uOttawa

L'Université canadienne
Canada's university

FACULTÉ DES ÉTUDES SUPÉRIEURES ET POSTOCTORALES

uOttawa

L'Université canadienne
Canada's university

FACULTY OF GRADUATE AND POSDOCTORAL STUDIES

Rosamund Dunkley

AUTEUR DE LA THÈSE / AUTHOR OF THESIS

M.Sc. (Biochemistry – Human and Molecular Genetics)

GRADE / DEGREE

Department of Biochemistry, Microbiology and Immunology

FACULTÉ, ÉCOLE, DÉPARTEMENT / FACULTY, SCHOOL, DEPARTMENT

Ubiquitos Over-Expression of Human X-Linked Inhibitor of Apoptosis (XIAP) in a Transgenic Mouse and Implications for Tumorigenesis

TITRE DE LA THÈSE / TITLE OF THESIS

P. Liston

DIRECTEUR (DIRECTRICE) DE LA THÈSE / THESIS SUPERVISOR

CO-DIRECTEUR (CO-DIRECTRICE) DE LA THÈSE / THESIS CO-SUPERVISOR

EXAMINATEURS (EXAMINATRICES) DE LA THÈSE / THESIS EXAMINERS

R. Aubin

L. Sabourin

Gary W. Slater

LE DOYEN DE LA FACULTÉ DES ÉTUDES SUPÉRIEURES ET POSTDOCTORALES /
DEAN OF THE FACULTY OF GRADUATE AND POSTDOCORAL STUDIES

Ubiquitous Over-expression of Human X-linked Inhibitor of Apoptosis (XIAP) in a Transgenic Mouse and Implications for Tumorigenesis

Rosamund Dunkley

Thesis Submitted to the Faculty of Graduate and Postdoctoral Studies
In partial fulfillment of the requirements
For the Degree of Master of Science in Biochemistry
with a specialization in Human and Molecular Genetics

Department of Biochemistry, Microbiology and Immunology
Faculty of Medicine
University of Ottawa

Your file Votre référence
ISBN: 0-494-11262-X
Our file Notre référence
ISBN: 0-494-11262-X

Abstract

The suppression of programmed cell death is an essential alteration in the transformation from normal to neoplastic growth. The X-linked inhibitor of apoptosis (XIAP) is a potent suppressor of apoptosis. It is a member of the Inhibitor of Apoptosis (IAP) family and functions by inhibiting caspases 3, 7 and 9 critical proteases in the process of programmed cell death. XIAP expression levels are frequently elevated in cancer cell lines and tumors, yet the link between XIAP expression and tumorigenesis has not been demonstrated experimentally. The objective of this project is to determine whether XIAP over-expression predisposes mice to cancer. A XIAP transgenic mouse model has been created with expression of the transgene driven by the ubiquitin C promoter. The UbiC-6-myc XIAP transgenics demonstrate ubiquitous over-expression of the human homolog of XIAP. Transgene over-expression was detected by western blot in all tissues tested including brain, retina, thymus, lung, heart, liver, kidney, pancreas, and spleen. The mice develop normally and show no unusual phenotype. Homozygous mice have been bred that show a further two-fold over-expression relative to their heterozygous littermates. Suppression of apoptosis has been documented in *in vitro* studies of mouse embryo fibroblasts and hepatocyte cultures. Transgenic XIAP provides protection against injury-induced apoptosis *in vivo* in a high dose streptozotocin induced pancreatic beta cell damage model in adult mice. The mice have been bred with an inducible c-myc oncogene transgenic strain that expresses c-myc in the beta cells of the islets of Langerhans when activated by tamoxifen (obtained from Dr. Gerard Evan). The myc/XIAP double transgenics responded in the same manner as the single c-myc transgenics and the beta cells underwent apoptosis. These results suggest a model where XIAP suppresses injury or stress induced apoptosis but is unable to block genetically pre-determined or oncogene-activated apoptosis.

Acknowledgements

Thank you to Dr. Peter Liston, my thesis supervisor for being so knowledgeable and always available for scientific advice. Thanks to the members of my thesis advisory committee including Dr. Alex Mackenzie, Dr. Ruth Slack and Dr. Doug Gray for sound guidance and constructive suggestions. Thank you to Sandra Hurley and Natasha Schokman for incredible technical assistance and support and to Juana Barcelo for assistance with mouse embryo fibroblast cultures. To Dr. Rashmi Kothary and Yves De Repentigny for performing the microinjections that created the UbiC-6myc XIAP transgenic mice and Dr. Lamorna Swigart-Brown and Dr. Gerard Evan for letting us use the c-myc transgenic mice in our experiments. To Phil Griffin, Adam Baker, and Charlie Thompson who all contributed to helping me understand the mysteries of immunohistochemistry. To Nigel Banner who created the macro that automated the cell counts. Thank you as well to the CIHR for providing funding for this project through grants to Dr. Peter Liston. And finally, thank you to everyone at the Apoptosis Research Centre and the CHEO Research Institute for your friendship and assistance throughout the duration of my project.

Dedication

To Tom for his love and support, it wouldn't have been possible without you
To my parents for always encouraging me to continue.

TABLE OF CONTENTS

LIST OF ABBREVIATIONS

° C - degrees Celsius

ABC – avidin biotin conjugated

Apaf – Apoptosis Protease Activating Factor

Bcl – B cell lymphoma

BIR – Baculoviral IAP Repeat

BIRP – BIR containing protein

BMI – Biochemistry, Microbiology, and Immunology

BMP – Bone Morphogenic Protein

BRUCE – BIR Repeat Containing Ubiquitin Conjugating Enzyme

CARD – Caspase Recruitment Domain

CARP – caspases-8- and -10-associated RING proteins

Caspase – Cysteine Aspartase

Ced – Cell death abnormal

C. Elegans - Caenorhabditis elegans

DAB - Diaminobenzidinetetrahydrochloride (peroxidase substrate)

dATP – deoxyadenosine Triphosphate

[α ^{32}P] dCTP – phosphorus –32 labelled deoxy–cytidine triphosphate

DD – death domain

DED –death effector domain

DIABLO – Direct IAP Binding Protein with Low pI

DISC – Death Inducing Signaling Complex

dNTP – deoxy-nucleotide triphosphate

DNA –deoxyribonucleic acid

EDTA- Ethylenediaminetetraacetic Acid

EGTA - Ethylene Glycol Bis-2-Aminoethyl Ether-N,N',N",n'-Tetraacetic Acid

ELISA - Enzyme Linked Immunosorbent Assay

ER- estrogen receptor

FADD – Fas Associated Death Domain

FLIP – FLICE Like Inhibitor Protein

g - gram

GAPDH - Glyceraldehyde-3-phosphate dehydrogenase

GSPT - G_1 to S phase transition protein

h - hour

HEPES - N-2-Hydroxyethylpiperazine-N'-2-Ethanesulfonic Acid

HIAP – Human Inhibitor of Apoptosis

HPS – Hemotoxylin, Phloxine, Saffron

HtrA - high-temperature requirement A

IAP – Inhibitor of Apoptosis

IBM – IAP Binding Motif

IgG - immunoglobulin G

ILPIP – hILP/XIAP-Interacting Protein

JNK – c-Jun Amino Terminal Kinase

Kb – Kilobase pairs

KCl – Potassium Chloride

kDa – Kilodaltons

MAP – Microtubule Associated Protein

MALT – Mucosa Associated Lymphoid Tissue

MEF – Mouse Embryo Fibroblasts

$MgCl_2$ – Magnesium Chloride

MIAP – Mouse Inhibitor of Apoptosis

min – Minute

ml– milliliter

mM – Millimolar

Mn (OAc) – Manganase acetate

mRNA – messenger RNA

NAIP – Neuronal Apoptosis Inhibitory Protein

NaCl – Sodium Chloride

NaOH – Sodium Hydroxide

NF-κB – Nuclear Factor kappa B

nm – nanometres

OCT – Optimal Cutting Temperature compound

OH- hydroxy

PBS – phosphate buffered saline

PBST – PBS with Tween

PCD – Programmed Cell Death

PCR – Polymerase Chain Reaction

PEG - polyethyleneglycol

PFA – Paraformaldehyde

pH - Potential of Hydrogen (measure of acidity)

PMSF – Phenylmethylsulfonyl Fluoride

PVDF - Polyvinylidene Fluoride

RNA – Ribonucleic Acid

RPM – Rotations Per Minute

rTh – thermostable recombinant DNA polymerase

RT- PCR – Reverse Transcriptase PCR

RZF – Ring Zinc Finger

SDS – Sodium Dodecyl Sulfate

SMA – Spinal Muscular Atrophy

SMAC – Second Mitochondrial-Derived Activator of Caspases

SSC – Standard Saline Citrate

SSPE – Standard Sodium Phosphate EDTA

TAB - TAK1-binding protein

TAE – Tris Acetate EDTA

TAK - TGF-beta Activated Kinase

TAM - Tamoxifen

TdT – Terminal Deoxynucleotidyl Transferase

TE – Tris EDTA

TGF -β – Trasnsforming Growth Factor β

TMB - 3, 3', 5, 5'- tetramethylbenzidine

TNF – Tumor Necrosis Factor

TRAF - TNF Receptor-Associated Factor

TRAIL - TNF-Related Apoptosis-Inducing Ligand

TsIAP – Testis-specific IAP

TUNEL – TdT-mediated dUTP Nick-End Labeling

UTR – Untranslated Region

UV - Ultraviolet

WST - 2-(4-Iodophenyl)-3-(4-nitrophenyl)-5-(2,4-disulfophenyl)-2H-tetrazolium, monosodium salt

XAF – XIAP Associated Factor

XIAP- X-linked Inhibitor of Apoptosis

LIST OF FIGURES

LIST OF TABLES

CHAPTER 1: INTRODUCTION

PART 1-1: PROGRAMMED CELL DEATH IN DEVELOPMENT AND DISEASE

Programmed cell death (PCD) is a critical cellular function that allows multi-cellular organisms to control development and respond to cellular stress and injury. It allows the organism to eliminate cells that have outlived their usefulness, become redundant, or which pose a threat to the health of the organism (Raff, 1998). There are at least three types of programmed cell death reviewed in (Assuncao Guimaraes and Linden, 2004), including the traditionally distinguished manifestations of programmed cell death, necrosis and apoptosis and a newly recognized form called autophagy.

Kerr and coworkers first identified two distinct forms of cell death in 1972 (Kerr, 2002). The first is a passive form of cell death called necrosis that can be recognized by its characteristic morphological changes. These consist of cytoplasm swelling, destruction of organelles, and destruction of the plasma membrane, leading to the release of intracellular contents and inflammation. The second type of cell death, apoptosis, has a very different morphological progression and was discovered to be a much more active process. Apoptosis was identified in single cells surrounded by healthy neighbours and was characterized by cell shrinkage, blebbing of the plasma membrane, maintenance of organelle integrity and condensation and fragmentation of DNA followed by ordered removal through phagocytosis (Assuncao Guimaraes and Linden, 2004).

A third cellular process named autophagy has recently been classified as a process of programmed cell death. Autophagy was initially implicated in the turnover of organelles. It

has been described as a means to resist starvation and as part of cellular remodelling during differentiation, metamorphosis, aging, and cell transformation, physiological whole-organism changes such as pregnancy and childbirth, and removal of anomalous cellular components after toxic insult. Autophagic cells contain autophagic vacuoli, the nucleoplasm and cytoplasm appear darkened, organelles such as the endoplasmic reticulum (ER) and mitochondria are dilated, and the plasma membrane loses its specialization.

Programmed cell death was first studied in development and is still most often recognised as the process that eliminates interdigital tissue from between the fingers during embryogenesis (Mirkes, 2002). Cell death is an integral part of the normal development of virtually every tissue and organ. During development, cell death helps sculpt parts of the body and is essential to metamorphosis, carving out cavities and eliminating structures that once served a function but are no longer needed, such as the tail of the tadpole during metamorphosis into a frog (Raff, 1998). The closure of the neural tube is one of the earliest instances of critical PCD in development. In fact, the entire structure of the nervous system is shaped through PCD as fifty percent of neurons generated during development are eliminated by cell death (Oppenheim, 1991).

Until very recently, PCD during development was assumed to occur predominantly, if not exclusively, by apoptosis. Necrosis was viewed as being largely caused by acute injury. It is now emerging that both necrotic and autophagic cell death occur during development as well. The relative contributions of each of these forms of PCD to normal development have yet to be established.

The molecular mechanisms of apoptosis were first elucidated by the discovery and characterization of *ced* (cell death abnormal) genes essential in the normal development of

Caenorhabditis elegans (C. elegans). Though *C. elegans* can survive embryogenesis with defects in PCD, in more complex organisms such as mice and *Drosophila melanogaster* defects in cell death pathways are often embryonic lethal (Raff, 1998).

More recently, apoptosis has been linked to several disease processes. Excessive cell death has been shown to contribute to the pathogenesis of a variety of neurological disorders. Examples include acute brain injury such as trauma, spinal chord injury, ischemic stroke and ischemia/reperfusion as well as chronic disease states such as Alzheimer's, Parkinson's, Huntington's, amyotrophic lateral sclerosis (ALS), spinal muscular atrophy, and diabetic neuropathy (Ekshyyan and Aw, 2004). In most of these disease or injury conditions most if not all of the morphological features of apoptosis are present.

On the other end of the spectrum, suppression of cell death has been identified as one of the six essential characteristics of all tumours (Hanahan and Weinberg, 2000). Tumour cells survive only by virtue of mutations that allow them to proliferate and to evade cell death signals. In fact, Hanahan and Weinberg argue that defects in apoptosis contribute to neoplastic transformation, progression and metastasis by creating a permissive environment for genetic instability and accumulation of gene mutations. Resistance to apoptosis can also enhance the escape of tumour cells from surveillance by the immune system. Moreover, because chemotherapy and irradiation act mostly by inducing apoptosis, dysregulation of apoptotic pathways can make cancer cells more resistant to therapy (Malaguarnera, 2004).

PART 1-2: APOPTOSIS

Apoptosis is a form of cell death that is tightly regulated by a complex web of extracellular and intracellular signals. The cell has developed an acutely sensitive network of sensors, effectors and inhibitors, that is responsive to a variety of apoptotic triggers including

immune system mediated cytotoxicity, cellular stress, DNA damage, and pathological injury. Apoptosis can be triggered by virtually every organelle including the nucleus, mitochondria, ER, Golgi apparatus and lysosomes (Ferri and Kroemer, 2001).

It seems that several organelles might initiate apoptosis by specific stress sensors and relay apoptosis-modulating signals to the rest of the cell (figure 1-1). The most well characterized pathways are divided into the intrinsic pathway that is sensitive to intracellular signals and triggers apoptosis through the mitochondria dependent pathway and the extrinsic pathway triggered by death receptors at the cell surface (Salvesen and Abrams, 2004). These pathways are not completely distinct and there are several points of cross-talk and amplification between effectors in each pathway (Ferri and Kroemer, 2001) . Extrinsic and intrinsic pathways and organelle-specific death signals converge, either by the local activation of caspases, a family of cysteine proteases that act as common death effector molecules in various forms of cell death (for example, caspase-12 in the ER, and caspase-2 in the Golgi) or by affecting mitochondrial membrane permeability.

a) Intrinsic pathway

The intrinsic pathway is regulated through permeabilization of the outer mitochondrial membrane (OMM) and the release of pro-apoptotic factors sequestered in the mitochondrial intermembrane space. Membrane integrity can be altered through differential expression of members of the Bcl-2 (B-cell leukemia/lymphoma-2) family.

i. Bcl-2 family members control outer mitochondrial membrane permeability

Bcl-2 was first discovered at the interchromosomal breakpoint of the t(14;18) translocation in follicular B cell lymphoma reviewed in (Sorenson, 2004). As this novel protein was being characterized, bcl-2 was presumed to be another of the growth promoting oncogenes.

Figure 1-1 Pathways of Apoptosis

Apoptotic pathways have traditionally been divided into extrinsic death receptor triggered pathways and intrinsic mitochondria driven pathways. Apoptosis can in fact be triggered by almost any organelle in the cell including the nucleus, lysosomes, Golgi apparatus and endoplasmic reticulum in addition to the mitochondria and plasma membrane receptors. These pathways converge on the activation of the caspase cascade. Apoptosis can be inhibited at several key points. Important regulators of the caspase cascade include inhibition of effector caspases by the inhibitors of apoptosis (IAP) family proteins. Another major point of regulation is mitochondrial membrane permeability (MMP), which is controlled by members of the Bcl-2 family. Several caspase-independent pathways have emerged, which are triggered by mitochondrial membrane permeability. Images adapted from (Ferri and Kroemer, 2001).

Nuclear triggers
Antimetabolites, topoisomerase inhibitors, DNA damaging agents, alkylating agents, γ-irradiation.

ER triggers
Tunicamycin, Brefeldin A, Thapsigargin

Lysosome triggers
Lysomotrophic detergents and photosensitizers

Plasma membrane triggers
TNF ligands

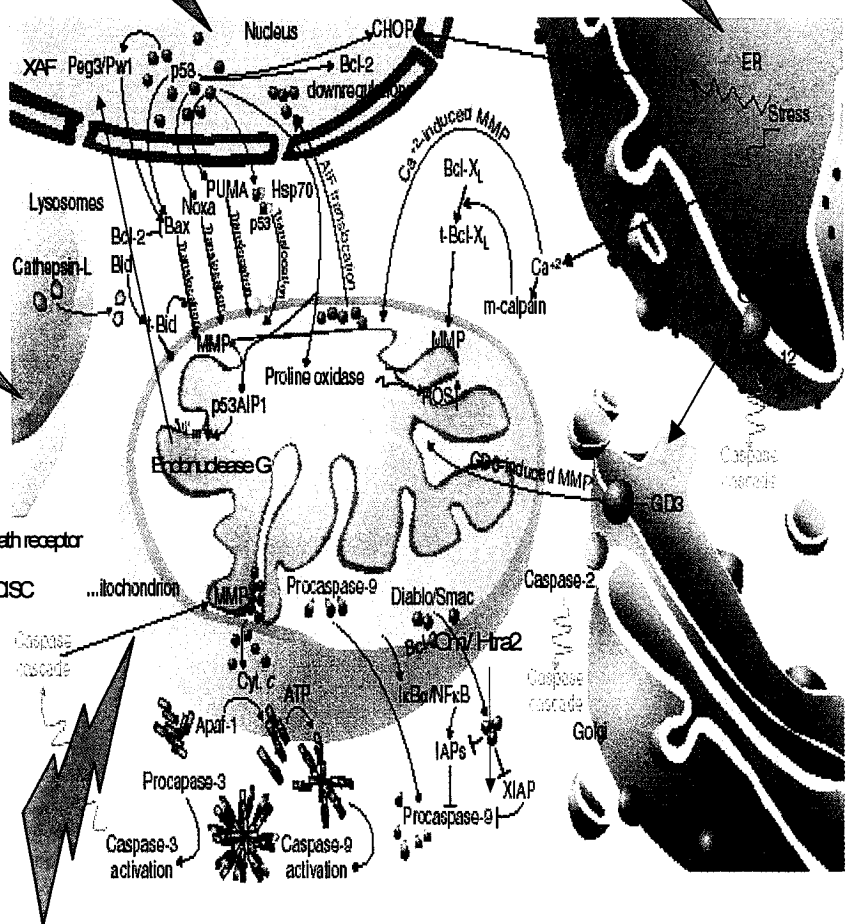

Mitochondria triggers
Chemotherapeutics, respiratory chain inhibitors, endogenous toxins ligands of Bcl-2 and Bcl-X, nonspecific stress mediators, reactive oxygen species, calcium concentration, nitrous oxide, viral and bacterial proteins

Figure 1-1

The discovery of its anti-apoptotic properties had an important impact on what types of proteins are considered proto-oncogenes. It also provided the first connection between apoptosis and tumorigenesis (Kirkin et al., 2004).

Bcl-2 family proteins are membrane bound proteins that have been found in the nuclear envelope, ER, mitochondria and plasma membrane. The structural homology between bcl-2 and the diphtheria toxin indicates a putative pore-forming structure. The bcl-2 family can be subdivided into three classes. The anti-apoptotic survival factors such as bcl-2, bcl-x_L, and bcl-w contain three to four bcl-2 homology (BH) domains. Anti-apoptotic members can block permeabilization of the membrane by oligomerizing to inhibit proper pore formation reviewed in (Sharpe et al., 2004). The pro-apoptotic death factors such as Bax and Bak contain BH1-BH3 domains. Pro-apoptotic members will promote pore formation through oligomerization. There is also the much larger class of BH3 only pro-apoptotic death factors such as Bad, Bid and Bim that act upstream in the pathway by antagonizing bcl-2 survival activity or activating Bax (Kirkin et al., 2004). The balance of activated pro-apoptotic and anti-apoptotic bcl-2 family members in a cell determines the permeabilization state of the outer mitochondrial membrane.

ii. Permeabilization of the mitochondria and release of pro-apoptotic factors

Permeabilization of the outer mitochondrial membrane by pro-apoptotic members of the bcl-2 family can release proteins from the intermembrane space. An example of this mechanism is the activation of BH3 only proteins Bid or Bim that induce homo-oligomerization of Bax or Bak channels. Bax and Bak channels allow the direct release of pro-apoptotic factors from the mitochondria (Orrenius, 2004).

Permeabilization can also occur through the induction of the permeability transition pore (PTP). Opening of the PTP can cause osmotic swelling of the mitochondrial matrix, rupture of the outer mitochondrial membrane and the release of cytochrome c. It has also been observed that a small fraction of mitochondria have open pores at any given time. This PTP flickering allows adenine exchange without large amplitude swelling or drop in membrane potential in the entire population (Orrenius, 2004).

Several different types of pro-apoptotic factors are released into the cytoplasm and trigger downstream events in the apoptotic cascade. Cytochrome c release promotes caspase activation through the formation of a multimeric complex called the apoptosome. Apoptosis-inducing factor (AIF) and endonuclease G are factors that are released and contribute to apoptotic nuclear DNA fragmentation in a caspase-independent manner (Cande et al., 2002). Second mitochondria-derived activator of caspase/Direct IAP-binding protein with low PI (Smac/DIABLO) and the serine protease high temperature requirement protein A2 (HtrA2/OMI) both interact with the Inhibitors of Apoptosis (IAPs) to promote caspase activation but also have caspase independent cytotoxicity (Saelens et al., 2004).

b) Extrinsic pathway

The extrinsic pathway triggers apoptosis in response to extra-cellular signals received through cell surface receptors. Ligation of death receptors of the tumour necrosis factor (TNF) receptor superfamily such as Fas (CD95/APO-1) or TNF-related apoptosis-inducing ligand (TRAIL) triggers receptor aggregation and recruitment of the adaptor molecule Fas-associated death domain (FADD). Subsequent recruitment of

caspase-8 or -10 to the complex completes the formation of the death inducing signalling complex (DISC) (Debatin and Krammer, 2004).

i. Death receptors

Death receptors are defined by a cytoplasmic domain of about 80 amino acids called the 'death domain', which plays a crucial role in transmitting the death signal from the cell surface to intracellular signalling pathways.

There are two essential elements required for TNF receptor activation. The first is the presence of a TNF receptor, a Type I transmembrane glycoprotein. The second element is the TNF ligand, a Type II protein, which exist in both a soluble and a membrane-bound form. In the TNF receptor family model, ligand binding causes trimerization of the receptor and triggers activation. Activation occurs because ligation of the receptor causes a clustering of the receptor death domains (DD) leading to the formation of a DISC complex. The DISC also contains the adaptor protein FADD that recruits caspase-8 through its DED (death effector domain). Caspase-8 clustering in the multimeric DISC complex promotes activation through induced proximity allowing it to cleave and activate downstream effector caspases.

Two classical examples of the TNF death receptor pathway are Fas (CD95) and TRAIL. The Fas (CD95) receptor is expressed in activated lymphocytes, as well as a variety of tissues and tumour cells. FasL (Fas ligand) is produced by activated T cells and plays a crucial role in the regulation of the immune system by triggering autocrine suicide or paracrine death in neighbouring lymphocytes or other target cells (Debatin and Krammer, 2004).

TRAIL is constitutively expressed in a wide range of tissues. The TRAIL ligand has five different receptors. TRAIL-R1 and R2 are agonistic receptors containing a conserved cytoplasmic death effector domain (DED) motif, which engages apoptosis machinery upon ligand binding (Shankar and Srivastava, 2004). TRAIL-R3, TRAIL-R4 and TRAIL-R5 receptors are antagonistic decoy receptors lacking cytoplasmic death domains that bind TRAIL but prevent the transmission of death signals.

ii. Cross talk between pathways

The extrinsic and intrinsic pathways are not mutually exclusive. The extrinsic pathway can trigger the activation of intrinsic proteins. For example upon death receptor ligation, activation of caspase-8 may result in cleavage of Bid, a BH3 only member of the Bcl-2 family. Truncated BID (tBID) translocates to the mitochondrial membrane and acts as a chaperone for the formation of Bak channels that release cytochrome c, initiating a mitochondrial amplification loop. The intrinsic pathway can also impact the extrinsic pathway such as occurs when caspase 6 is activated downstream of mitochondrial events and provides feedback to the receptor pathway by cleaving caspase-8 (Debatin and Krammer, 2004). These are two examples of the many ways in which these pathways can merge and amplify each other.

iii. DNA damage induced apoptosis and p53

DNA damage triggers apoptosis through a unique mechanism that employs both the intrinsic and extrinsic pathways. The decision by a cell to trigger apoptosis in response to DNA damage is linked to its inability to eliminate the damage through DNA repair and cell cycle arrest. One of the more important mediators of this decision point is p53. P53, a key tumour suppressor, can act as a transcriptional activator of genes encoding

apoptotic effectors. It can directly activate transcription of several genes encoding pro-apoptotic bcl-2 family members most notably Bax and the BH3-only proteins Noxa and PUMA (Norbury and Zhivotovsky, 2004). P53 can also activate transcription of Fas following DNA damage rendering the cell more susceptible to Fas ligand induced apoptosis and cytotoxic T lymphocyte-mediated killing. P53 can also downregulate transcription of IAP-family proteins such as survivin (Zhou et al., 2002).

c) Caspases

The extrinsic and the intrinsic pathways converge on the caspases. Caspases are cysteine proteases that cleave proteins after aspartate residues (Salvesen and Abrams, 2004). They have been recognized as the principal molecular machines that execute apoptosis. There are eleven known human caspases with different substrate specificity that are involved in apoptosis signalling and cytokine processing (Debatin and Krammer, 2004). These can be divided into subgroups based on substrate specificity, domain composition or presumed roles *in vivo* (Salvesen and Abrams, 2004). Caspases 2, 8, 9, and 10 are often called initiator caspases. Each contains a large pro-domain which often promotes recruitment to a higher order complex. These 6-7 helix bundles direct caspases to their activation platforms. Caspases 3, 6, and 7 have short pro-domains and are often referred to as effector caspases. Caspases 1, 4, 5 and 14 have not been associated with apoptosis but instead are involved in cytokine activation.

i. Initiator Caspases

The initiator caspases lie at an important decision point in a cell's life. They convert the death signal into action. There are three possible roles for initiator caspases: sensing and integrating different inputs so that they can be transmitted to a common execution phase, signal amplification by generating substantial amounts of active executioner

caspases, and finally acting as a regulatory point before commitment to death (Salvesen and Abrams, 2004).

In the extrinsic pathway, caspases 8 and 10 are recruited and activated through induced proximity. They interact with adaptor molecules such as FADD that provide a link to death receptors through DEDs. In the intrinsic pathway, caspase 9 is recruited to the apoptosome through the adaptor protein Apaf-1 via its CARD – CARD interaction. In both pathways, the formation of a higher order complex such as the DISC or the apoptosome requires sufficient signal for multiple caspases to be recruited to the same complex before activation can occur.

ii. Effector caspases

In contrast to the relatively complex methods of activating initiator caspases, the activation of effector caspases occurs through direct proteolysis at internal sites. Caspases 3, 6, and 7 exist in the cell as inactive zymogens. These zymogens are present as dimers, but cleavage within their linker segments is required for activation. Once cleaved, the effector caspases can cleave other effectors providing further signal amplification.

iii. Caspase Substrates

There are a large variety of caspase substrates in the cell. Proteolytic cleavage of cytoskeletal proteins such as fodrin, gelsolin, actin, plectrin, cytokeratin and lamin promotes loss of overall cell shape, nuclear condensation and budding (Debatin, 2004). Many of the morphological changes first observed by Kerr that characterize classical apoptosis result from cleavage of these substrates by effector caspases.

PART 1-3: INHIBITORS OF APOPTOSIS

The inhibitors of apoptosis (IAPs) are a family of endogenous caspase inhibitors. Originally discovered in baculoviruses, the IAPs are highly conserved across taxa from viruses to insects to mammals. IAPs are characterized by the presence of one or more baculoviral IAP repeat (BIR) domains. BIR domains consist of a 70-80 amino acid cysteine- and histidine-rich folding domain that chelates a zinc ion forming a compact globular structure of four to five alpha helices and a variable number of beta sheets (Liston et al., 2003). In addition to their ability to bind and inhibit caspases, IAPs have been shown to participate in cell cycle regulation and modulation of receptor-mediated signal transduction (Nachmias et al., 2004).

Several BIR containing proteins (BIRPs) have been identified in unicellular organisms that do not undergo apoptosis. These proteins are important for cytokinesis, and it has been proposed that these BIRPs are ancient progenitors that may have evolved into the current IAPs through gene duplication events (Miller, 1999).

a) IAP family members

i) There are eight identified mammalian IAP family members. Neuronal apoptosis inhibitory protein (NAIP) was the first mammalian IAP identified during a positional cloning effort to identify the gene responsible for spinal muscular atrophy (Roy et al., 1995). Soon after the discovery of NAIP, three other IAPs were discovered including the X-linked inhibitor of apoptosis (XIAP), cellular IAP 1 (c-IAP1/HIAP2) and cellular IAP 2 (c-IAP-2/HIAP1). These four IAPs all contain three BIR domains and all but NAIP also share homologous really interesting new gene (RING) zinc finger domains at their carboxyl terminus. The remaining members of the mammalian IAP family,

Figure 1-2 Inhibitors of Apoptosis (IAP) family members

The eight members of the mammalian IAP family. All IAP members contain at least one conserved BIR domain (pink). XIAP, HIAP1, HIAP2, and NAIP each have 3 BIR domains each with its own binding affinities. XIAP, HIAP1, HIAP2, Ts-IAP and Livin also share homology in the RZF domain (yellow) that acts as an E3 ubiquitin ligase. Other conserved domains are identified at the bottom of the figure including the CARD or caspase recruitment domain (green) of HIAP1 and HIAP2, the coiled-coil domain (blue) of Survivin and the ubiqitin-conjugating domain (orange) of BRUCE.

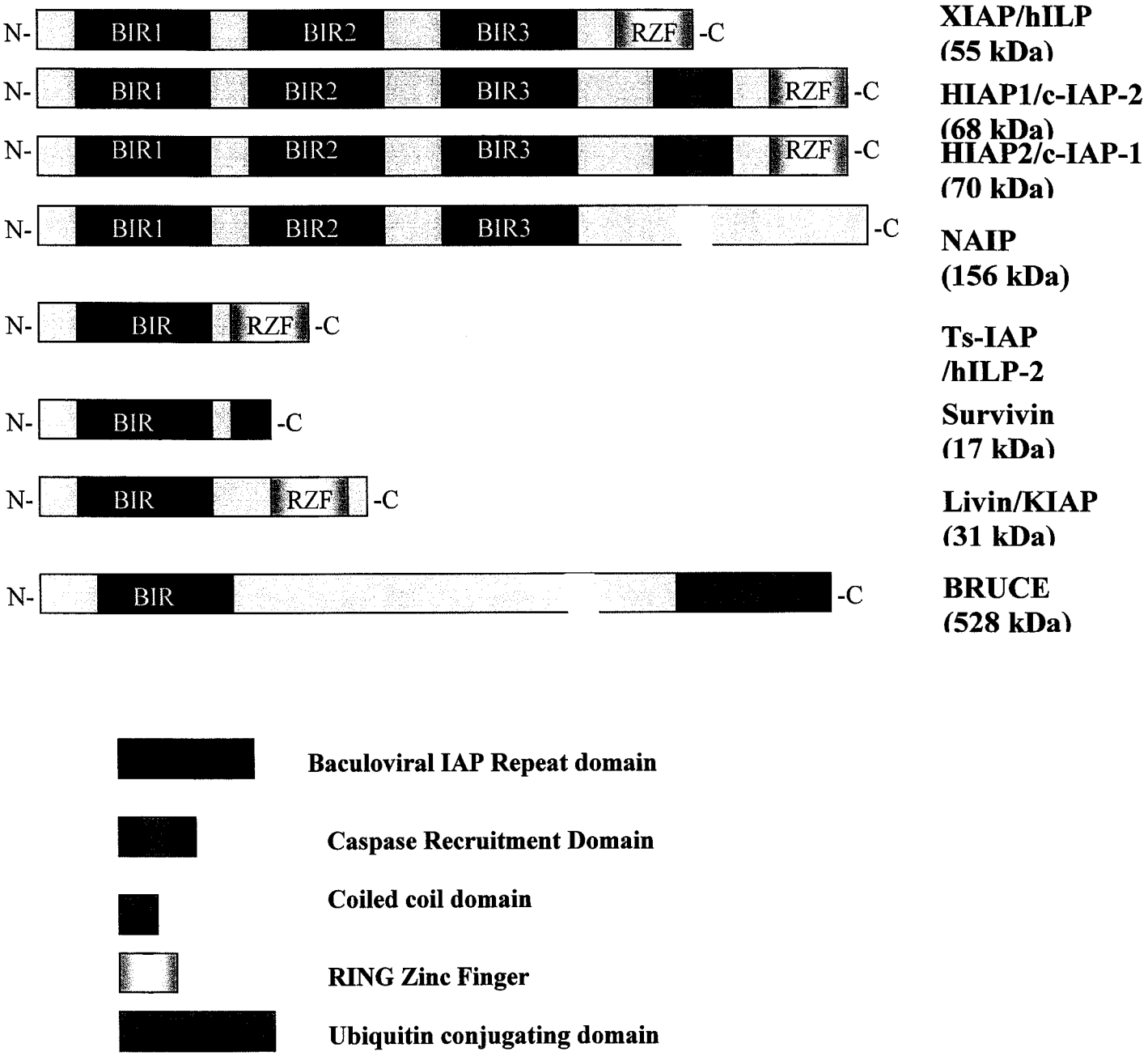
N-
BIR1
BIR2
BIR3
RZF
-C
XIAP/hILP
(55 kDa)
HIAP1/c-IAP-2
(68 kDa)
HIAP2/c-IAP-1
(70 kDa)
NAIP
(156 kDa)
BIR
Ts-IAP
/hILP-2
Survivin
(17 kDa)
Livin/KIAP
(31 kDa)
BRUCE
(528 kDa)
Baculoviral IAP Repeat domain
Caspase Recruitment Domain
Coiled coil domain
RING Zinc Finger
Ubiquitin conjugating domain

Figure 1-2

Survivin, Livin, testes-specific IAP (Ts-IAP), and BRUCE each contain one BIR domain.

b) Common functions and domains

Baculoviral IAP Repeats (BIR) domains

The ability of IAPs to bind and inhibit caspases is linked to the presence of the BIR domains. In IAPs containing three BIR domains, BIR2 and its upstream linker are involved in binding effector caspases 3 and 7, while BIR3 interacts with the initiator caspase 9. The linker region upstream of BIR2 stretches across the active site of caspase 3 to inhibit substrate entry (Huang et al., 2003) and the linker alone is sufficient to inhibit caspase-3 activity. In contrast, the linker is not sufficient for caspase-7 inhibition. This interaction requires stabilisation by the amino terminus of the BIR2 domain with the small subunit of caspase-7 for complete inhibition. This creates a scenario where inhibition of caspase-3 is competitive while inhibition of caspase-7 employs both a competitive and a non-competitive mechanism.

The inhibition of caspase-9 occurs by a completely different mechanism that is not surprising based on the very different activation mechanism needed for the activation of initiator caspases. Caspase-9 can undergo a self-cleavage event in the linker region between its p20 and p10 subunits. The BIR3 domain directly binds caspase-9 via this newly exposed amino terminus and the interaction is stabilized through additional contacts with the enzyme (Shi, 2004). Up to this point, there are no known caspase interactions with BIR1 and it is has the least conserved sequence homology of all of the BIRs in the 3 BIR domain IAPs (Liston et al., 2003).

Each of the single BIR IAPs has its own specificity. Survivin inhibits caspases-3 and –7, Livin binds caspases-3, -7, and –9, Ts-IAP inhibits caspase-9 and BRUCE interacts with caspase-3. Initially, it was surprising that all eight IAPs had affinities for the same three of

the eleven mammalian caspases. Subsequently, two families of proteins have been identified that inhibit the activity of the initiator caspases of the extrinsic pathway. Both FLICE/ Caspase-8 like inhibitor protein (FLIP) (Boatright et al., 2004) and caspases-8- and -10-associated RING proteins (CARPs) (McDonald and El-Deiry, 2004) regulated caspase-8 and –10 recruitment, activity and stability. The IAPs remain as the only identified cellular inhibitors of the terminal caspase cascade. The apparent redundancy amongst the IAPs is decreased because each of the IAPs displays unique aspects of expression and recruitment to signalling complexes.

ii) RING zinc finger

RING zinc fingers (RZF) are a subclass of zinc finger domains that chelate two zinc ions in a characteristic cross-brace arrangement (Liston et al., 2003). Usually found at the amino terminus of proteins that act as E3 ubiquitin ligases, the IAP family RZFs are invariably found at the carboxyl terminus. E3 ligases are adapters, recruiting target proteins to complexes containing E2 ubiquitin-conjugating enzymes where they can be activated by E1 ubiquitin activating enzymes and degraded in the proteosome (Yang and Yu, 2003).

There is some debate as to the targets of ubiquitination by the IAPs. It has been suggested that the RZF is present to provoke the ubiquitination and consequent proteosomal degradation of the IAPs themselves and therefore serve a pro-apoptotic function (Yang and Yu, 2003). In other work, it has been shown that IAPs can trigger the ubiquitination of caspases-3 and –7 by triggering degradation of the entire complex. This would be serving an anti-apoptotic function (Suzuki et al., 2001). It has also been shown that IAPs are able to ubiquitinate Smac, an IAP inhibitor, once again re-affirming the anti-apoptotic nature of the E3 ligase activity (Hu and Yang, 2003).

c) Non-conformist IAPs

i) BRUCE

BRUCE, a giant BIR containing protein is not often considered a canonical IAP. Originally identified through a screen for ubiquitin conjugating enzymes, BRUCE has a single BIR domain with homology to the Survivin BIR but is also a chimeric E2/E3 ubiquitin enzyme (Bartke et al., 2004). Recent work has shown that in addition to its functions as an ubiquitin enzyme, over-expression of BRUCE can protect cells against apoptosis by binding and inhibiting caspase-3. BRUCE was also shown to interact with Smac and HtrA2, IAP inhibitors (Bartke et al., 2004). Therefore, though its main function is not that of an apoptosis inhibitor BRUCE is still a valid member of the IAP family.

ii) Survivin

Though it is considered an IAP, Survivin has much more significant functional homology with the BIRPs found in unicellular organisms such as yeast. Its main function is ensuring proper cytokinesis and its anti-apoptotic functions are secondary. Survivin is expressed at mitosis and localizes to various components of the mitotic apparatus including centrosomes and microtubules of the metaphase and anaphase spindle (Altieri, 2003).

PART 1-4: X-LINKED INHIBITOR OF APOPTOSIS (XIAP)

XIAP mRNA is expressed ubiquitously in all adult and fetal tissues except peripheral blood leukocytes (Deveraux and Reed, 1999). XIAP is an important regulator of apoptosis. XIAP's role has been demonstrated in the suppression of apoptosis induced by TNFα, Fas, serum or growth factor withdrawal, ischemia, chemotherapy and radiotherapy (LaCasse et al., 1998),(Holcik and Korneluk, 2000). Over-expression of XIAP is protective against several forms of apoptosis *in vivo* including ischemia (Xu et al., 1999), neuronal axotomy

Figure 1-3 Specific interactions between XIAP domains, Smac, and caspases

A) A map of XIAP's domain structure including the amino acids at which each domain begins and ends.

B) Crystal structure showing the linker (blue and purple) and BIR2 (red and mauve) interaction with caspase-7 (yellow and green). XIAP tightly binds the active site of caspases-3 and -7 by a short peptide sequence in the linker region preceding BIR2. This binding occludes substrate entry and catalysis, resulting in complete inhibition of caspase-3 and –7.

C) Crystal structure of the BIR3 (blue) interaction with caspase-9 (green and red). XIAP-BIR3 domain forms a heterodimer with the caspase-9 monomer. This effectively traps caspase-9 because caspase-9 requires homodimerization to become active. The XIAP-BIR3 domain not only sequesters caspase-9 in a monomeric state but also traps the active site loops in their unproductive conformations.

D) Crystal structure of the Smac dimer and the interaction between Smac and BIR3. Smac interacts directly with a groove on the surface of the BIR-3 domain of XIAP. The amino terminal IBM (AVPI) displaces a very similar motif (ATPF) on the small subunit of caspase-9 that occupies the same BIR3 surface groove as Smac. Each of the BIR2 and BIR3 domains alone is not a good binding partner, but because Smac is a dimer it can efficiently antagonize inhibition of both effector and initiator caspases by binding in a 2:1 stoichiometric complex.

E) The AVPI sequence of the Smac dimer (purple) interacting with BIR3 (light blue) of XIAP

All crystal structures adapted from Huang et al 2001

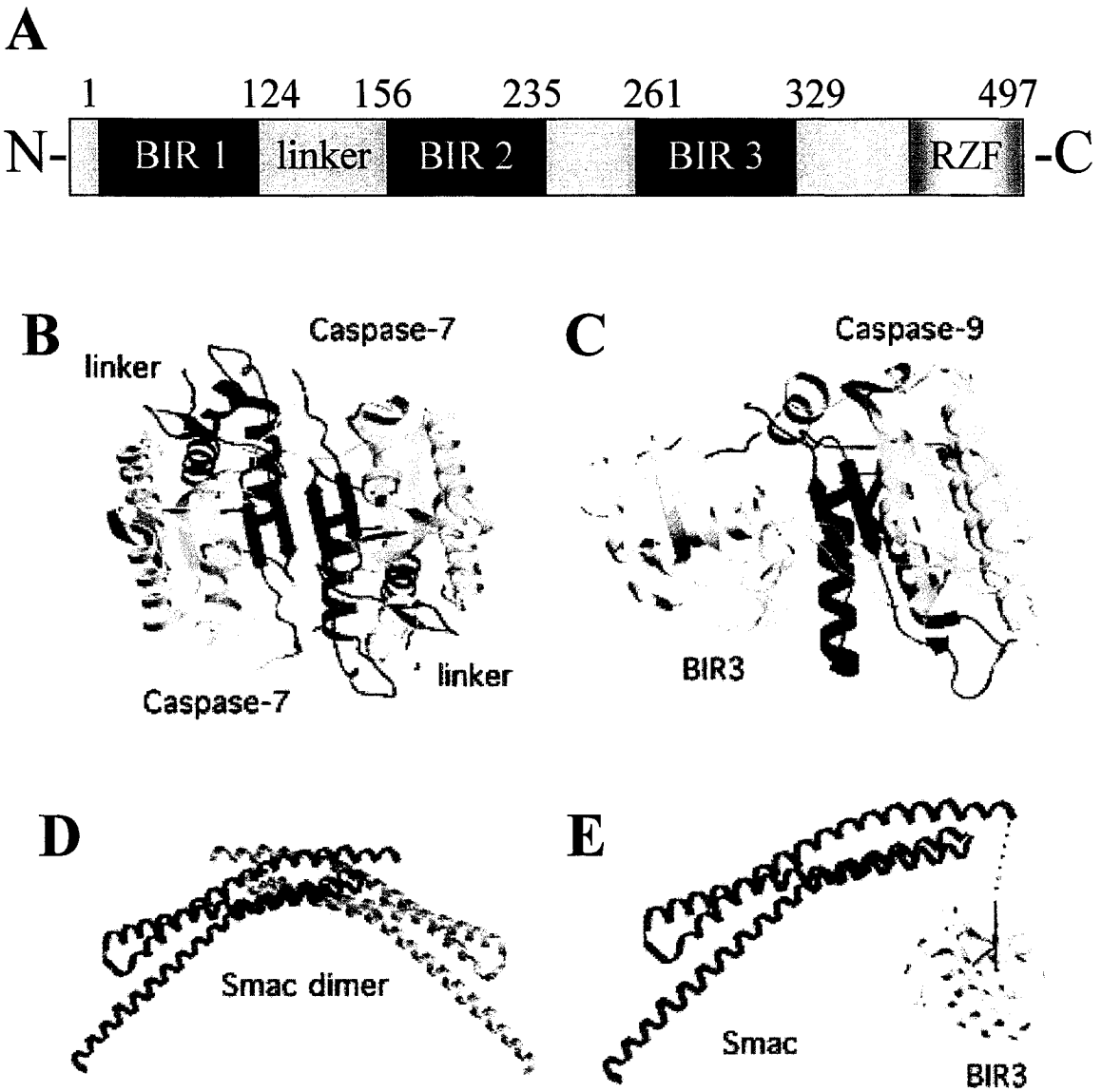
A
1
124
156
235
261
329
497
N-
BIR 1
linker
BIR 2
BIR 3
RZF
-C
B
Caspase-7
linker
Caspase-7
linker
C
Caspase-9
BIR3
D
Smac dimer
E
Smac
BIR3

Figure 1-3

(Kugler et al., 2000), kainic acid-induced neuronal death (Korhonen et al., 2001), and thymocyte apoptosis (Conte et al., 2001).

a) Potent caspase inhibitor

There are several mechanisms through which XIAP exerts its anti-apoptotic effect but the most significant up to this point has been its role in caspase inhibition.

i) Inhibition of caspase-3 and -7

XIAP is the IAP with the highest affinity for caspases. XIAP-BIR2 inhibits caspases-3 and –7 with a $K_i < 2$ nM (Deveraux and Reed, 1999). XIAP demonstrates a marked preference for the activated form of caspase-3 (Suzuki et al., 2001). This is possible because XIAP tightly binds the active site of caspases-3 and -7 by a short peptide sequence in the linker region preceding BIR2 as shown in figure 1-3. This binding occludes substrate entry and catalysis, resulting in complete inhibition of caspase-3 and -7 (Shiozaki et al., 2003).

ii) Inhibition of caspase-9

Crystallography studies have shown that the XIAP-BIR3 domain forms a heterodimer with the caspase-9 monomer as shown in figure 1-3. This effectively traps caspase-9 because caspase-9 requires homodimerization to become active (Shiozaki et al., 2003). The XIAP-BIR3 domain not only sequesters caspase-9 in a monomeric state but also traps the active site loops in their unproductive conformations.

iii) Inhibition co-dependence allows XIAP to bind both caspases

XIAP can not only bind and inhibit caspase-3, -7 and -9 but the maintenance of the BIR3-caspase-9 interaction is dependent upon XIAP's ability to simultaneously bind and inhibit active caspase-3 via its linker-BIR2 domain (Bratton et al., 2002). The ability of XIAP to bind both caspase-9 and -3 within the same complex provides a two-pronged approach to caspase inhibition. Not only can it prevent further amplification of an intrinsic mitochondria

dependent signal through inhibition of caspase-9 activation, but it can also prevent an extrinsic death receptor induced signal downstream of the DISC by inhibiting caspase-3. This approach allows XIAP to prevent cross talk and amplification between pathways. This potency in preventing apoptosis in both extrinsic and intrinsic pathways is demonstrated through the observation that XIAP can prevent both Fas and Bax induced apoptosis exclusively through inhibition of caspases (Bratton et al., 2002).

XIAP is active on the periphery of the apoptosome (Bratton et al., 2002). XIAP specifically associates with the apoptosome via an interaction with the small subunit of caspase-9, protecting the p12 subunit from further cleavage to the p10 form (Shiozaki et al., 2003). Analysis of the protein constituents of native apoptosomes has revealed the presence of XIAP but not the other IAPs (Hill et al., 2004) further highlighting the functional uniqueness of this IAP as the central regulator of apoptosis.

b) E3 ubiquitin ligase activity

The BIR domains are not the only important functional domains in XIAP. The carboxyl terminal RING zinc finger motif plays a significant functional role. The RZF domain of XIAP is essential for the reduction of caspase-3 through proteosomal degradation (Suzuki et al., 2001). The E3 ubiquitin ligase activity of the RZF promotes the degradation of caspase-3 and enhances the anti-apoptotic activity of XIAP. But the E3 ligase activity is complex and its effects have also been considered pro-apoptotic.

XIAP can promote the ubiquitination not only of caspase-3 but also of itself. Ubiquitination of XIAP occurs at two lysine residues (Lys^{322} and Lys^{328}) both located on the surface of the BIR3 domain. In particular, Lys^{322} lies next to the Smac interacting groove (Shin et al., 2003). Mutation of these lysine residues did not affect XIAP protection from Bax or Fas induced apoptosis (Shin et al., 2003) casting doubt on whether ubiquitination of

XIAP alters its anti-apoptotic potential. In other studies auto-ubiquitination and proteosomal degradation of XIAP appeared to be necessary to allow apoptosis to proceed unhindered (Nachmias et al., 2004). Taken together, XIAP's E3 ligase activity cannot be decisively categorized as either pro- or anti-apoptotic. In fact, the RZF may actually help to shift the balance towards pro- and anti-apoptotic activities based on unknown signals within the cell.

c) XIAP inhibitors

XIAP binding proteins promote apoptosis in the cell by removing IAP mediated inhibition of caspases. Four small cytoplasmic proteins control apoptosis in *Drosophila*. It was subsequently found that Reaper, HID, Grim, and Sickle all function by binding and inhibiting the activity of the *Drosophila* IAP homologue DIAP1. No significant sequence homology exists among the proteins except at the amino terminus. The first four amino acids had a highly conserved sequence termed the IAP binding motif (IBM). This IBM was capable of binding to the core of the BIR domains, displacing caspases or preventing them from binding and therefore relieving caspase inhibition (Vaux and Silke, 2003).

Mammalian counterparts containing IBM sequences have also been identified, but with a slight variation. These mammalian IBM sequences only become amino terminal after the mitochondrial localization signal has been removed. Apoptosis in *Drosophila* is not controlled by the mitochondrial release of cytochrome c in the same way as mammalian apoptosis. Two of the mammalian IAP binding proteins, Smac and Omi are encoded by nuclear genes and targeted to the mitochondria. They are sequestered in the intermembrane space until they are processed, removing the mitochondria localization sequence and revealing an amino terminal IBM. Once processed and released Smac and Omi can interact with XIAP and interfere with caspase inhibition.

i) Smac/DIABLO

Smac is the best characterized of the IAP inhibitors. It has been shown that Smac can interact directly with a groove on the surface of the BIR-3 domain of XIAP. Smac's IBM (AVPI) displaces a very similar motif (ATPF) on the small subunit of caspase-9 that occupies the same BIR3 surface groove as Smac (Huang et al., 2003). Smac has a weaker interaction with XIAP-BIR2. In fact, Smac does not effectively displace caspase 7 but rather forms a ternary complex with linker-BIR2 and caspase-7. Each of the BIR2 and BIR3 domains alone is not a good binding partner, but because Smac is a dimer it can efficiently antagonize inhibition of both effector and initiator caspases by binding in a 2:1 stoichiometric complex (Huang et al., 2003).

ii) Omi/HtrA2

Omi is a homotrimeric mitochondrial serine protease. It undergoes the same processing as Smac revealing an N-terminal IBM (AVPS) when it is released from the mitochondria. Other than competitive binding for the BIR domains of IAPs, there is not much similarity between Smac and Omi in regards to their physical characteristics and biochemical activities (Yang et al., 2003). Omi can cleave all of the IAPs tested except for Survivin, though it shows the highest cleavage efficiency for c-IAP1. In contrast to Smac's stoichiometric antagonism of IAPs, Omi cleavage is catalytic and irreversible, and is more efficient in inactivating IAPs (Yang et al., 2003).

iii) GSPT1 (G_1 to S phase transition protein)

GSPT1 is a newly characterized human IBM-containing protein that differs from Smac and Omi in that it is processed and released from the endoplasmic reticulum rather than the mitochondria. Proteolytic cleavage of a 69-residue leader sequence exposes the IBM

(AKPF) that can bind to IAPs, inhibit their activity or target them for proteasome-mediated degradation (Hegde et al., 2003). It is not clear yet what triggers GSPT1 cleavage, whether it is sensitive to ER stress or if it has a cell cycle dependent role.

iv) XAF

In contrast to the other three XIAP inhibitors, XAF1 does not contain an IBM motif. Identified through a yeast two-hybrid screen, XAF1 is a nuclear protein that directly interacts with endogenous XIAP. XAF1 sequesters XIAP in nuclear inclusions and reverses the protective effect of XIAP over-expression in cell lines (Liston et al., 2001). Capable of forming seven zinc-finger motifs, XAF appears to undergo alternative splicing leading to at least four distinct mRNA transcripts. XAF has been shown to antagonize XIAP mediated inhibition of caspase-3 activity *in vitro* (Liston et al., 2001).

d) XIAP in signal transduction pathways

XIAP, in addition to its role as an endogenous caspase inhibitor, interacts with several pro-survival pathways in the cell. These multiple roles of XIAP as a direct inhibitor of apoptosis and as a survival co-factor make it a crucial checkpoint in the fate of the cell.

XIAP can bind to the cytoplasmic domain of the type 1 bone morphogenetic protein (BMP) receptor and can affect BMP-regulated dorsal-ventral polarity in a *Xenopus* developmental model (Lewis et al., 2004). Furthermore, XIAP can associate with TGF-beta activated kinase (TAK1) resulting in the synergistic activation of TGF-β-dependent transcription of XIAP (Lewis et al., 2004).

Unlike c-IAP1 and c-IAP2, XIAP is not responsive to NF kappa B mediated transcriptional activation but overexpression of XIAP has been shown to induce NF-κB-dependent transcription (Levkau et al., 2001).

Figure 1-4: XIAP signalling interactions

XIAP interacts with several pro-survival signalling pathways. Serine 87 in BIR1 can be phosphorylated by Akt, which also interacts with p53. XIAP can bind to the BMP1 receptor leading to alterations in development. XIAP also interacts with TAK1 of the TGF-β pathway. No specific domains have been mapped except that the BIR domains are necessary for the interaction. The interaction with TAK1 may also involve TAB1, TAB2, TRAF6 and ILPIP in a complex that activates JNK signaling. The RZF domain is important for signaling to the NF-κB pathway.

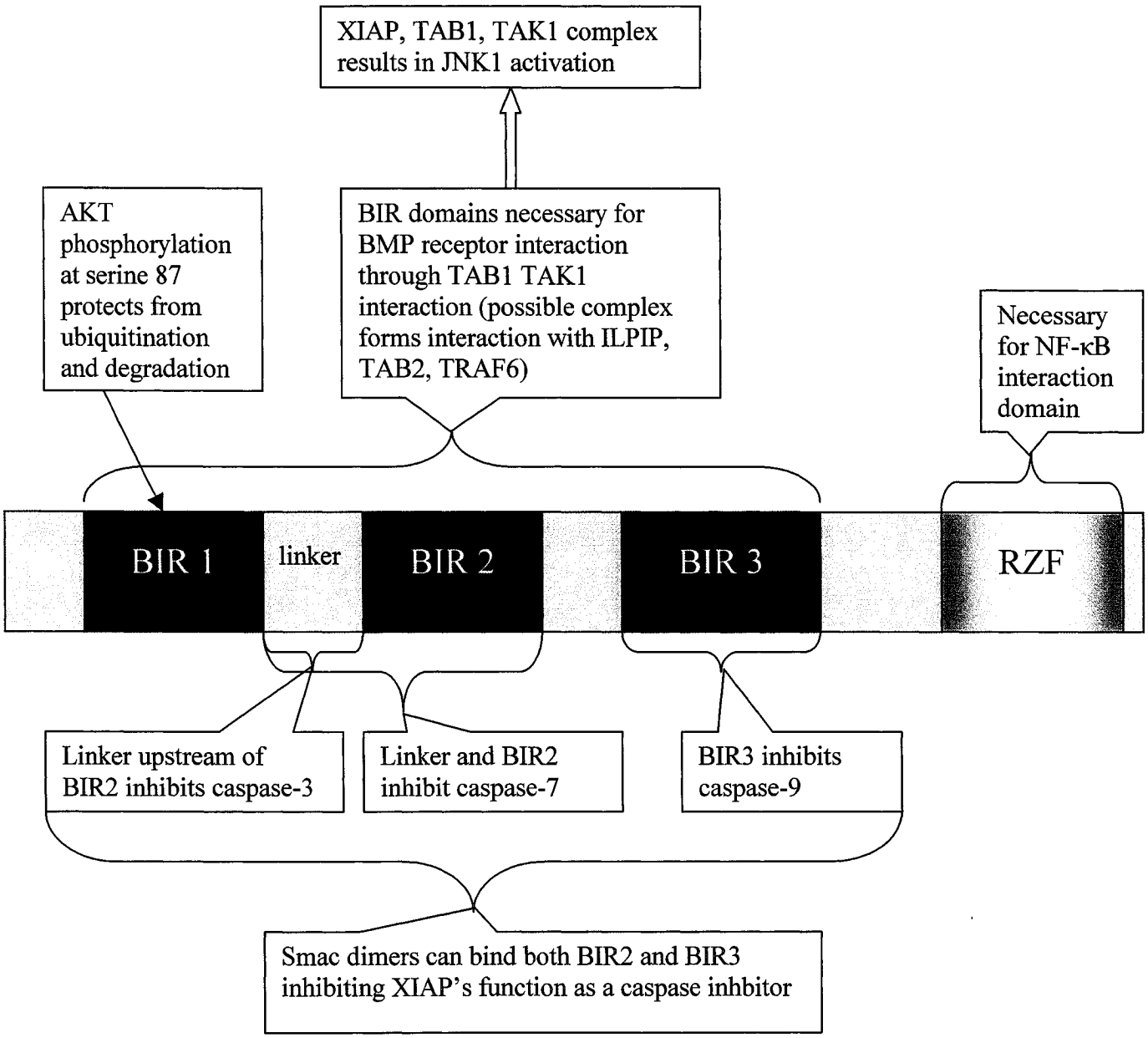
XIAP, TAB1, TAK1 complex results in JNK1 activation
AKT phosphorylation at serine 87 protects from ubiquitination and degradation
BIR domains necessary for BMP receptor interaction through TAB1 TAK1 interaction (possible complex forms interaction with ILPIP, TAB2, TRAF6)
Necessary for NF-κB interaction domain
BIR 1
linker
BIR 2
BIR 3
RZF
Linker upstream of BIR2 inhibits caspase-3
Linker and BIR2 inhibit caspase-7
BIR3 inhibits caspase-9
Smac dimers can bind both BIR2 and BIR3 inhibiting XIAP's function as a caspase inhbitor

Figure 1-4

Another stress responsive pathway, the N- terminal c-Jun kinase (JNK) pathway can be activated by the over-expression of XIAP and is thought to play a role in XIAP's protective effect (Sanna et al., 2002a).

It is not totally clear how XIAP interacts with these pathways but it has been proposed that XIAP may form a complex withTAK1 and its adaptors, TAK1-binding proteins (TAB1 and TAB2), which binds directly to BIR domains, and newly discovered hILP/XIAP-Interacting Protein (ILPIP) (Sanna et al., 2002b). This putative complex and the synergistic activity of TAK1 and TAB1 have been reported to induce JNK1 activation. It is also thought that the activation of NF-κB can result from activation of IκB kinase by TAK1 (Lewis et al., 2004).

XIAP has also been linked to the Akt survival pathway. Phosphorylation of XIAP by Akt protects XIAP from ubiquitination and degradation in response to cisplatin. Auto-ubiquitination of XIAP is also inhibited by Akt (Cheng et al., 2002; Dan et al., 2004). XIAP's interaction with signalling pathways has been mapped to several specific domains and is not dependent on XIAP's caspase inhibitory activity (Lewis et al., 2004). NF-κB activation requires an intact RZF and XIAP's E3 ubiquitin ligase activity. The amino-terminal portion of the loop domain between BIR3 and the RZF and part of BIR3 itself are necessary for XIAP's interaction with the TGF-β pathway while TAB1 and TAK1 require intact BIR domains for binding.

PART 1-5: APOPTOSIS AND CANCER

a) Six essential alterations in cancer

Cancer cells are fundamentally different from ordinary tissue. Hanahan and Weinberg defined six essential characteristics shared by all types of cancer. These characteristics include self-sufficiency in growth signals, insensitivity to anti-growth signals, tissue invasion and metastasis, limitless potential to replicate, sustained angiogenesis and resistance to apoptosis (Hanahan and Weinberg, 2000). At the same time, most anti-cancer drugs and radiation therapy eliminate cancer cells either directly by triggering apoptosis or indirectly by interfering with cellular processes thereby stressing the cell until it undergoes apoptosis (Kaufmann and Vaux, 2003).

b) Effects of inhibition of apoptosis on the progression of tumorigenesis

The effects of inhibiting apoptosis are significant in the transformation of normal cells into neoplastic cancer cells (Hanahan and Weinberg, 2000). Inhibition of apoptosis allows resistance to immune-based destruction, disobeyance of cell cycle checkpoints that would normally induce apoptosis, facilitates growth factor/hormone independent survival, and supports anchorage-independent survival during metastasis. Finally, it reduces dependence on oxygen and nutrients. However, alterations in apoptotic pathways are not sufficient to trigger tumour formation as demonstrated in knockout mice that are missing several key genes in the apoptotic pathway including Fas, FasL, Bak, Bax, Bim, Apaf-1, or caspase-2, -3 or –8 (Kaufmann and Vaux, 2003).

c) Inhibition of apoptosis and chemotherapy resistance

Not only does inhibition of apoptosis impact on tumour formation, it also promotes resistance to cytotoxic anti-cancer drugs and radiation. The majority of cancer therapies, whether directly or indirectly, exert their cytotoxic effect through apoptotic mechanisms (Debatin, 2004). Though there is a high level of redundancy and cross-talk between

apoptotic pathways, mutations or silencing of decision points in these pathways increases the ability of cancer cells to resist treatment and continue to progress. Certain apoptotic regulators such as the IAPs or Bcl-2 family members have been shown to be up-regulated in response to chemotherapy and radiation (Lima et al., 2004).

d) Accumulation of multiple, somatic genetic lesions for malignant progression

Inhibition of apoptosis creates a permissive environment for genetic instability and accumulation of gene mutations. Changes in apoptotic genes do not normally cause cancer by themselves but if a mutation is present and a secondary mutation does occur in a gene that promotes proliferation or alteration of cell cycle checkpoints, the resulting cancer can be much more potent and malignant form. This multiple hits hypothesis is beautifully demonstrated by the bcl-2/myc double transgenic which develops tumours when only days old (Strasser et al., 1993) while bcl-2 transgenics have a 12-18 month latency period (Zhou 2001). This multiple lesion accumulation is also seen in the progression of colon polyps into malignant adenocarcinomas (Sedivy et al., 2000).

PART 1- 6: IAPS AND CANCER

By inhibiting cell death, IAPs provide a mechanism to allow mutated cells to be rescued from apoptosis and to promote malignant transformation. IAPs are not generally considered prototypical oncogenes since IAPs are involved in cancer progression as opposed to initiation (Nachmias et al., 2004). Nevertheless, the inhibition of apoptosis by IAPs does play an important role in tumorigenesis and IAPs have been shown to be upregulated in large variety of cancer cells.

a) Evidence that the IAPs participate in tumorigenesis

i) HIAP1/MLT fusions

Chromosomal translocations in cancer have become fertile ground for discovering new apoptosis regulatory genes including Bcl-2 and Bcl-10. A newly characterized translocation t(11;18) in mucosa-associated lymphoid tissue (MALT) lymphoma generates a fusion protein. The fusion protein consists of HIAP1/c-IAP2 and MALT1, a newly characterized gene containing a death domain, two immunoglobulin-like domains and a caspase-like domain (Dierlamm et al., 1999). The HIAP1-MLT fusion protein can induce NF-κB activation. A positive feedback loop is thus created because the HIAP1-MLT fusion protein is expressed from the NF-κB inducible HIAP1 promoter (Hosokawa et al., 2004). The fusion protein also exhibits anti-apoptotic functions when expressed in cells exposed to UV or etoposide. The HIAP1-MLT fusion protein also binds to IAP inhibitors, Smac and Omi, as well as TRAF2 (Hosokawa et al., 2004). The distinctly anti-apoptotic properties of the fusion protein and the presence of HIAP1 are important evidence of the IAPs contribution to the initiation of cancer.

ii) XIAP and other IAPs are over-expressed in tumour cell lines and contribute to chemotherapy resistance.

XIAP is highly over-expressed in many tumour cell lines of the NCI panel (Fong et al., 2000). Over-expression of XIAP in chemotherapy sensitive pancreatic tumour cell line dramatically increased resistance to apoptosis after treatment with TRAIL or Fas (Trauzold et al., 2003). XIAP has also been shown to contribute to cisplatin resistance in human ovarian cancer (Li et al., 2001) and prostate cancer cells (Amantana et al., 2004). In human breast cancer, an NF-κB induced increase in XIAP expression caused a remarkable resistance to apoptosis induced by paclitaxel, adriamycin, and beta-lapachone (Lin et al.,

2004). In renal cell carcinomas, there is an increase in XIAP protein levels between early and advanced tumour stages (Yan et al., 2004).

Often several of the IAPs will be upregulated in cancer cell lines. Overexpression of survivin or XIAP attenuated the apoptosis induced by roscovitine and TRAIL in glioma cells (Kim et al., 2004). Resistant pancreatic carcinoma cell lines show strongly elevated levels of c-IAP2, XIAP and survivin (Trauzold et al., 2003). Significantly elevated levels of Survivin mRNA and slightly elevated levels of other IAP family members have been found in esophageal cancer (Nemoto et al., 2004).

b) Strategies to inhibit XIAP expression

From a therapeutic perspective, reducing IAP expression provides the potential not only to improve the efficacy of chemotherapy and radiation by removing resistance to apoptosis but also to slow the growth and progression of tumours. As endogenous inhibitors of apoptosis, IAPs are ideal targets for down-regulation and both XIAP and Survivin have been identified as promising targets in cancer therapy.

i) Silencing through anti-sense

Based on its high expression in a variety of cancer cell lines, the down-regulation of XIAP has been targeted to enhance sensitivity to chemotherapeutics and to slow tumour progression. Anti-sense therapy has proven effective in a wide variety of cancer cell lines including breast (Lin et al., 2004), bladder (Bilim et al., 2003), lung (Hu et al., 2003) and leukemia (Carter et al., 2003). Anti-sense XIAP has anti-tumour establishment activity in xenograft models of non-small cell lung cancer (NSCLC). It can also work synergistically with vinorelbine (VNB) to significantly reduce the rate of tumour establishment and increase anti-tumour activity over that obtained with anti-sense or VNB alone (Hu et al.,

2003). Most recently, clinical trials to test anti-sense XIAP therapies for treatment of cancer have been established in the UK.

ii) RNAi

RNAi has also proven to be a very effective tool in silencing XIAP. In breast cancer cell lines, down-regulation of XIAP by RNAi enhances the effects of etoposide and doxorubicin (Lima et al., 2004). Small interfering RNA (siRNA) targeted to XIAP overcame resistance in ceramide-resistant human glioma cells (Hatano et al., 2004). TRAIL resistance was overcome in melanoma cell lines by interfering with expression of inhibitors of apoptosis using RNAi (Chawla-Sarkar et al., 2004).

iii) Small molecule inhibitors of XIAP

Smac screening assays have been developed to search for small molecule inhibitors of XIAP that could be developed into drugs (Glover et al., 2003; Kipp et al., 2002). The first compound to be discovered by this method was embelin, a Japanese Ardisia herb, which has been identified as a small molecular weight inhibitor that binds to XIAP BIR3 with an affinity similar to Smac (Nikolovska-Coleska et al., 2004).

Another screening assay has been developed based on the reversal of XIAP mediated inhibition of caspase-3. This method has identified a class of polyphenylureas with XIAP-inhibitory activity (Schimmer et al., 2004). These compounds have been reported to directly induce apoptosis of many types of tumour cell lines in culture, and sensitize cancer cells to chemotherapeutic drugs. Peptides have also been identified that inhibit XIAP and may be used to develop anti-cancer drugs (Tamm et al., 2003).

Phenoxodiol, a novel nontoxic drug, has been demonstrated to control FLIP/XIAP function and has the potential to eliminate tumour cells through Fas-mediated apoptosis.

Ovarian cancer cells that are resistant to conventional chemotherapy, undergo apoptosis following phenoxodiol treatment (Kamsteeg et al., 2003).

b) Blocking XIAP function using endogenous inhibitors

i) Smac antagonizes IAPs and works with TRAIL to enhance tumour apoptosis

The ability of Smac to efficiently relieve caspase inhibition has been exploited in the synthesis of Smac peptides containing the conserved amino terminal IBM. Smac peptides seem to enhance the pro-apoptotic effects of drug doses that are themselves minimally toxic to cancer cells (Arnt and Kaufmann, 2003). There also appears to be a synergy between Smac and TRAIL. Smac peptides have been found to enhance the ability of TRAIL to reduce the size of glioblastomas *in situ* (Fulda et al., 2002). Another group showed the same effect using adenoviral infection with Smac. They found that Smac antagonizes the IAPs in hepatocellular carcinoma tumour cells and enhances tumour cell death induced by TRAIL (Pei et al., 2004).

ii) XAF1: candidate tumor suppressor

Surprisingly, though XAF1 mRNA expression is widespread throughout normal tissue, its expression in a majority NCI 60 panel of cancer cell lines is low to absent making it a candidate tumour suppressor (Liston et al., 2001). An interferon stimulated gene, XAF1 augments TRAIL induced apoptosis in melanoma cell lines (Leaman et al., 2002). XAF1 has also been found to be silenced by hypermethylation in gastric carcinoma (Byun et al., 2003).

PART 1-7: HYPOTHESIS

Inhibition of apoptosis in and of itself does not generally cause spontaneous cancers (Kaufmann and Vaux, 2003). However, inhibition of apoptosis is an important factor in

the progression of tumorigenesis. Many types of cancer have significant alterations in their apoptotic machinery. XIAP is highly over-expressed in many tumour cell lines and primary tumour biopsy samples and yet there is little direct evidence of the role XIAP plays in tumour establishment, growth, metastasis, and resistance to chemotherapy *in vivo* (Hu 2003).

I propose to test the hypothesis that constitutive XIAP over-expression will manifest itself as enhanced tumour formation rates in combination with established human oncogenes. I therefore created a line of transgenics which express XIAP under the control of the Ubiquitin C promoter. The ensuing resistance to apoptosis is thus predicted to create an environment where other carcinogenic events will complement the over-expression of XIAP to cause these mice to be more susceptible to cancer.

PART 1-8: STATEMENT OF PURPOSE AND OBJECTIVES

Statement of purpose

The purpose of this project is to establish and characterize UbiC-6myc-XIAP transgenic mice and to observe the changes seen in transgenics with a known oncogene or in the absence of a known tumour suppressor. These two different models will be informative in characterizing the role of XIAP in tumorigenesis.

Objective 1: Establishing a transgenic mouse colony

The colony of transgenic mice was bred to create both a homozygous high expression line and a heterozygous line on a pure C57BL6 background. Genotyping by Southern blot and PCR were done to establish transmission of the transgene to offspring. RNA expression was profiled and protein expression was characterized in a variety of tissues.

Objective 2: To determine if XIAP over-expression has any effects on development

Embryos were analyzed for gross morphology at four different stages in development with an emphasis on interdigital tissue apoptosis. Neuronal development was also analyzed for any changes particularly supernumerary neurons that would indicate a lack of developmental apoptosis.

Objective 3: Validation of transgene function *in vitro* and *in vivo*

Two primary cell types were analyzed for protection from apoptosis *in vitro*. Triggers included exposure to both the intrinsic and extrinsic pathway as well as general cellular stress. An *in vivo* injury model of streptozotocin induced pancreatic beta cell apoptosis was used to evaluate differences between transgenic and wildtype mice.

Objective 4: To determine if over-expression of XIAP has any effects on tumorigenesis with known oncogenes.

The model used to determine if XIAP is involved in tumorigenesis involved the over-expression of the c-myc oncogene, which is involved in proliferation.

CHAPTER 2: MATERIALS AND METHODS

PART 2-1: Creation of transgenics

The transgenics were created by microinjection of the construct that consisted of the Ubiquitin C promoter fused to a 6-myc epitope tag fused to the amino terminal of the human XIAP coding region. The carboxyl terminal was fused to a polyadenylation signal. The construct was microinjected into the male pronucleus of the zygotes by the lab of Rashmi Kothary.

Breeding protocol for backcrossing and creation of homozygotes

All animals were housed in the University of Ottawa Animal Care and Veterinary Services facility at the Roger Guindon Campus. Breeding took place within the facility under breeding protocol BMI-35 and CHEO-74.

Genomic DNA Isolation

Genomic DNA was isolated from tails at weaning (Laird et al 1991). Tails are digested for 12 to 18 hours with shaking at 55°C in 0.5 ml of lysis buffer (100 mM Tris.HCl pH 8.5, 5 mM EDTA, 0.2% SDS, 200 mM NaCl, 100 ug Proteinase K/ml). After lysis, the tail mixture was spun at 13 000 rpm for 5 minutes and a phenol/chloroform extraction was performed (Current Protocols in Molecular Biology). Briefly, an equal volume of purification grade phenol/water/chloroform (Applied Biosystems) is added to the isolated supernatant and mixed. The mixture was centrifuged for 10 minutes at 13 000 rpm and the aqueous layer was removed. The phenol/water/chloroform extraction was repeated on the aqueous layer.

A chloroform extraction was then performed (same as above except chloroform added in place of phenol/water/chloroform). An equal volume of isopropanol was added and mixed then centrifuged for 15 minutes at 13 000 rpm. The supernatant was aspirated and the pellet was re-suspended in 250 µl of 70% ethanol. The tubes were incubated at room temperature for 10 to 15

minutes, centrifuged at 13 000 rpm for 10 minutes, the pellet was dried and re-suspended in 50 µl of TE (Tris EDTA) buffer and stored at -20°C. The DNA concentration was determined using a Cary 50 Bio UV visible spectrophotometer.

Southern Blot

5 µg of genomic DNA was digested with *EcoR*1 and *BamH*1 at 37°C for 12 to 18 hours and loaded onto a 1% agarose gel in TAE buffer and run at 70 V. The gel was transferred for 12-18 hours onto nylon membrane (Pall B Biodyne) using 0.4 N NaOH transfer solution and Whatman paper wick. The membrane was neutralized for 15 minutes with shaking in 0.2 M Tris pH 7.5 containing 2 X SSC and baked for 30 minutes at 80°C. The membrane was pre-hybridized in 10 % PEG solution (10% PEG, 1.5X SSPE, 7% SDS, 12.5 mL deionised water) for 1.5 hours at 65°C. The XIAP coding region probe was labelled with $dCTP^{32}$ with a Rediprime labelling kit and Nick column. Non-specific hybridization was blocked using salmon sperm DNA and the membrane was hybridized for 12 to 18 hours at 65° C. The membrane was washed with increasing stringency and temperature ranging from 2X SSC at room temperature to 0.1X SSC at 65°C. Membranes were exposed to film for 24 to 72 hours at - 80°C and then developed.

Phosphor Imager Analysis

Membranes were incubated with a phosphor screen (Kodak) for 24 to 72 hours and band intensity was quantified using the Storm phosphor-imager and Image Quant 5.1 software. Two separate transgenic bands were compared in intensity to endogenous bands within a sample. Ratio of 2.0 or greater was determined to be homozygous, ratios between 1.0 and 2.0 heterozygous and lanes with no transgenic bands were determined to be wildtype. Ratios of less than 1.0 or with a large discrepancy between the two bands were classified as indeterminate.

PCR for genotyping

2 µl of genomic DNA isolated from the tail was added to 5 µl of 10X PCR buffer, 5 µl of 2 mM dNTPs, 2 µl of 50 mM $MgCl_2$ and the following primers.

Table 2-1 Primer pairs used for genotyping transgenic mice by PCR

Gene Name	Forward primer	Reverse Primer
Human XIAP	5'-CAGGATCCATGTCTGATGCTG TGAGTTCTG- 3'	5'-GACTCGAGCTAAGTAGTTCTT ACCAGACACTCCTCAAG–3'
c-myc	5'-CCAAAGGTTGG CAGCCCTCATGTC-3'	5'-AGGGTCAAGTTGG ACAGTGTCAGAGTC-3'
P53	5'ACACACCTGTAGCTCCAGCAC3'	5'AGCGTCTCACGACCTCCGTC3'
P53 (null) 3rd primer	5'-GTGTTCCGGCTGTCAGCGCA-3'	

A 30µl mineral oil overlay was added to each tube. Using the Perkin Elmer DNA Thermal Cycler 480 the DNA was denatured for 10 minutes at 94°C and then amplified for 35 cycles (50°C for 2 minutes, 72°C for 1 minute and 94°C for 2 minutes) then annealed at 72°C for 10 minutes and stored at 4°C. Results were visualized by loading 8 µl of amplified sample DNA with 2µl of 5x loading dye and running at 80 V on 1% agarose gel with TAE buffer.

RNA Isolation

Mice were euthanized by intraperitoneal injection 0.1 ml of Somnitol. The spleen, kidney, liver, thymus, heart, lung, pancreas and brain were removed and placed directly into triazol (Gibco/BRL). Tissues were homogenized for 1 minute using the Polytron Pro 200 homogenizer. 1 ml of homogenate was removed and placed into Eppendorf tubes. 200 ul of chloroform was added and mixed then centrifuged for 15 minutes at 60 000 g at 10°C. The aqueous layer was removed and added to 0.5 mL of isopropanol and incubated at room temperature for 10 minutes. The mixture was then centrifuged for 10 minutes at 10 °C for 60 000 g and the supernatant was discarded. 1 ml of 75% ethanol was added, mixed and centrifuged at 10 °C for 5 minutes. The supernatant was discarded and the pellet dried and re-dissolved in RNase free water (Sigma). If

further purification was needed an Rneasy Mini Kit (Quiagen) was used. The RNA was quantified using the spectrophotometer and stored at -80°C.

Taqman RT-PCR

The procedure followed was included with the Taqman EZ RT-PCR kit (Applied Biosystems). Briefly a master mix was prepared with the following reagents: 31.625% Rnase-free water, 25% 5X EZ-Buffer, 15% 25 mM Mn(Oac), 15% dNTP 10 mM, 5% rTh polymerase, 1.25% Amperase UNG, 50 nM RGAPDH probe, 100 nM RGAPDH forward primer, 100 nM RGAPDH reverse primer. GAPDH was used as a control for the reaction. Reactions were completed with the following primer pairs and probes.

Table 2-2 Primer pairs used for quantitative RT-PCR analysis of endogenous and transgene-encoded IAP levels

Gene name	Forward primer	Reverse Primer
Human XIAP	5'GGTGATAAAGTAAAGTGCTTTCACTGT 3'	5'TCAGTAGTTCTTACCAGACACTCCTC A3'
Mouse XIAP	5'-CTGAAAAAACACCACCGCTAA-3'	5'-CTAAATCCCATTCGTATAGCTTCTTG'3'
Mouse HIAP1	5'-AAGTTCAAGCTGGCTATCCTCATC-3'	5'-ACGATTGCTGCGTCTGCA-3'
Mouse HIAP2	5'-TACGGATGAAGGGTCAGGAGTTT-3'	5'-TCTGTAGGGTCAGCATTTTCTTCTC-3'

Table 2-3 Probes used for quantitative RT-PCR analysis of endogenous and transgene-encoded IAP levels

Gene name	Probe
Human XIAP	5'(FAM) CAACATGCTAAATGGTATCCAGGGTGCAAATATC (TAMRA)-3'
Mouse XIAP	5'-(FAM) AATCGATGATACCATCTTCCAGAATCCTATGGTG (TAMRA)-3'
Mouse HIAP1	5'-(FAM) TTGAGCAGCTATTATCTACGTCAGACTCCCCA (TAMRA)-3'
Mouse HIAP2	5'-(FAM) CTTCTTGAGCAGCTGTTGTCCACTTCAGACA (TAMRA)-3'

For each reaction, the concentration of the IAP probe was 200 nM and the forward and reverse primers were each 600 nM. 2.5 ug of DNA were run for each sample. The analysis of results was done within the Taqman program and then transferred into Microsoft Excel. Results were quantified in relation to rodent GAPDH controls.

Protein Extraction

Mice were euthanized by intraperitoneal injection of 0.1 ml of Somnitol (Animal Care and Veterinary Services) and liver, kidney, pancreas, heart, lung, thymus, brain and retinas were removed and placed on ice. Organs were weighed and 5 volumes of homogenizing buffer (10 mM Tris 6.8, 150 mM NaCl, 2 mM $MgCl_2$, 1 mM PMSF) were added. The organs were homogenized using the Polytron (see above in RNA extraction) for 1 minute. An equal volume of homogenizing buffer with 2% SDS was added and samples were boiled for 20 minutes. Samples were sonicated and 1 mL of homogenate was removed and centrifuged at 4°C for 10 minutes at 130 000 rpm. The supernatant was removed and centrifuged again for 15 minutes at the same speed and temperature. The supernatant was removed and stored at -20°C.

Western Blot

10 µl of sample with 5 µl of 2X Laemmli protein sample buffer (Bio-Rad) was loaded onto 10% SDS-PAGE separating gel (10% bisacrylamide, 375 mM Tris-HCl pH 8.8, 0.1% SDS, 0.05% ammonium persulfate) and an upper stacking gel (4% acrylamide/0.1% bisacrylamide, 125 mM Tris-HCl pH 6.8, 0.1% SDS, 0.05% ammonium persulfate) with Precision Plus dual colour protein standards (BIO-RAD) and run at 80 V. Proteins were transferred to PVDF membranes using a semi-dry Hoeffer semiphor transfer apparatus at 20 V for 25 minutes. Membranes were blocked overnight at 4°C in 5% skim milk in PBST (1X PBS with 0.1% Tween-20). Primary antibodies were incubated for 1 hour with shaking at room temperature. Antibodies used included polyclonal anti-XIAP (1:2000) made in house and monoclonal anti-c-myc (1:2000)

from Sigma. Primary and secondary antibodies were diluted in 5% skim milk in PBST. Blots were washed in PBST and incubated with secondary antibodies for 1 hour at room temperature. Secondary antibodies were horseradish peroxidase conjugated anti-rabbit IgG (1:2000) and anti-mouse IgG (1:5000) from Amersham. Blots were washed again and incubated with ECL plus reagent (Amersham) for 5 minutes at room temperature and exposed to film for 30 seconds to 10 minutes.

Perfusion, Freezing and Cryostat sectioning

Mice were anaesthetized using 0.1 ml of Somnitol and perfused with 10 ml of saline and 10 ml of 4% PFA in PBS through the left ventricle using a 27 gauge butterfly needle. Organs were removed, fixed overnight in 4% PFA and transferred into 10% sucrose for 24-48 hours. Organs were embedded in OCT freezing medium (Tissue Tek), frozen on dry ice and stored at -80°C. 10 –16 μm sections were cut using a Microm HM 500 vacutome cryostat and mounted onto Superfrost Plus (Fisher) slides. Slides were stored at -20°C

Immunofluorescence

Slides were thawed to room temperature and sections were circled with a hydrophobic barrier using a Pap pen (ESBE Scientific). Slides were boiled intermittently in the microwave in citric acid pH 6.0 (2.1 g in 1.0L) for 10 minutes for antigen exposure. Slides were blocked (blocking solution: 5% goat serum, 0.3% Triton-X in PBS) for 30 minutes at room temperature. The slides were incubated with primary antibody (0.3% Triton-X, 1% goat serum, primary antibody (see table) diluted in PBS) for 12 to 18 hours at 4°C.

Table 2-4 Table of primary and secondary antibodies used in immunofluorescence including the dilutions and the company from which the antibodies were purchased

Primary Antibody Immunofluorescence	Source	Dilution	Secondary Antibody	Source	Dilution
Polyclonal anti-XIAP	Made in lab	1:500	Anti-rabbit Alexa Fluor 488	Molecular Probes	1:200

Monoclonal anti-myc	Sigma	1:200	Anti-mouse Alexa Fluor 488	Molecular Probes	1:200
Monoclonal NeuN antibody (A60)	Dr. McBurney	1:200	Anti-mouse Alexa Fluor 488	Molecular Probes	1:200

Slides were washed with PBS and incubated with secondary antibody (0.3% Triton-X, 1% goat serum, secondary antibody (see table) diluted in PBS) for 3 hours at room temperature without exposure to light. Slides were washed with PBS, mounted using Prolong anti-fade mounting media (Molecular Probes). Sections were examined on a Zeiss Axiophot fluorescent microscope. Images were integrated and captured using Northern Eclipse software. Slides were stored in the dark at -20°C.

Immunohistochemistry

Slides were quenched with 0.3% hydrogen peroxide in PBS, washed in PBS and incubated in blocking solution (2% goat serum, 0.3% Triton-X, 5% BSA in PBS) for 20 minutes. The slides were washed in PBS and incubated in primary antibody (see chart for antibody dilutions) for 1 hour.

Table 2-5 Table of primary and secondary antibodies used in immunohistochemistry including the dilutions and the company from which the antibodies were purchased

Primary Antibody Immunohistochemistry	Source	Dilution	Secondary Antibody	Source	Dilution
Monoclonal anti-cleaved caspase-3	Cell Signalling	1:50	Anti-mouse IgG	Cell Signalling	1:200
Anti-insulin	Dako	Diluted by manufacturer	Anti-guinea pig IgG	Vector	1:250

The slides were washed again in PBS and incubated with secondary antibody (0.3% Triton-X, 1% goat serum, and appropriate secondary antibody diluted in PBS) for 30 minutes. The slides were washed a third time in PBS then signal was detected using an avidin biotin conjugated system (ABC Kit from Vector) and visualized using DAB (Vector). Slides were mounted in

Vectashield mounting media (Vector) and cover slips were sealed around the edges with nail polish. Slides were then examined using bright field and phase contrast microscopy on a Zeiss Axiophot microscope. Images were captured using Northern Eclipse microscopy analysis software. Slides were stored at room temperature.

Part 2-2: Analysis of Embryogenesis

Embryo collection and photography

Timed breedings were established and females were monitored for plugs. Time points were determined under the assumption that conception occurred 0.5 days before a plug was detected. Litters from heterozygous X wild-type crosses were sacrificed at day 10, 12, 15, 17.5 of gestation. Embryos were removed and placed into PBS under a dissecting microscope and photographed at different magnifications depending on their size using a Nikon Coolpix 4500 digital camera. Tails (for days 12-17.5) or placental material (Day 10) were removed and used for genotyping. The embryos were fixed in 4% PFA in PBS overnight and then switched into 10% sucrose in PBS for 24-72 hours. Embryos were embedded in OCT and frozen on dry ice. Sections were collected on the cryostat by the method described above.

NeuN cell counts

Sections of the cerebellum, cortex, and olfactory lobes from transgenic and wildtype brains were probed with NeuN antibody (Dr. McBurney) by the method described in the immunofluorescence section. Different areas of the brain including anterior and posterior cortical regions, cerebellum and olfactory lobes were compared for neuronal cell counts. Northern Eclipse software including a macro developed by Nigel Banner (Zeiss) was used to count every neuron that fluoresced in each image. Size exclusion was set so that objects under 5

pixels in size were not counted. Threshold intensity was optimized for each region of the brain. It was set at 80 for the cortex, 100 for the dentate gyrus and 118 for the cerebellum. At least ten different slides were counted for each section.

Part 2-3: Primary cell cultures and *in vivo* models

Mouse Embryo Fibroblasts –culturing conditions and drug treatments

Timed breeding was determined in the same manner as for the embryo panel. Mothers were sacrificed at day 13.5 of gestation. Each embryo was removed and placed into a separate 10 cm plate in PBS. The heads, limbs and liver were removed and used for genotyping. The remaining embryonic tissue was minced and trypsinized. The resulting cell mixture was placed into a 50 mL conical tube, allowed to settle for 2 minutes and the supernatant was mixed with MEF media (Dulbecco's Modification of Eagles Medium (DMEM), 1% L-glutamine, 1% non-essential amino acids, 10% fetal calf serum). The cells were then centrifuged at 1000 rpm at 10°C for 5 minutes. The pellet was resuspended in MEF media and the cells were left to grow overnight in T-150 flasks in a 37°C incubator with 5% CO_2. The media was changed and the MEFs were frozen in liquid nitrogen.

MEFs were thawed and passaged twice before experiments were performed. 1×10^3 cells were cultured in 100 μL of media in each well of a 96 well plate. Etoposide was diluted in DMSO and each well received the same liquid volume. The doses of etoposide administered were 0, 1, 2, 5, 10, 25, 50, 75, 100, and 250 μM. Each MEF line received each dose in triplicate. Viability was assessed using a WST-1 metabolic assay (see below).

Hepatocyte –Isolation and culturing conditions

Mice were given an intraperitoneal injection of 0.1 mL of Somnitol. Once the mouse was unresponsive a catheter was threaded into the inferior vena cava and the liver was perfused with 50 mL EGTA (8.3g/L NaCl, 0.5 g/L KCl, 2.4g/L HEPES, 190 mg/L in distilled water, pH 7.4)

and then 50 mL collagenase (0.5 mg/mL collagenase in 100 mL HEPES II buffer (3.9 g/L NaCl, 0.5 g/L KCl, 0.7 g $CaCl_2$–$2H_20$, 2.4 g HEPES in distilled water, pH 7.6)). The perfused liver was then put into 10 mL Williams Media E in a 10 cm plate. Cells were centrifuged for 6 minutes at 850 rpm in a 50 mL conical tube. The supernatant was discarded and the cells were re-suspended in 40 mL of media. The centrifugation step was repeated and then the cells were resuspended in complete Williams Media (10% FBS, 2% antibiotic-antimycotic mixture, 0.2% gentamicin, 1% L-glutamine in Williams Media E) and incubated at 37°C with 5% CO_2. Cells were plated at 10 million cells per 10 cm plate.

WST-1 viability assays

Cells were assessed for viability after treatment with apoptotic triggers *in vitro*. Media was removed and cells were washed with PBS. 10% WST-1 cell proliferation reagent (Roche) diluted in media was added to each well. Cells were incubated at 37°C. After 1, 2, 3, and 4 hours, 100 μL from each well was aliquoted into a 96 well plate. The absorbance at each time point was evaluated at wavelengths of 450 nm and 600nm on the Spectra Max 340 platereader (Molecular Devices).

Islet Isolation

Mice were euthanized by 0.2ml of Somnitol delivered by intraperintoneal injection. The abdomen was swabbed with 70% ethanol and cut open. The pancreas was excised and placed into a 35 mm dish. A 3 ml syringe was filled with a Dnase/ Collagenase P solution (0.1 mg/ml DNase (Invitrogen), 20 mg/ml Collagenase P (Sigma) supplemented with Hanks Balanced Salt Solution (HPSS)) that was kept at 37 ˚C in water bath. The DNase/Collagenase P solution was injected into the pancreas and incubated for 30 minutes at 37 ˚C in an incubator. The pancreas was broken apart by pipetting and the islets were picked under a dissecting microscope and stored in HBSS on ice. Two rounds of islet

picking were completed. The islet mixture was centrifuged at 130 000 rpm for 5 minutes and the supernatant was discarded. The pellet was kept at –20 °C and used for western blotting.

Glucose Tolerance Test

Mice were fasted for a four-hour period and given a bolus injection of 2g/kg of glucose. Each dose was adjusted to the mouse's body weight as measured on the day of injection. Blood glucose was monitored (as described below), before injection and 15, 30, 60, 90 and 120 minutes post injection. The results of the glucose tolerance test represent 18 animals (6 wildtype and 12 transgenic) and the data presented is the average for each genotype at each time point.

Single high dose streptozotocin treatment and blood glucose measurements

Fasting blood glucose was monitored throughout streptozotocin experiments both pre- and post-injection. Food was taken away for four hours and then the saphenous vein of the hind limb was punctured with an 18-gauge needle. A blood droplet was allowed to form and blood glucose was analyzed using the One Touch Ultra glucometer (Lifescan). Pressure was applied to the site to stop bleeding. A separate test strip was used for each reading. Readings were taken on four sequential days pre-injection and four readings were taken post-injection.

Streptozotocin (Sigma) was given based on a dose of 150 mg/kg. Mice were weighed and each mouse received a dose adjusted to its body weight. Control mice received only the vehicle that consisted of sodium citrate buffer pH 4.5. Streptozotocin was stored at -20°C and not exposed to light. Streptozotocin was only stable in the sodium citrate solution for 15-20 minutes so doses were pre-weighed and only mixed with the vehicle immediately prior to injection. Intraperitoneal injections of streptozotocin or sodium citrate vehicle were administered after a four-hour fasting period. Body weight was monitored every day and subcutaneous injections of saline were given to mice that lost more than 1 g in 24 hours.

Mice were sacrificed after a maximum of 10 days after injection and the pancreas was excised and analyzed by immunohistochemistry. 36 animals (14 wildtype and 22 transgenic) were divided into three separate experimental groups. All results are the pooled averages of all three experiments.

Statistics

Results from the streptozotocin experiments were evaluated for significance using a two-tailed, unpaired Student's t test. Error bars when present on graphs represent the standard error.

Part 2-4: Creation of double transgenics and tamoxifen injection protocol

Breeding of double transgenics

The human insulin promoter (Pins) c-myc tamoxifen inducible estrogen receptor fused (ER^{TAM}) transgenic mice were received from Dr. Gerard Evan and bred with both homozygous and heterozygous transgenic UbiC-6myc-XIAP mice. Six litters of mice were produced from the mating. Offspring were genotyped by PCR (see genotyping by PCR for primers and conditions) for the presence of the c-myc transgene and by Southern blot for the presence of the XIAP transgene. Based on the results of both the PCR and the southern blot, animals were assigned to four categories: myc-/XIAP-, myc+/XIAP-, myc -/XIAP +, and myc+/XIAP+.

C-myc activation by tamoxifen injection

25 mg of 4-hydroxy (4-OH) tamoxifen (Sigma) was suspended in 5 ml of peanut oil under sterile conditions. The mixture was sonicated 4 times for 15 seconds at an amplitude of 25% using a Vibra Cell probe sonicator (Sonics & Materials). Once a homogenous suspension was achieved 0.2 ml of the peanut oil suspension was loaded into a 21-gauge syringe. Five animals of from each of the four genotypes were used for the experiment resulting in 20

mice in total. The mice were given daily intraperitoneal injections of 1mg of 4-OH tamoxifen suspended in 200 μl of peanut oil for six consecutive days. Body weight was monitored daily. Blood glucose readings were taken after a four-hour fast on days 1, 3, and 6 of injections.

Mice were sacrificed by an intraperitoneal injection of 0.1 ml of Somnitol (ACVS) at seven days. Blood glucose readings were also taken on the day of sacrifice. Mice were perfused with 10 ml of saline. Pancreata were removed, immersed in OCT and frozen on dry ice. 10 micron sections were cut on the cryostat as described above. Sections were labelled with hemotoxolyin, phloxine and saffron (HPS) for histology. Sections were also collected and used for insulin immunohistochemistry (see above) and TUNEL analysis (see below).

TUNEL analysis

TUNEL analysis was done using the ApopTag Fluorescein *In Situ* Apoptosis Detection Kit (Serologicals Corporation). Briefly, sections were fixed by incubation in pre-cooled ethanol:acetic acid (2:1) for 5 minutes at -20°C. The sections were then washed in PBS and equilibration buffer was applied and incubated for 10 seconds at room temperature. Terminal deoxynucleotide transferase (TdT) enzyme was added and incubated in a humidified chamber for 1 hour at 37°C. The slides were then incubated with stop/wash buffer for 10 minutes then washed in PBS. Anti-digoxigenin conjugate was added and incubated for 30 minutes at room temperature in the dark. The specimens were washed in PBS and then mounted in Prolong anti-fade. The sections were examined using a Zeiss Axiophot fluorescence microscope. Images were integrated and captured using Northern Eclipse software. Slides were stored at -20°C in the dark.

CHAPTER 3: RESULTS

Part 3-1: Establishment of a transgenic mouse colony

Three different transgenic XIAP over-expressing mouse models have been published to date. The first XIAP transgenic was driven by a thymocyte specific Lck^{pr} promoter (Conte et al., 2001). In this model, thymocytes and T-cells accumulated in lymphoid tissue, T cell maturation was perturbed, and transgenic thymocytes resisted a variety of apoptotic triggers both *in vitro* and *in vivo*. The two additional XIAP transgenic mouse models used neuron specific promoters. Expression of XIAP driven by the neuron specific enolase (NSE) promoter driven XIAP attenuated the effects of MPTP induced toxicity in dopaminergic neurons (Crocker et al., 2003). The Thy 1.2 promoter driven XIAP transgenics showed less damage after transient cerebral ischemia and protection from brain damage due to neonatal hypoxia-ischemia (Trapp et al., 2003; Wang et al., 2004).

All three of the published XIAP transgenics targeted a specific organ or cell type. The purpose of creating the Ubiquitin C promoter driven transgenics was to observe the effects of ubiquitous over-expression of XIAP in all tissues, and during embryogenesis, and to develop an animal model to test whether XIAP directly participates in tumorigenesis.

a) Analysis of transmission of transgene to offspring

i) Founders

Twenty-six candidate founders microinjected with the Ubi-6myc XIAP construct were born. Of the twenty-six potential founders twelve were identified as positive for the transgene when tested by Southern blot as shown in figure 3-1. These results were confirmed by PCR.

Figure 3-1 Detection of the presence of the human XIAP transgene in colony founders

Twenty-six potential founders were genotyped and twelve were positive by Southern blots for the human transgene. Genomic DNA was extracted from tail samples and digested with *BamHI* and *BglII*. The XIAP coding region probe was labeled with P^{32}-dCTP and used for Southern blot analysis. Each founder had a distinct banding pattern though two endogenous bands are visible in every lane. Relative copy number was estimated by setting the least intense band (402) as one and estimating the relative intensity of all other bands as a ratio with that least intense band.

A) Founders 402, 404, 407, 409, 410, 411,412 were positive for the transgene while 403, 405, 406, 408 and 413 were negative

B) Founders 414, 416, 420, 421, 424, and 426 were identified as positive and founders 415, 417,418, 419, 422, 423, and 425 were negative.

C) A schematic diagram of the construct that was used to create the transgenics. The construct consisted of the Ubiquitin C promoter with the 6-myc epitope tag fused to the amino terminus of the human XIAP coding region. The construct also included SV40 splice sites and a poly-adenylation signal.

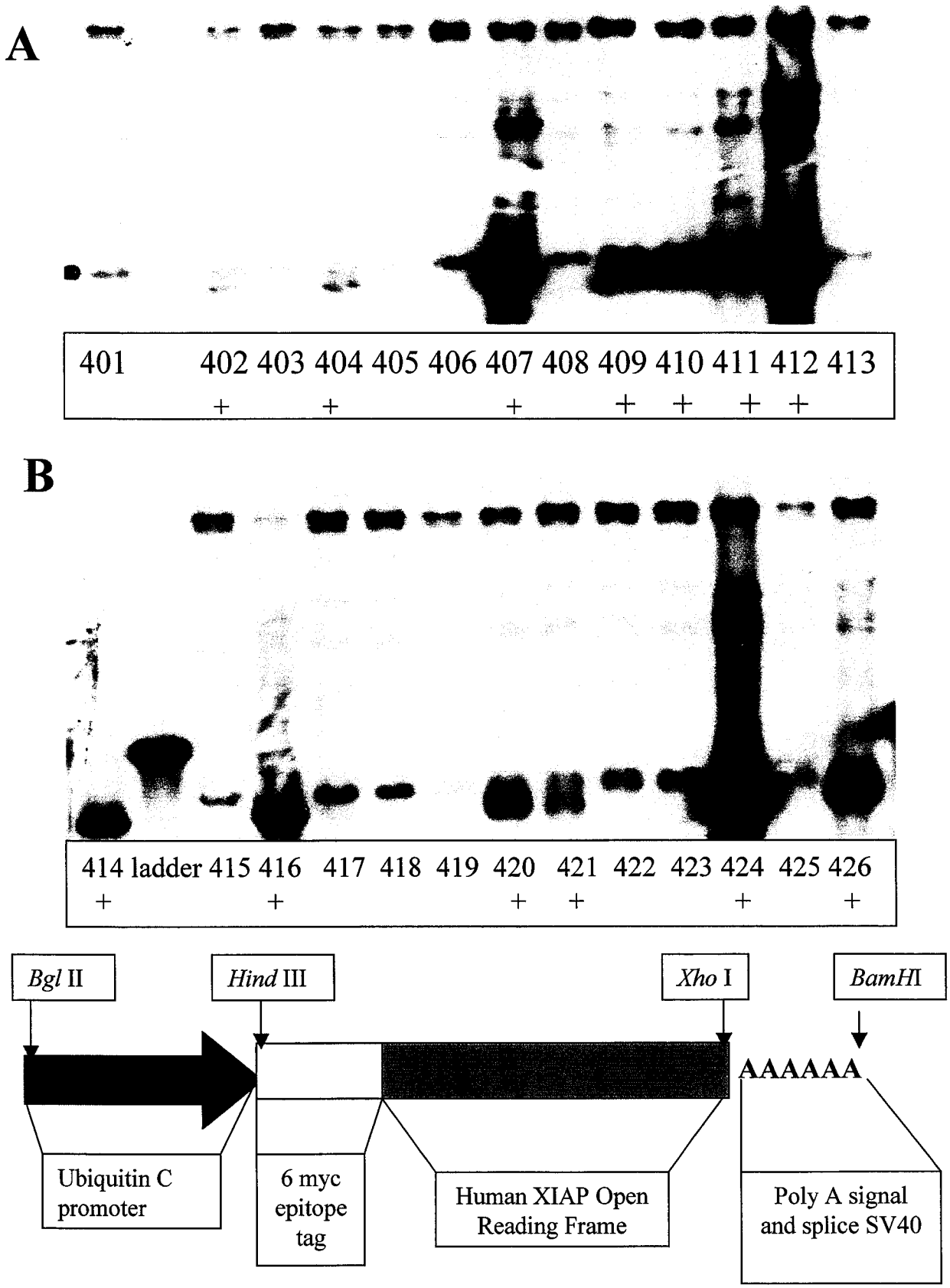
A
401 402 403 404 405 406 407 408 409 410 411 412 413
+ + + + + + +
B
414 ladder 415 416 417 418 419 420 421 422 423 424 425 426
+ + + + + +
C
Bgl II
Hind III
Xho I
BamHI
AAAAAA
Ubiquitin C promoter
6 myc epitope tag
Human XIAP Open Reading Frame
Poly A signal and splice SV40

Figure 3-1

The relative copy number ranged from the lowest intensity band in founder 402 to more than ten times that intensity in the 407 and 411 lines. Two lines, 416 and 426, were chosen as moderate expressers based on their intermediate band intensity relative to 402.

All twelve of the transgenic founders were successful in producing offspring. The transmission rate of the transgene varied widely between lines. All of the offspring from each mouse line was genotyped to verify transgene transmission to the F1 generation. On the basis of Southern blots, the offspring were scored as positive for the transgene or as wild-type littermates that do not carry any copies of the human XIAP transgene. Genotypes were confirmed by PCR.

b) Detection of the presence of transgene-encoded human XIAP protein and profiling of tissue specific expression

Samples including liver, kidney, spleen, pancreas, brain, thymus, lung, and heart were analyzed by Western blot to determine the protein expression of the human XIAP transgene. The levels of XIAP protein expression were compared in littermates that carried the transgene, labelled as transgenic (tg), and those that did not, labelled as wildtype (wt).

A monoclonal anti-c-myc antibody was used to detect the epitope tag of the transgene-encoded protein. All of the transgenic samples tested expressed the transgene-encoded protein while none of the wildtype samples contained any anti-c-myc reactive proteins at 67 kDa as shown in figure 3-2. This confirmed the accuracy of the genotyping and the ubiquitous nature of protein expression. There was some cross-reactivity at lower molecular weights.

Figure 3-2 Detection of the transgene-encoded protein by western blot using a monoclonal antibody specific the transgene-encoded c-myc epitope tag and a polyclonal anti-XIAP antibody.

A panel of organs from a mouse from the 402 line was tested for the expression of the transgene-encoded protein. The Western blots include tissues harvested from a high expression transgenic mouse and its wildtype littermate. For each tissue type tested samples from the transgenic animal (tg) are paired with samples from the wildtype animal (wt).

A) The western blot was probed with monoclonal anti-myc, which detects the myc tagged transgene encoded protein at the molecular weight of 67 kDa. From left to right, samples on the membrane include liver, kidney, spleen and pancreas.

B) The western blot was also probed with monoclonal anti-c-myc and samples on the membrane include brain, thymus, lung and heart.

C) The western blot was probed with polyclonal anti- XIAP. Transgene encoded human XIAP migrates at the molecular weight of 67 kDa. The endogenous mouse XIAP migrates at the molecular weight of 55 kDa. From left to right, samples on the membrane include liver, kidney, spleen and pancreas.

D) The western blot was also probed with polyclonal anti-XIAP and samples on the membrane include brain, thymus, lung and heart.

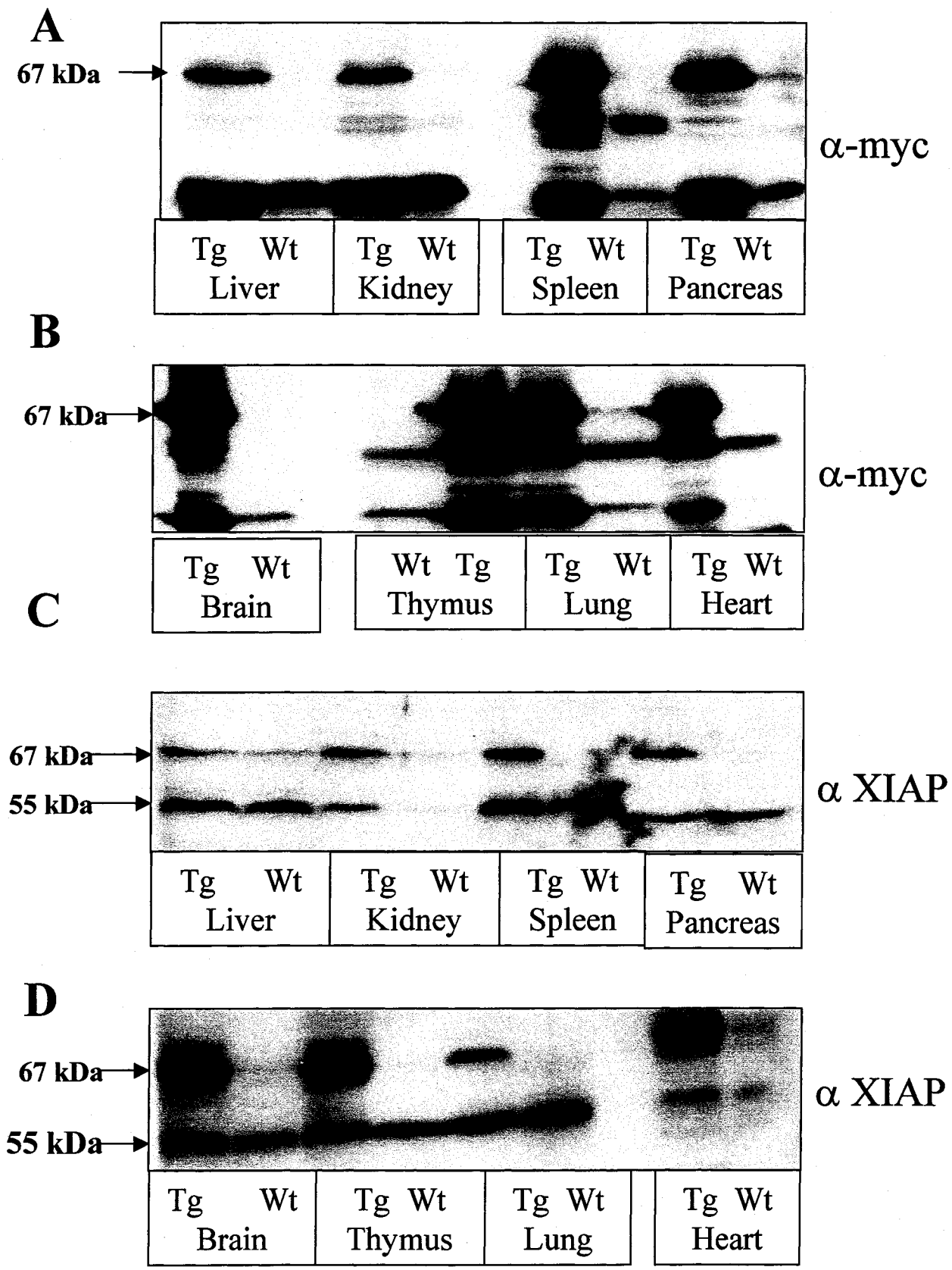
A
67 kDa
α-myc
Tg Wt
Liver
Tg Wt
Kidney
Tg Wt
Spleen
Tg Wt
Pancreas
B
67 kDa
α-myc
Tg Wt
Brain
Wt Tg
Thymus
Tg Wt
Lung
Tg Wt
Heart
C
67 kDa
55 kDa
α XIAP
Tg Wt
Liver
Tg Wt
Kidney
Tg Wt
Spleen
Tg Wt
Pancreas
D
67 kDa
55 kDa
α XIAP
Tg Wt
Brain
Tg Wt
Thymus
Tg Wt
Lung
Tg Wt
Heart

Figure 3-2

Blots were also probed with a polyclonal XIAP antibody that recognizes both the endogenous mouse and the transgenic human form of the protein. It was possible to compare the level of transgene-encoded protein expression to endogenous levels because the transgenic protein migrates at a higher level (65-67 kDa) than the endogenous protein (55-57 kDa) due to the 110 amino acid 6myc epitope tag fused to its amino-terminus (see figure 3-1 for schematic of construct). The polyclonal antibody detected human XIAP in every tissue tested but there was significant variation in transgenic XIAP expression among tissues as shown in figure 3-2. Certain tissues such as thymus and brain expressed the transgenic XIAP protein at a much higher level relative to the endogenous protein than other tissues such as lung. There was a non-specific band detected by the polyclonal antibody at 67 kDa in the wildtype liver sample but the c-myc antibody did not detect it so it was attributed to cross-reactivity.

ii) Analysis of tissue-specific XIAP expression by immunofluorescence

Tissues were analyzed by immunofluorescence using the monoclonal c-myc antibody and the polyclonal anti-XIAP antibody. This was done to establish which cell types within specific tissues express the XIAP transgene. Expression of the c-myc epitope tag was detected in sections of the brain and thymus from transgenic animals as shown in figure 3-3. The pattern of expression within the brain and the thymus confirms the ubiquitous nature of the transgene-encoded protein expression. Expression was seen in all layers of the cortex as well as the hippocampus, dentate gyrus, and cerebellum. In the cortex (shown in figure 3-3a) there is a cell body specific stain but there is also a ubiquitous stain that does not appear to be cell type specific.

Figure 3-3 Analysis of tissue specific XIAP expression using a monoclonal anti-myc antibody to detect the transgene-encoded protein.

Tissues were probed with monoclonal anti-c-myc (1:500), which recognizes the 6-myc epitope tag on the transgene- encoded human XIAP protein. The fluorescent conjugated secondary antibody was Alexa 488 (1:200). Images were captured at 40 times magnification. Sections from the wildtype animal are located on the left and the sections from the transgenic animal are on the right. In all sections the expression of the myc tag is detectable in the transgenic but not in the wildtype animals.
A) Sections from the cortex of the brain
B) Sections from the dentate gyrus.
C) Sections from the thymus.

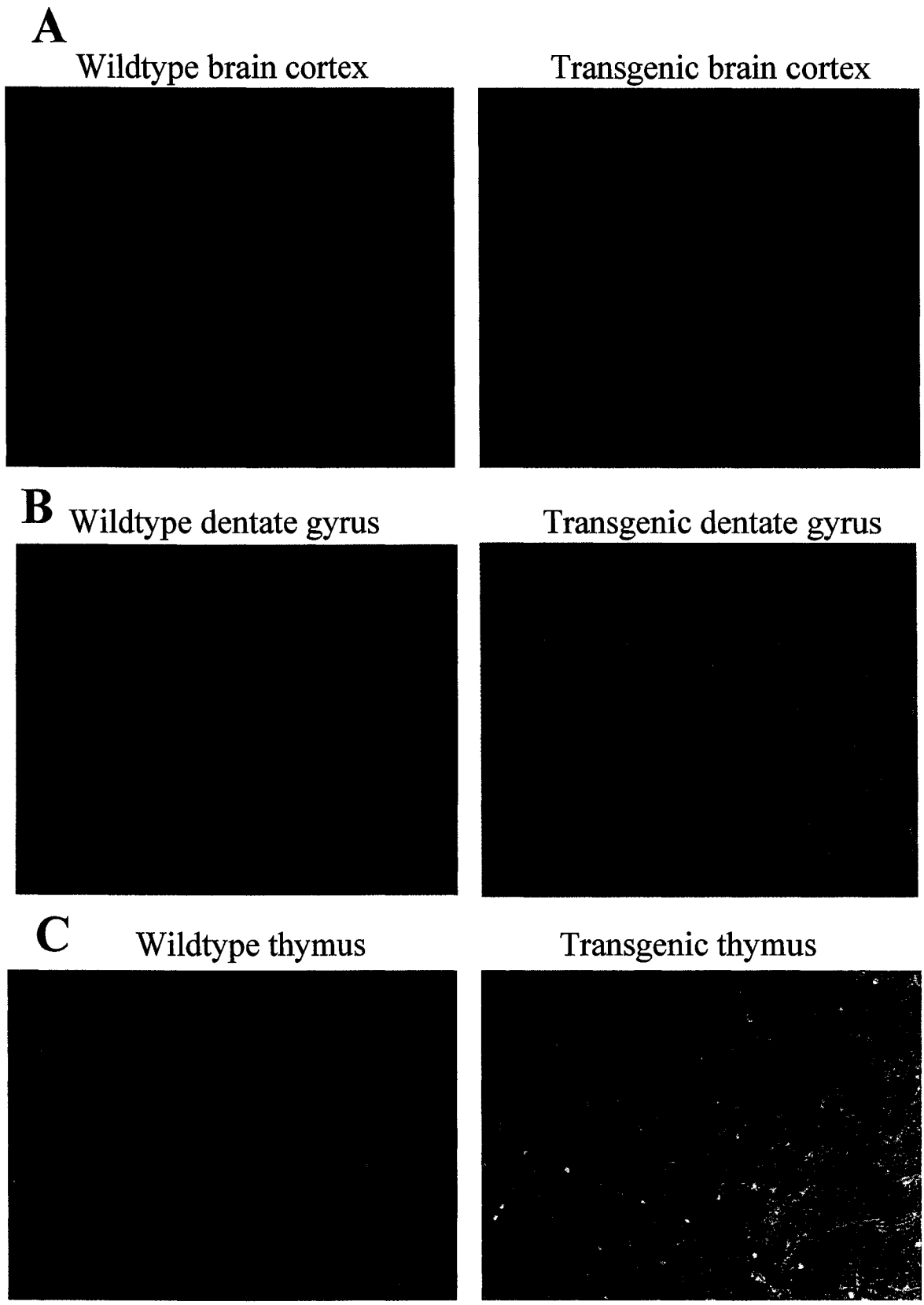
A
Wildtype brain cortex
Transgenic brain cortex
B
Wildtype dentate gyrus
Transgenic dentate gyrus
C
Wildtype thymus
Transgenic thymus

Figure 3-3

In the dentate gyrus and hippocampus, the over-expression also appears most visible in the cell bodies. In the thymus, the expression does not appear to be cell type specific.

c) Determination of high and moderate expression lines

High expression lines were chosen based on the degree of protein expression in the brain. Offspring from each line were compared based on the results of blots probed with both anti-c-myc and anti-XIAP as shown in figure 3-4. The protein expression results from the western blots indicated that the highest expressing line was line 402 while lines 426 and 416 showed moderate expression. Line 402 showed a consistent two-fold over-expression versus moderate expression lines.

ii) Determination of levels of expression in moderate and high expression line by real time quantitative reverse transcriptase PCR analysis

Real-time quantitative reverse transcriptase-PCR (RT-PCR) (Taqman) was used to analyze tissue samples from representative organs including the brain, pancreas and liver. The levels of human XIAP mRNA were compared to confirm the highest expression line by quantifying the amount of transgenic message. The amount of RNA message varied between tissues but there was a consistent two to one ratio of expression between the high expression and the moderate expression lines as shown in figure 3-4.

iii) Levels of endogenous mouse XIAP, MIAP-1 and MIAP-2 transcripts are not consistently suppressed in the tissues tested.

The quantitative analysis of endogenous IAP family members by RT-PCR was used to verify that the presence of the transgene was not interfering with endogenous murine IAPs. Previous work on the XIAP knockout mouse suggested that the other IAPs increased expression in order to compensate for the loss of XIAP (Harlin et al., 2001).

Figure 3-4 Determination of high and moderate expression lines based on quantitative RT-PCR and western blot analysis

Protein extracts from the brains of offspring from all twelve lines were compared. Six of the lines are shown including 402, 426, 416, 407, 410, and 420.

A) The membrane was probed with monoclonal anti-c-myc antibody

B) The membrane was probed with the polyclonal anti-XIAP antibody. Line 402 was chosen as the high expression line while lines 426, and 416 were chosen as the moderate expression lines.

C) The difference in messenger RNA expression between the high expression line 402 and the moderate expression line 416 is quantified using real time reverse transcriptase PCR (Taqman). In brain, spleen, and pancreas there is consistently an approximately two to one ratio between the amount of mRNA in the high expression line and the moderate expression line. The RNA was amplified using human XIAP primers that only recognize the transgene-encoded RNA and not endogenous XIAP. All samples were standardized by analysis of GAPDH mRNA expression levels. Expression levels of the transgene were set at one for the moderate expression line 416.

A

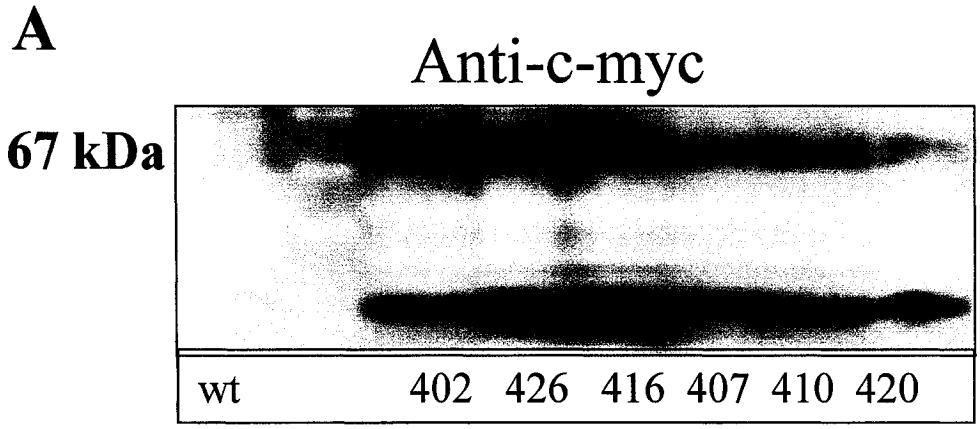

B

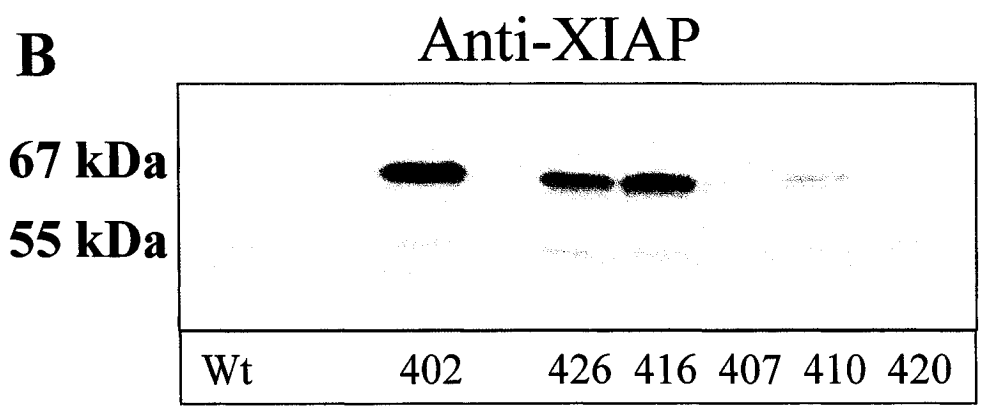

C

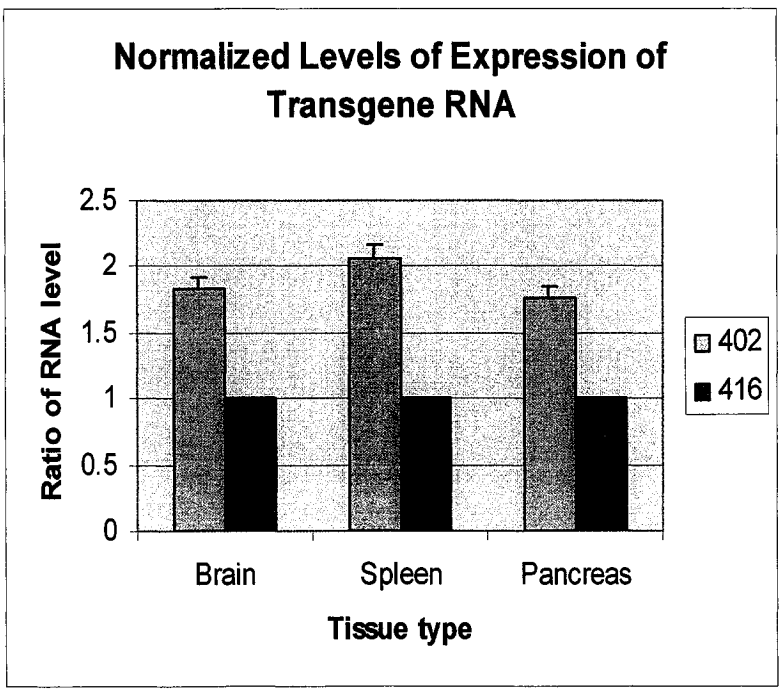

Figure 3-4

We therefore sought to determine whether constitutive over-expression of XIAP would trigger a compensatory decrease in either the endogenous XIAP or other murine IAPs (MIAP1 and MIAP2).

RNA samples were amplified with primers to the endogenous mouse XIAP, MIAP-1 and MIAP-2 (mouse cIAP-2 and cIAP-1 homologues) to determine if there are any changes or compensatory decreases in the endogenous IAP levels. Full organ panels from both transgenic and wildtype littermates from the 402 high expression line and the 426 moderate expression line were tested. There was variation in mRNA levels but nothing that was replicated in both the high expression animal and the moderate expression animal as shown in figure 3-5. The spleen was the only organ that showed suppression of all three IAPs in the moderate line and mXIAP suppression in the high expression line. There were more tissue samples that showed a higher level of endogenous IAP mRNA levels than suppression. These observations are not consistent with the hypothesis of compensatory decreases in endogenous IAP mRNA levels.

d) Creation of a homozygous high expression line of XIAP transgenics

Mating of heterozygous siblings from high expression line number 402 was established to generate homozygous lines. Animals were determined to be homozygous based on Phoshor Imager analysis of band intensities. Southern blots were probed for the human XIAP transgene, and band intensity was normalized to the two endogenous XIAP bands created in the characteristic-banding pattern of the 402 transgenics. A band intensity increase of approximately two fold was considered indicative of a homozygous animal (see figure 3-6 for values table). Homozygous animals were identified and then paired to create a homozygous line.

Figure 3-5 Determination of levels mRNA of endogenous MIAP-1, MIAP-2 and mXIAP by quantitative RT-PCR analysis

Samples of RNA were extracted from the heart, pancreas, spleen, liver, lung, brain, thymus and kidney. Primers for mouse XIAP, MIAP1 and MIAP2 were used to amplify mRNA from each sample. For each pair of reactions the wildtype mRNA level was set as 1 and transgenic mRNA levels are shown as ratios of the wildtype level. There is some variation in the ratios between wildtype and transgenic samples but nothing consistent between both the high and moderate expression transgenic lines. Samples from the pancreas were omitted because the RNA had degraded and did not give an accurate quantitative reading.

A) 402 high expression transgenic and wildtype littermate.

B) 426 moderate expression transgenic and wildtype littermate.

A

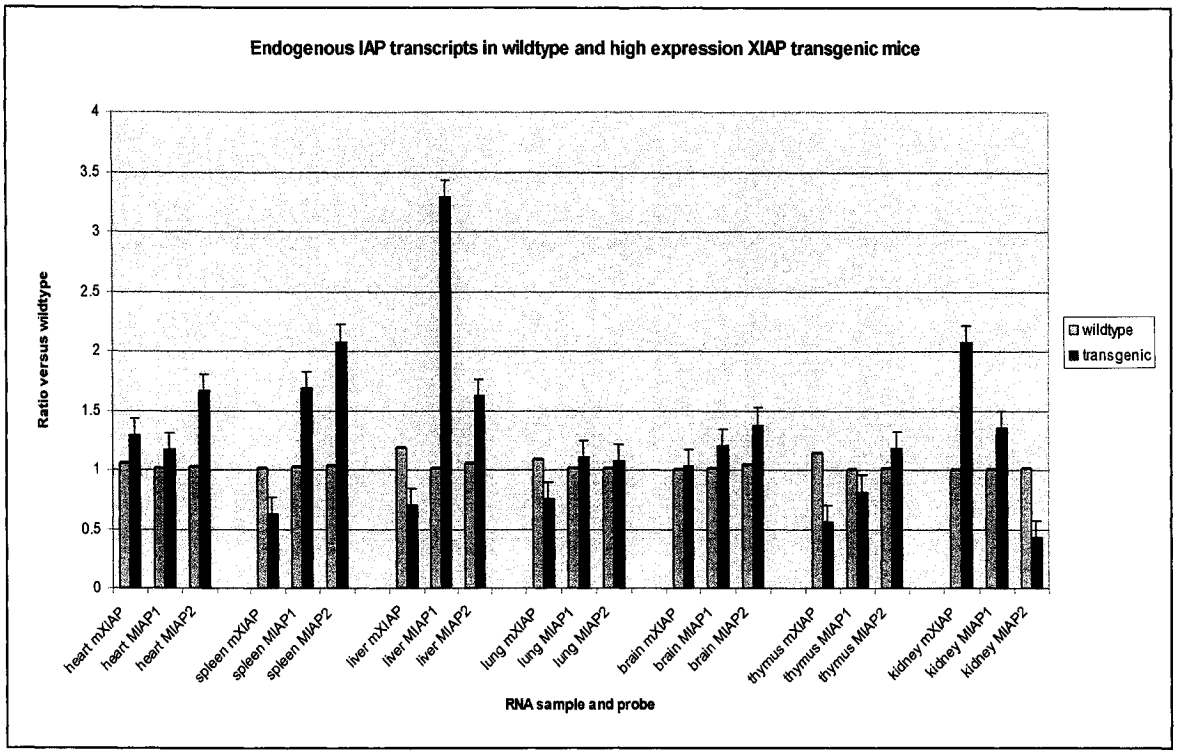
Endogenous IAP transcripts in wildtype and high expression XIAP transgenic mice
Ratio versus wildtype
4
3.5
3
2.5
2
1.5
1
0.5
0
wildtype
transgenic
heart mXIAP
heart MIAP1
heart MIAP2
spleen mXIAP
spleen MIAP1
spleen MIAP2
liver mXIAP
liver MIAP1
liver MIAP2
lung mXIAP
lung MIAP1
lung MIAP2
brain mXIAP
brain MIAP1
brain MIAP2
thymus mXIAP
thymus MIAP1
thymus MIAP2
kidney mXIAP
kidney MIAP1
kidney MIAP2
RNA sample and probe

B

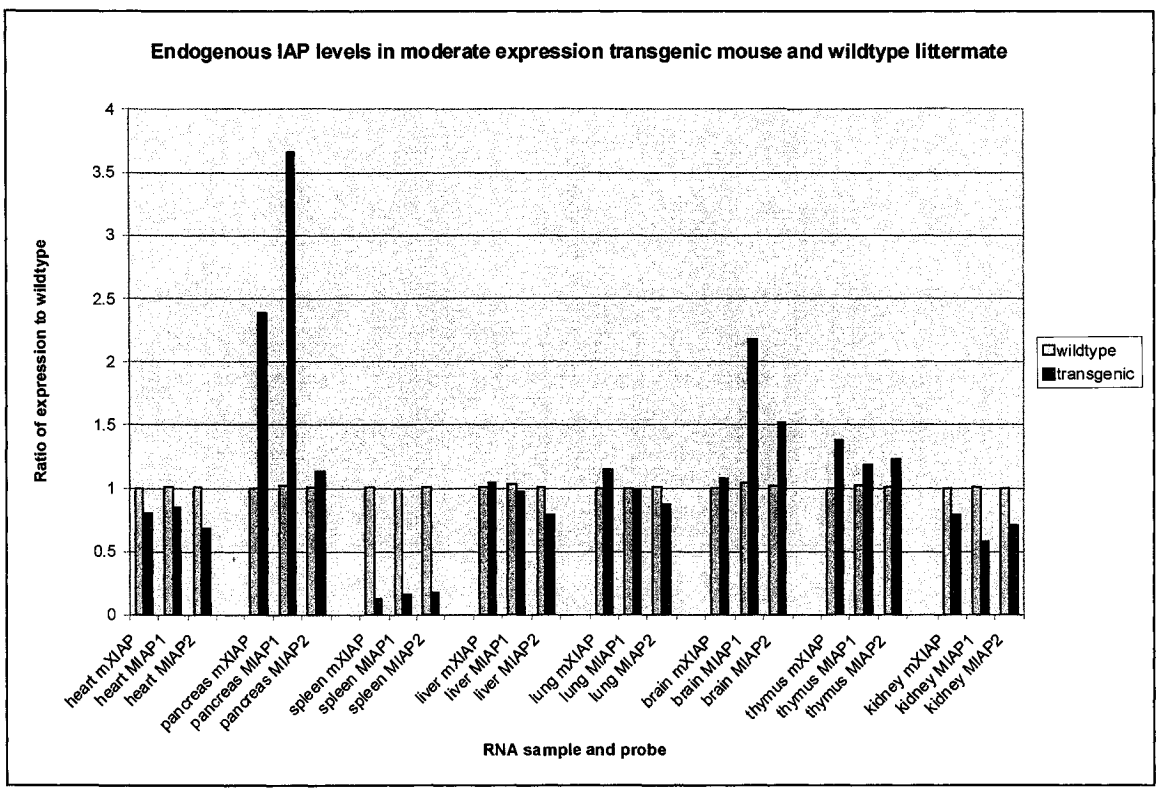
Endogenous IAP levels in moderate expression transgenic mouse and wildtype littermate
Ratio of expression to wildtype
4
3.5
3
2.5
2
1.5
1
0.5
0
wildtype
transgenic
heart mXIAP
heart MIAP1
heart MIAP2
pancreas mXIAP
pancreas MIAP1
pancreas MIAP2
spleen mXIAP
spleen MIAP1
spleen MIAP2
liver mXIAP
liver MIAP1
liver MIAP2
lung mXIAP
lung MIAP1
lung MIAP2
brain mXIAP
brain MIAP1
brain MIAP2
thymus mXIAP
thymus MIAP1
thymus MIAP2
kidney mXIAP
kidney MIAP1
kidney MIAP2
RNA sample and probe

Figure 3-5

Compensation for sex differences in the endogenous levels of XIAP

Because XIAP is an X-linked gene, females carry two copies while males carry only one. This dosage effect does not impact on expression because of X-chromosome inactivation but it does impact on the dosage of the endogenous gene when doing densitometry calculations. Separating the sexes and calculating ratios and background independently for male and female offspring circumvented this problem.

i) Determination of relative protein expression in homozygous and heterozygous transgenics by western blot and immunofluorescence

Protein samples were extracted from the brains of homozygous and heterozygous animals from high expression line 402. Western blots showed a 2-fold increase in expression of the c-myc epitope tagged XIAP protein in the homozygous versus the heterozygous animals. This increase was also detected by immunofluorescence as shown in figure 3-7.

Figure 3-6 Identification of homozygous transgenic animals by Phosphor Imager analysis

A) Southern blot that was used for genotyping litters from a heterozygous/heterozygous cross from the high expression line. The samples are numbered by lane. Samples in lanes 1 through 9 are from female animals and samples in lanes 10 through 15 are from male animals. The two dashed arrows indicate the endogenous bands, end 1(bottom dashed arrow) and end 2 (top dashed arrow). The two endogenous bands are the only bands present in the wild type offspring in lane 7. The two normal arrows indicate the transgenic bands, trans 1(bottom arrow) and trans 2 (top arrow). The third transgenic band was not used in calculations.

B) The first table is a table with the intensity of each the four bands quantified in each lane (shown as end1, end2, trans1, and trans2 in table B). Two separate ratios were determined for each lane. The first ratio was trans1 divided by end 1 (trans1/end1 in table B) and the second ratio was trans 2 divided by end 2 (trans2/end2 in table B). An initial genotype is assigned based on the two uncorrected ratios (genotype in table B).

To get the corrected genotype the ratio was compared to background. Each ratio was calculated separately.

C) The table shows the correction for background in the wild type lanes for the trans1/end1 ratio from table B.

D) The table shows the correction for background in the wild type lanes for the trans2/end2 ratio.

The background is determined as the average intensity of the empty area where the transgenic bands would be in the wild type lanes (background in tables C and D). The ratio corrected for background appears in the ratio column of tables C and D. Background was calculated separately for males and females. The corrected genotype for each ratio is shown as genotype in tables C and D. The genotype determined in the first table is then confirmed if the genotype determined in the second and third table based on the corrected ratios are the same. If the two ratios were not the same the sample was labelled as indeterminate and the animal was not used in experiments or breeding

A

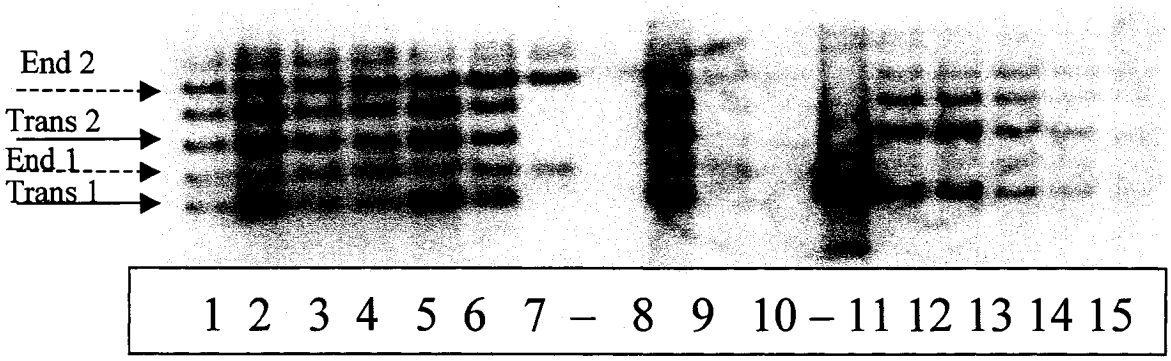

B

	end.1	end.2	trans.1	trans.2	tran1/end1	tran2/end2	genotype
lane 1	268470.42	307594.80	291623.98	270448.87	1.09	0.88	hetero
lane 2	393395.91	447679.09	535544.16	673909.28	1.36	1.51	homo
lane 3	343837.30	380186.49	386234.45	390970.38	1.12	1.03	hetero
lane 4	424042.23	416006.19	458365.60	421860.39	1.08	1.01	hetero
lane 5	404288.70	447506.01	653855.39	626870.63	1.62	1.40	homo
lane 6	399461.96	445623.67	435372.46	373539.76	1.09	0.84	hetero
lane 7	365905.10	388392.62	241285.12	217166.49	0.66	0.56	wildtype
lane 8	504525.10	517751.21	651961.25	632886.96	1.29	1.22	indetermin
lane 9	343454.64	278205.65	382024.65	223118.52	1.11	0.80	wildtype
lane 10	221938.73	189749.55	250002.70	172099.70	1.13	0.91	wildtype
lane 11	414555.20	358457.87	517254.77	487209.82	1.25	1.36	indetermin
lane 12	331698.35	299279.75	431731.53	513283.07	1.30	1.72	homo
lane 13	285653.71	345447.17	414855.88	393858.21	1.45	1.14	indetermin
lane 14	198755.86	218067.05	300987.70	224968.18	1.51	1.03	indetermin
lane 15	230129.54	167463.46	214404.29	209964.04	0.93	1.25	hetero

C

	band 1 analysis		
lane	background	ratio	genotype
1	0.12	1.25	hetero
2	0.40	4.10	homo
3	0.16	1.63	hetero
4	0.11	1.19	hetero
5	0.65	6.76	homo
6	0.12	1.29	hetero
7	0.00		
8	0.33	3.39	homo
9	0.00		
10	0.00		
11	0.28	2.92	homo
12	0.34	3.48	homo
13	0.49	5.05	homo
14	0.55	5.69	homo
15	-0.03	-0.36	hetero

D

	band 2 analysis		
lane	background	ratio	genotype
1	0.12	0.50	hetero
2	0.75	3.04	homo
3	0.27	1.10	hetero
4	0.26	1.05	hetero
5	0.64	2.61	homo
6	0.08	0.33	hetero
7	0.00		wildtype
8	0.47	1.89	homo
9	0.00		wildtype
10	0.00		wildtype
11	0.60	2.44	homo
12	0.96	3.89	homo
13	0.38	1.56	hetero
14	0.28	1.12	hetero
15	0.50	2.02	homo

Figure 3-6

Figure 3-7 Determination of the relative transgene-encoded protein levels in homozygous and heterozygous animals by anti- XIAP immuno-reactivity in the brain

A) Brain protein lysates were probed with the monoclonal anti-c-myc antibody. The western blot shows a two-fold over-expression of the epitope tagged protein at 67 kDa in the homozygous sample versus the heterozygous sample and an absence of the epitope tag in the wildtype sample.

B) In the blot on the right, lysates probed with polyclonal anti-XIAP antibody show transgenic (67 kDa) and endogenous (55kDa) XIAP levels in the same three samples. There appears to be a slightly cross-reactive band just below 67 kDa in the anti-XIAP blot but it is not present in the anti-c-myc probed blot of the same samples.

Frozen 10-micron sections from the cortex of the brain were labelled with anti-XIAP (1:100) and Alexa 488 secondary antibody. Images were captured at a magnification objective of 40 with 5 integrations of the image.

C) The secondary antibody control shows no significant background fluorescence from the secondary antibody.

D) The cell bodies express XIAP in the wild type sections.

E) In the heterozygous transgenic section there is intense ubiquitous background fluorescence. The fluorescent conjugated antibody appears to detect protein expressed throughout the tissue with intensification in the cell bodies.
F) The homozygous transgenic section shows the same intense ubiquitous background fluorescence as in E.

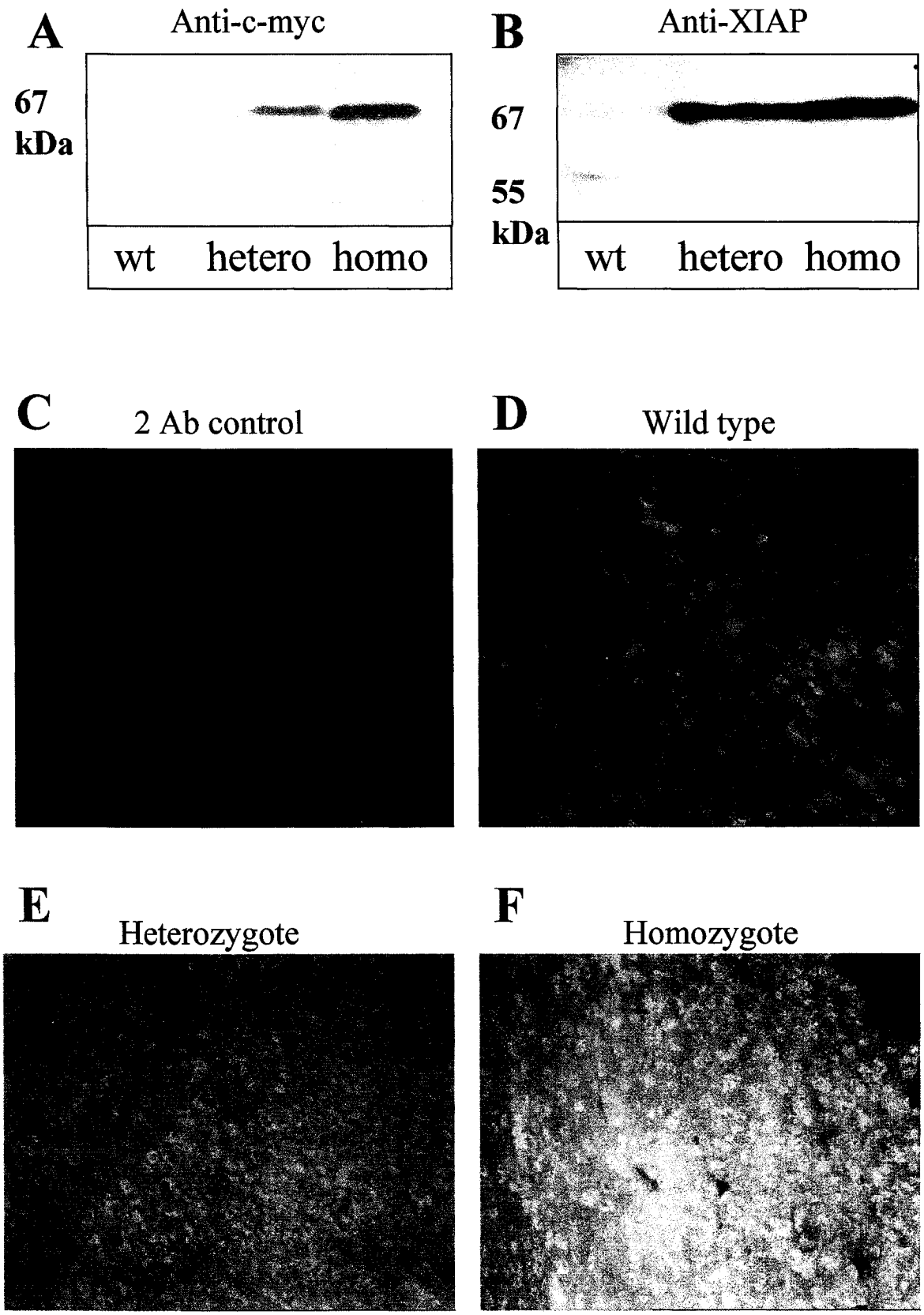
A
Anti-c-myc
67
kDa
wt
hetero
homo
B
Anti-XIAP
67
55
kDa
wt
hetero
homo
C
2 Ab control
D
Wild type
E
Heterozygote
F
Homozygote

Figure 3-7

Part 3-2: The Effects of XIAP over-expression in development

a) Examination of gross morphology in embryos at days E10, E12, E15, E17.5 of development

Embryos were harvested at day E10, E12, E15, and E17.5 of gestation to observe transgenic development and compare it to the development of wild-type littermates. Embryos were photographed to observe gross morphology and limb buds were sectioned to observe any changes in interdigital tissue apoptosis. Interdigital tissue apoptosis is one of the classic sites of apoptosis during development. Members of the BMP family and Smad, two classes of molecules that interact with XIAP in signalling pathways have been shown to be present during interdigital tissue apoptosis.

The four different stages examined represent important milestones in development as described by MH Kaufman in The Atlas of Mouse Development. Day 10 embryos are stage 16, have 30-34 somites, and represent the first appearance of the hind limb bud (Kaufman 1992). This stage is also important for the formation of the lens placode of the eye and primary bronchi in the lungs. The next stage examined was Day 12. It was significant because this was the latest stage where interdigital tissue was present and the cell death that occurs during the regression of the interdigital tissue could be examined. In the vascular system, Day 12 represents the beginning of the partition of arterial trunk. Day 12 also marks the appearance of the tongue, thymus and parathyroid primordium. In the eyes the lens vesicle becomes detached (Kaufman 1992). It is also a milestone for sexual differentiation of gonads. Day 15 embryos were chosen because the digits are fully differentiated in the limbs. In the vascular system, coronary vessels appear, and in the eye the ganglionic cells of retina form. Day 17.5 represents most of the external morphological features of a newborn

though there is an increased degree of differentiation in the eye that continues until after birth (Kaufman 1992).

Wildtype and transgenic embryos are shown at each of the four stages in figure 3-8. Transgenic and wildtype embryos appear identical at each stage. The normal morphology exhibited by transgenics indicates that XIAP expression does not result in significant changes in gross morphology.

b) Effects of transgene-encoded XIAP on neuronal cell counts

Neuronal cell counts were determined to be an important indicator of normal apoptosis in neuronal development. Supernumerary neurons would be indicative of abnormalities in cell death during development. Neuronal development was chosen because the brain was the organ most likely to show a developmental phenotype since it had the highest ratio of transgenic to endogenous protein expression.

The possibility of supernumerary neurons in the XIAP transgenics was also explored because of the documented presence of supernumerary neurons in many mouse models where there is inhibition of apoptosis during central nervous system development.

These models include Bcl-2 transgenics(Coleman et al., 1999; Dubois-Dauphin et al., 1994; Martinou et al., 1994; Zanjani et al., 1997), Bax knockouts (White et al., 1998), caspase-9 knockouts (Kuida, 2000), caspase-3 knockouts (Leonard et al., 2002) and Apaf-1 knockouts (Yoshida et al., 1998). There was significant strain-based variation in the developmental defects, especially in the severity of the phenotypes for caspase-3, -9 and Apaf1 knockouts. The C57BL6 strain that the XIAP transgenics were created in was the strain that had much less severe developmental defects in the knockouts.

Figure 3-8 Wild type and transgenic embryos photographed at days E10, E12, E15, E17.5 of development.

Embryos were removed at important developmental stages to determine if there were any changes in morphology between transgenic and wildtype animals. Each litter was harvested at the time points listed above and animals were photographed and placed in PBS. Tails were removed and used for genotyping. Transgenic animals are shown on the left and wildtype animals are on the right. Representative animals from four different litters are shown.

A) Littermates photographed at Day 10 of gestation at 3 times magnification.
B) Animals shown are at Day 12 at 2 times magnification.
C) Day 15 embryos at 1 times magnification
D) Day 17.5 embryos at 0.75 times magnification.

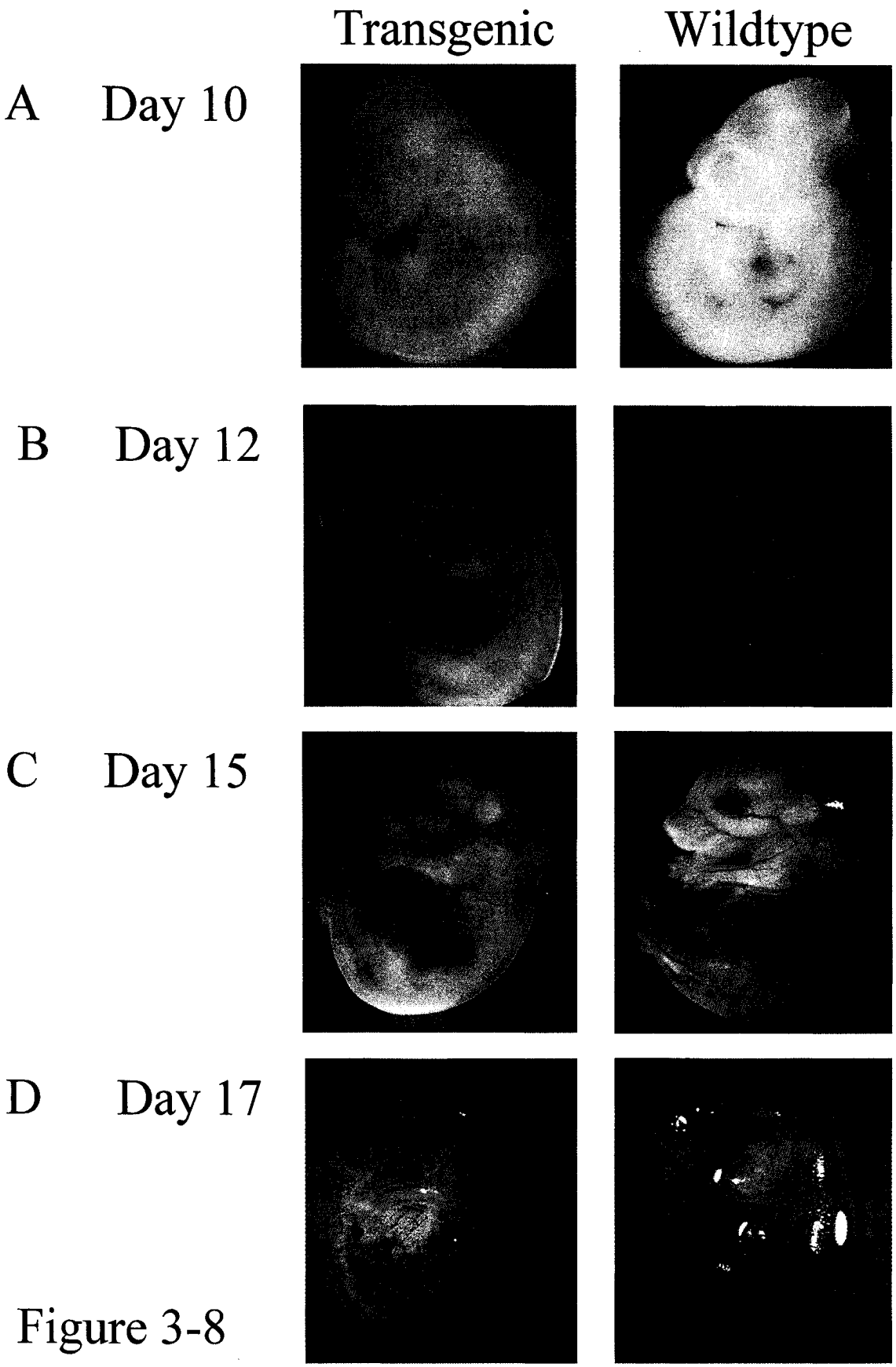

Figure 3-8

Wild type and transgenic brains were sectioned and stained with NeuN (A60) neuronal specific antibody. Different areas of the brain including anterior and posterior cortical regions, cerebellum and olfactory lobes were compared for neuronal cell counts (see figure 3-9). Size exclusion was set so that objects under 5 pixels in size were not counted. Threshold intensity was optimized for each region of the brain. The threshold varied from 80 in the cerebellum to 100 in the dentate gyrus and 118 in the cortex. At least ten different slides were counted for each section. Neurons were counted for 5 different animals per group with 20 images per section per animal. A two-tailed student's t-test was performed for results from each region. There was no significant difference ($p = 0.116504$) in the number of neurons in cerebellum and an insignificant decrease ($p = 0.539132$) in the posterior cortex.

Figure 3-9 Images of brain sections probed with NeuN for neuronal cell counts and graphic comparison of cell counts

Sections of the brain were labelled with NeuN (A60) antibody and Alexa 488 secondary antibody.
A) The dentate gyrus probed with NeuN at 10X magnification.
B) The dentate gyrus probed with NeuN at 40X magnification.
C) The cerebellum probed with NeuN at 10Xmagnication
D) The cerebellum probed with NeuN at 40X magnification

Cells were counted using image detection software from Northern Eclipse. All cell counts were done at 40X magnification. For each image labelled objects smaller than 5 pixels in size were not counted. Cells that reached threshold intensity of 80 in the cortex, 100 in the dentate gyrus and 118 in the cerebellum were counted.

E) Cell counts are shown for the cerebellum and the cortex of transgenic brains (red) and wildtype brains (blue). Neurons were counted for 5 different animals per group with 20 images per section per animal. Each bar represents the average for the genotype. A two-tailed student's t-test was performed for results from each region. There was no significant difference in the number of neurons in cerebellum ($p=0.05$) and no significant difference in the number of neurons in the posterior cortex ($p = 0.05$).

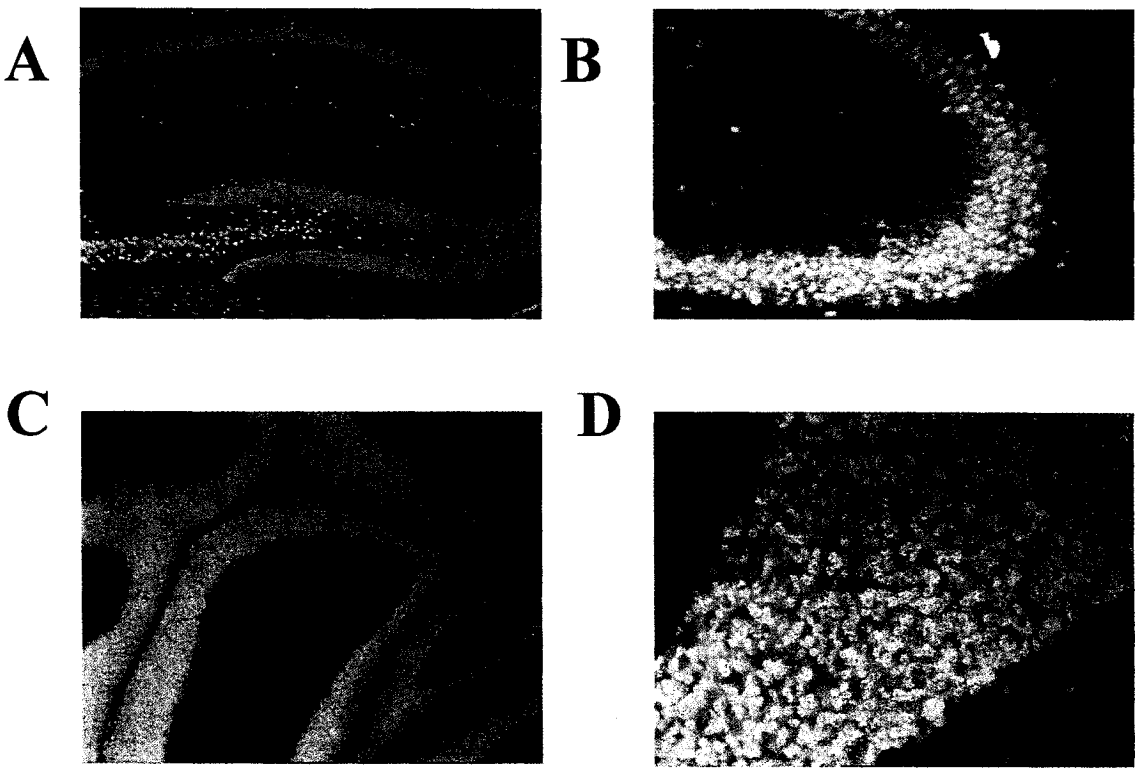
A
B
C
D

E

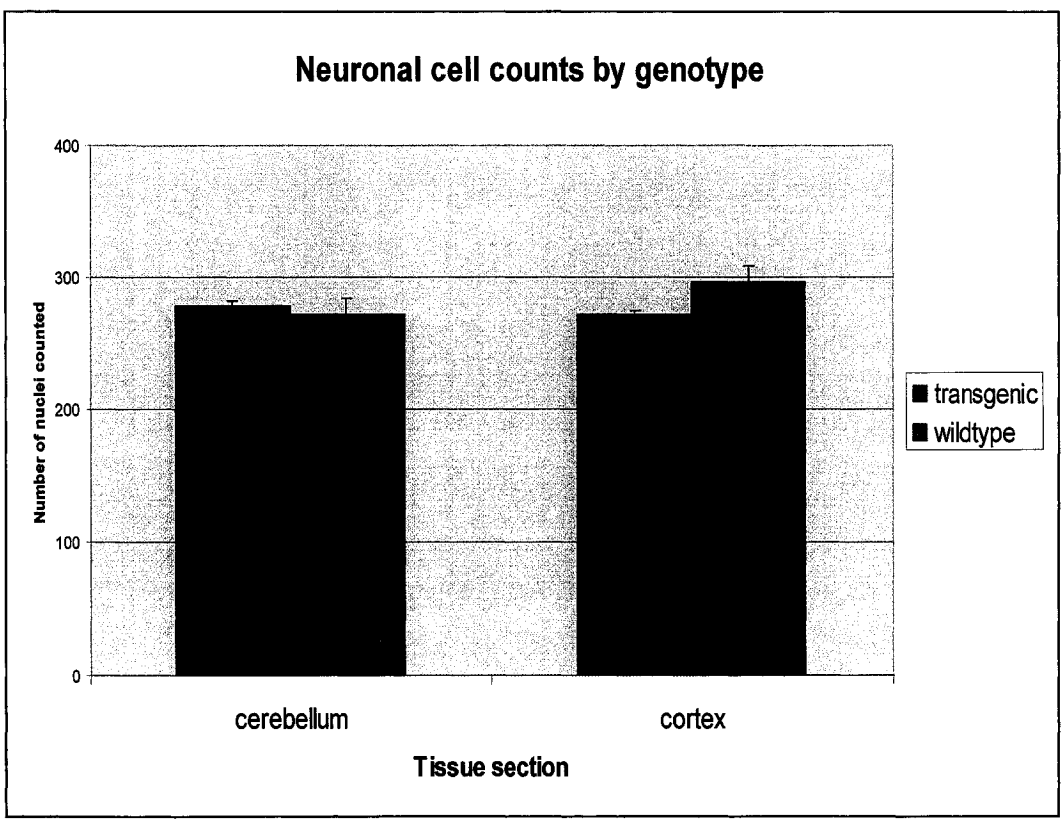
Neuronal cell counts by genotype
Number of nuclei counted
400
300
200
100
0
cerebellum
cortex
Tissue section
transgenic
wildtype

Figure 3-9

Part 3-3: Analysis of transgene-encoded protein function *in vitro* and *in vivo*

In order to confirm that the transgene-encoded protein was functional, tissue explants and whole animals were tested for suppression of apoptosis. XIAP has been shown to suppress apoptosis induced by TNFα, Fas, serum or growth factor withdrawal, ischemia, chemotherapy and radiotherapy (LaCasse et al., 1998). Over-expression of XIAP is protective against several forms of apoptosis *in vivo* including ischemia (Xu et al., 1999), neuronal axotomy (Kugler et al., 2000), kainic acid-induced neuronal death (Korhonen et al., 2001), and thymocyte apoptosis (Conte et al., 2001).

a) *In vitro* cell death assays show that transgenic protein is functionally suppressing apoptosis

Two types of primary cell cultures were established for *in vitro* cell death assays. Mouse embryo fibroblasts were cultured and treated with etoposide, a trigger that induces apoptosis through the intrinsic pathway. Primary hepatocytes cultures were treated with monoclonal anti-Fas that triggers cell death through the death receptor mediated extrinsic pathway. For both cell types cell viability was quantified using a metabolic WST assay.

i) Analysis of transgene-encoded XIAP function in primary mouse embryo fibroblasts (MEF) cultures after treatment with etoposide

There were two significant reasons that MEFs were chosen as one of the primary cell cultures. The first is that they are undifferentiated cells that are still actively dividing so they are susceptible to the effects of etoposide. The second is that the use of embryonic cell cultures provided a means to determine whether the protein product of the XIAP transgene was present during development. Each MEF culture was derived from a single embryo. The genotypes were determined by DNA analysis of embryonic tissue not employed in

generating the MEF cultures. XIAP protein expression in the MEFs was determined by Western blot as shown in figure 3-10.

Transgenic and wildtype MEFs were compared for cell death sensitivity. Three XIAP transgenic cultures and three wild-type cultures were assayed. The cells were plated on 96 well plates in triplicate at 1 $x10^4$ per ml and incubated at 37°C with 5% CO_2 for 24 hours. At 24 hours post seeding, media was removed and the cells were exposed to etoposide for 72 hours. Etoposide, a topoisomerase inhibitor that causes actively dividing cells to undergo apoptosis, triggers apoptosis through the intrinsic pathway. A full range of doses from 1 μM to 250 μM was used in the assay. MEFs were exposed to etoposide for 72 hours. The transgenic cultures showed a higher viability at all doses tested compared to the wild type (see figure 3-10).

ii) Analysis of transgene-encoded XIAP function in primary hepatocytes treated with monoclonal anti-Fas antibody

The second primary cell line chosen was hepatocytes. Hepatocytes provided a good contrast to MEFs in that they are fully differentiated and specialized cells. Protein expression in the liver had already been established (see figure 3-2). Hepatocytes were isolated from mice by a collagenase liver perfusion protocol. Cells were treated with doses of anti-Fas ranging from 0 to 250 ng/ml. Anti-Fas antibody induces an aggregation of the Fas receptor, triggering apoptosis through the extrinsic pathway. At all doses tested the transgenic hepatocytes were more resistant to apoptosis than wild-type hepatocytes given the same dose as shown in figure 3-11. Each dose was administered in quadruplicate.

Figure 3-10 Survival of mouse embryo fibroblasts (MEFs) after treatment with etoposide, an intrinsic pathway trigger

A) Western blot probed with anti-c-myc show XIAP protein expression in each of the MEF lines used in death assays.

B) The same Western blot was also probed with anti-XIAP. Lines R2, R5, R7 expressed transgene-encoded protein and lines R4, R6, R8 were wildtype. DNA was also extracted from the embryos during the creation of the fibroblast lines. All lines were genotyped by PCR. Line R3 was the only line that was genotyped as positive but did not express any transgene-encoded XIAP protein. The positive control (pc) consisted of lysates from Hela cells transfected with the pcDNA3-6myc XIAP expression plasmid.

C) Etoposide death assay is shown with doses ranging from 0 to 100 μM of etoposide. The transgenics (pink) were more viable at all doses tested that the wildtypes (blue). Each line represents the average of three different MEF cultures derived from the same transgenic line. The graph is of a representative experiment. Viability was assessed using a WST-1 metabolic assay. The WST-1 reagent is a tetrazolium salt that gets cleaved by metabolic enzymes causing a colour change that can be detected by measuring the absorbance using a spectrophotometer.

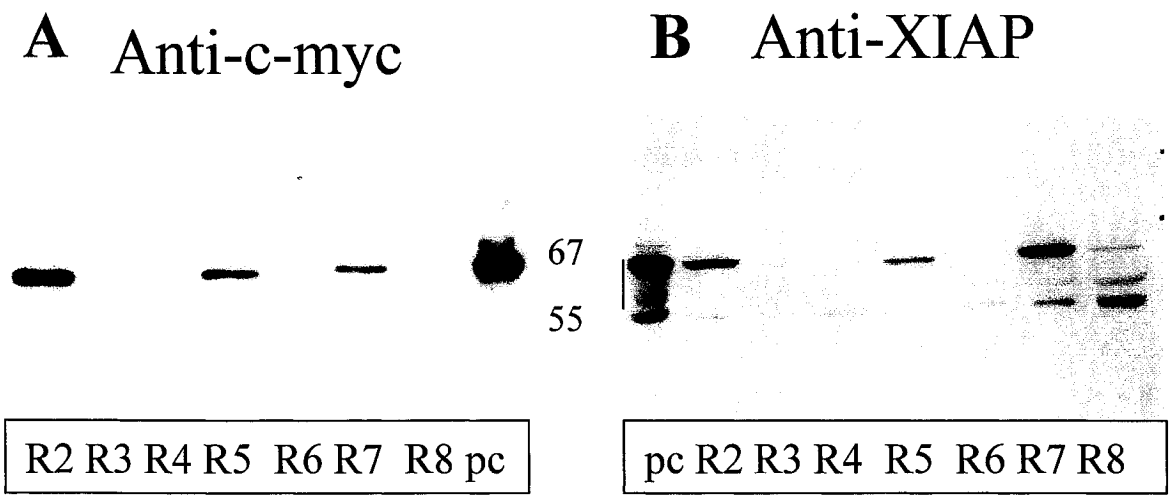
A Anti-c-myc
B Anti-XIAP
67
55
R2 R3 R4 R5 R6 R7 R8 pc
pc R2 R3 R4 R5 R6 R7 R8

C

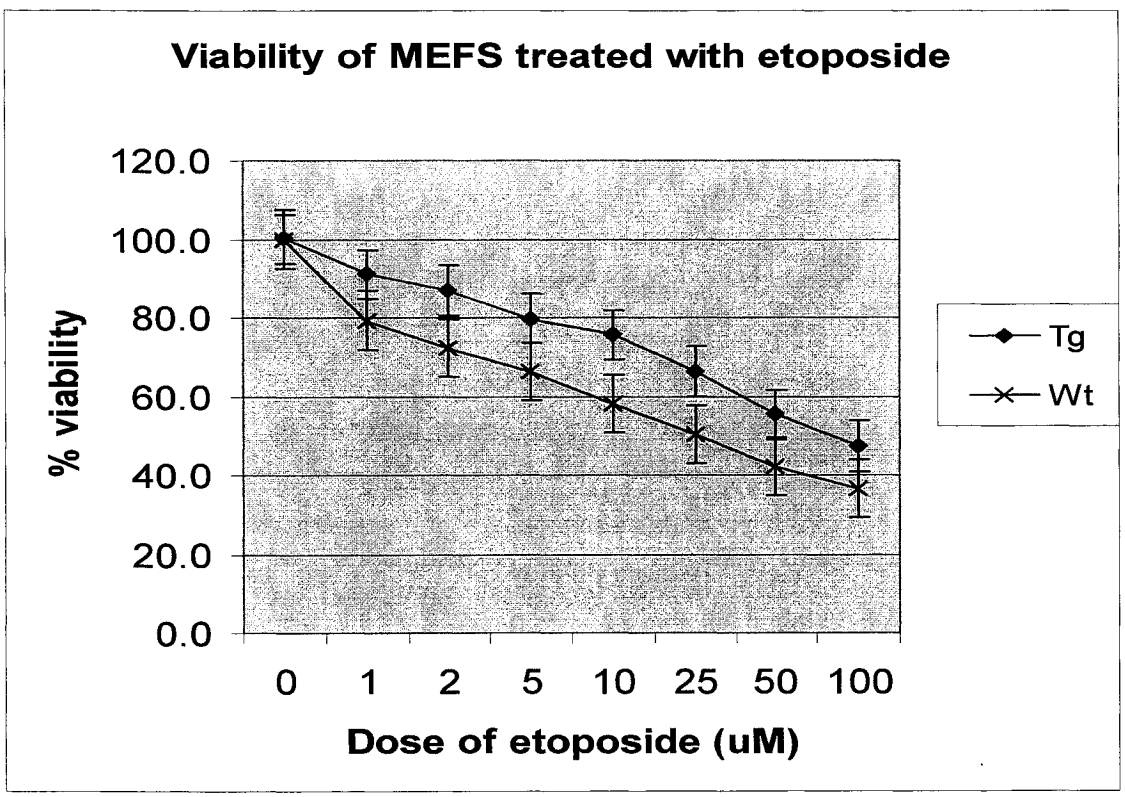
Viability of MEFS treated with etoposide
120.0
100.0
80.0
60.0
40.0
20.0
0.0
% viability
0
1
2
5
10
25
50
100
Dose of etoposide (uM)
Tg
Wt

Figure 3-10

Figure 3-11 Survival of primary hepatocytes after treatment with anti-Fas alone or with cyclohexamide

Survival curve of hepatocytes treated with anti-Fas antibody in doses ranging form 0 to 250 ng/mL. Anti-Fas antibody triggers apoptosis through the extrinsic death receptor pathway. Viability was assessed by the WST-1 assay which measures metabolic activity. The transgenic hepatocytes (pink) were more viable at all doses than the wildtype hepatocytes (blue). Each dose was administered in quadruplicate and each data point represents the average for each dose.

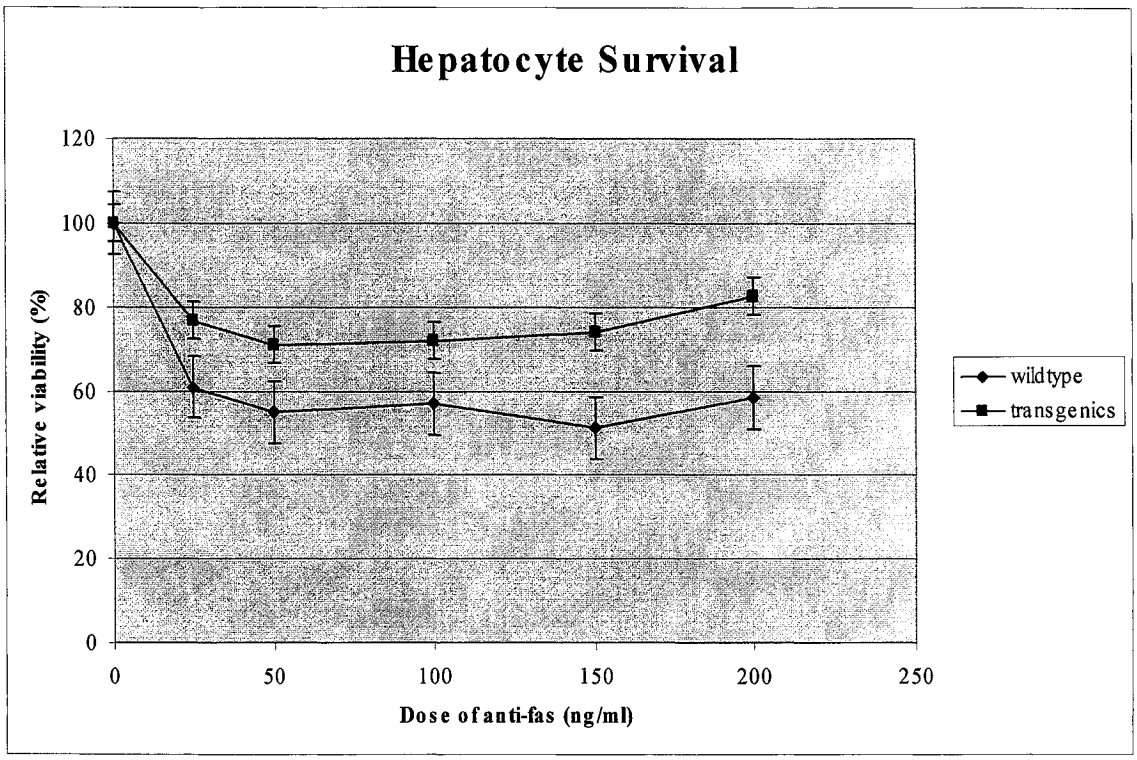
Hepatocyte Survival
Relative viability (%)
120
100
80
60
40
20
0
0
50
100
150
200
250
Dose of anti-fas (ng/ml)
wildtype
transgenics

Figure 3-11

iii) The effect of cyclohexamide on resistance of transgenic hepatocytes treated with high doses of anti-Fas

Hepatocytes were also treated with anti-Fas in combination with 10ug/ml cyclohexamide. Cyclohexamide, a protein synthesis inhibitor, increases the apoptotic effect of anti-Fas. Transgenics are still resistant to anti-Fas mediated apoptosis at lower doses but the difference in viability decreases at higher doses of anti-Fas (see figure 3-11). This decrease in viability is an indication that the additional cellular stress of eliminating protein synthesis overwhelms the effects of the suppression of apoptosis by XIAP when a high level of death inducing signal is present.

b) Functional suppression of apoptosis in *in vivo* injury models

Because of the ubiquitous nature of the transgene over-expression there were many different types of injury models that could be used to determine if the over-expression of XIAP was suppressing apoptosis. The thymus and the brain were both high expression tissues but the suppression of apoptosis is well documented in these tissues in the thymocyte specific transgenic (Conte et al., 2001) and the neuron specific transgenic (Crocker et al., 2003; Trapp et al., 2003; Wang et al., 2004).

The pancreas was chosen for several reasons. The first is that there are well-documented injury models available that mimic *Diabetes mellitus* by inducing apoptosis in the beta cells of the islets of Langerhans. The second is that one of the key objectives in generating the transgenic mice was to determine if XIAP directly contributes to tumorigenesis. The model system chosen employs an inducible myc oncogene expressed solely in the beta cells of the pancreas. Before proceeding with these experiments, it was crucial to establish that the transgene encoded XIAP protein is functional in the pancreatic

beta cells. In order to confirm functionality, we employed high-dose streptozotocin model of beta cell injury. The pancreas was targeted using streptozotocin, a DNA damaging agent that targets beta cells in the islets of Langerhans (Blasiak et al., 2004).

a) High single dose streptozotocin pancreatic beta cell injury model

The pancreatic beta cell injury model was used to determine the specific protection that over-expression of XIAP confers to the beta cells in the islets of Langherhans. Streptozotocin is a DNA damaging agent that destroys beta cells in the islets of Langerhans in the pancreas mimicking the effects of beta cell destruction in *diabetes mellitus*. Streptozotocin can be administered as a single high dose or in a series of consecutive low dose injections.

The method chosen for these experiments was a single high dose, causing apoptosis through the generation of oxygen free radicals. XIAP has shown protection against oxygen free radical induced apoptosis in the MPTP induced toxicity (Crocker et al., 2003) and neuronal axotomy (Perrelet et al., 2004). The low dose experimental method triggers an autoimmune mediated destruction of the pancreas. While the low dose method is more reflective of diabetes progression, the objective was to confirm apoptosis suppression in an acute injury model.

i) Examination of XIAP expression in the islets of Langherhans in the pancreas

Isolated islets from wildtype and transgenic animals were compared for transgene-encoded XIAP expression. Using the monoclonal anti-c-myc antibody it was determined that the transgenics do express the transgene-encoded protein in the islets of Langerhans as shown in figure 3-12.

Figure 3-12 Transgene-encoded XIAP expression and glucose tolerance in the islets of Langherhans in wildtype and transgenic animals

A) Islets were isolated from both wild type and transgenic mice. Transgene-encoded XIAP expression was detected by western blot using the monoclonal c-myc antibody. Wild type islets did not express transgene-encoded protein but the transgenic islets did express the transgene-encoded XIAP.

B) The results of a glucose tolerance test. Untreated mice including 6 wildtype (blue), 6 heterozygous transgenics (yellow) and 6 homozygous transgenics (pink) were fasted for four hours and given a bolus injection of glucose (2g/kg). Blood glucose was monitored at 0, 15, 30, 60, 90, and 120 minutes after injection. Significant differences in glucose tolerance were observed between wildtype and heterozygous transgenics as well as between wildtype and homozygous animals but not between heterozygous and homozygous transgenics. The differences were observed at all time points except 30 min at $p=0.01$ in an unpaired, 2 tailed Student's t-test. Error bars for each data point represent standard error.

A

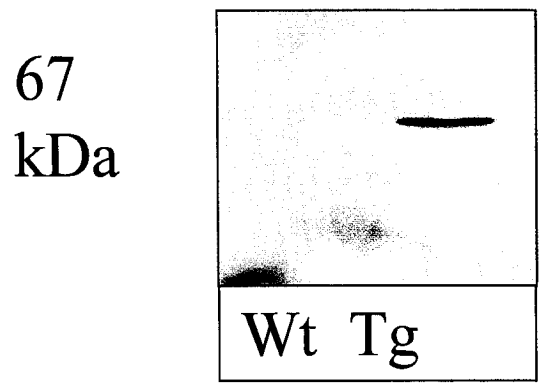

B

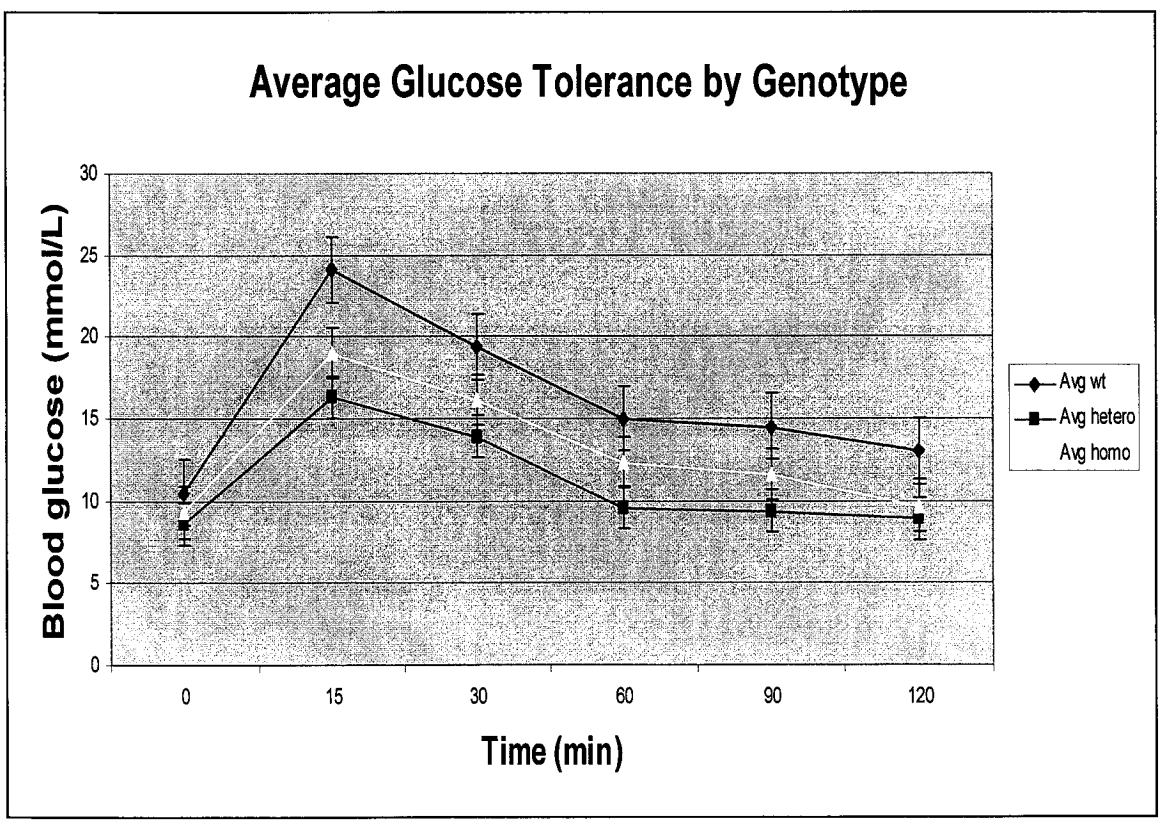

Figure 3-12

Figure 3-12a Transgene expression in the islets of Langherhans

Pancreas sections were double labelled with anti-myc antibody (green fluorescence) that recognizes an epitope fused to the transgene and Hoescht (blue fluorescence) that labels the nuclei. Images were captured at 40 times magnification.

A) In the wildtype section, there is no green labeling because no transgenic protein is present. Nuclei are visible in blue. Areas of high nuclear density indicate the presence of an islet.

B) In the section from the heterozygous transgenic, green labeling is present throughout the acinar and islet cells. Nuclei are visible as blue spots.

C) In the section from the homozygous transgenic, the intensity of the green labeling increases throughout the tissue. Nuclei remain visible at the same intensity as in the wildtype and heterozygous sections.

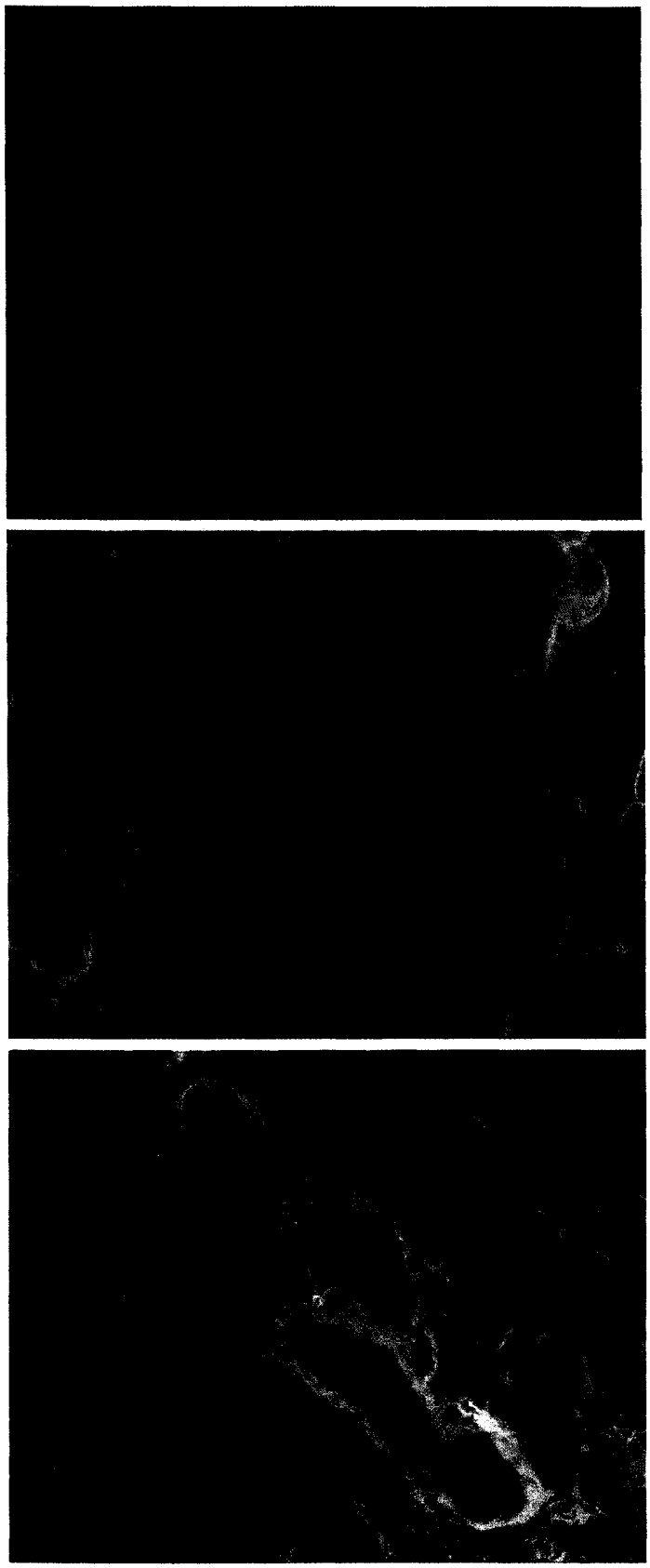

Figure 3-12a

ii) Analysis of response to glucose challenge by genotype

Glucose tolerance tests are used to determine how well the pancreas functions. The test measures how long it takes the body to return blood glucose to baseline after challenge with a bolus injection of glucose. Animals were fasted for 4 hours and then injected with a dose of 2g/kg of glucose. Blood glucose was tested at 6 time points over 2 hours. Significant differences in glucose tolerance between wild type and transgenic animals were seen at all time points except 30 min at $p=0.01$ in an unpaired, 2 tailed Student's t-test. There was no difference between the fasting baseline blood glucose between genotypes but both the heterozygous and homozygous transgenics had lower blood glucose levels after challenge and returned to baseline faster (figure 3-12). Transgenics animals are more tolerant to glucose challenge than wild types. These results indicate that the transgenic animals regulate blood glucose more effectively than wild types.

b) Analysis of response to high dose streptozotocin in different genotypes

i) Analysis of differences in fasting blood glucose levels between genotypes before treatment

Fasting blood glucose readings where taken over a two-week period to establish a baseline for both the transgenics and the wild types before injection. Thirty-four mice were included in experiments. No significant differences were discovered between any of the genotypes at baseline levels in a student's t-test at $p<0.01$ (figure 3-13).

ii) Analysis of blood glucose levels for transgenic and wildtype animals after high dose streptozotocin treatment

The initial experiment was performed with six animals; five animals injected with 150 mg/kg of streptozoticin and one animal that received citrate buffer vehicle only.

Figure 3-13 Blood glucose levels of wildtype, heterozygous and homozygous transgenic animals before and after treatment with a high dose of streptozotocin

A) Fasting blood glucose levels for the three genotypes, wildtype (blue), heterozygous transgenic (pink), and homozygous transgenic (red). Each bar represents the average of four different fasting blood glucose measurements for 13 wild types, 6 heterozygotes, and 15 homozygotes. Error bars represent standard error.

B) Results of streptozotocin test presenting data from three independent experiments. Nine wild types, three heterozygotes, and ten homozygotes received streptozotocin treatment. Four wild types, three heterozygotes and five homozygotes received injections with vehicle only. Because there was no significant difference in glucose tolerance between heterozygous and homozygous transgenic animals, these results were pooled to generate a larger data pool that would be more statistically significant. The lines plot the average results for each of the four groups. The average for the treated wild types is represented as "STZ wildtype" with dark blue diamonds. The treated transgenics including both heterozygous and homozygous are represented with pink squares as "STZ transgenic". The average blood glucose of the wildtypes that received an injection of vehicle only is represented as the "control wildtype" with yellow triangles. The average of the heterozygous and homozygous transgenic that received vehicle only is represented as "control wildtype" with cyan/light blue "x". The results shown are the pooled averages for each group at each time point for three different experiments. Based on student's t-tests there is a significant protection of the transgenic animals versus their wildtype littermates. The error bars represent standard error.

A

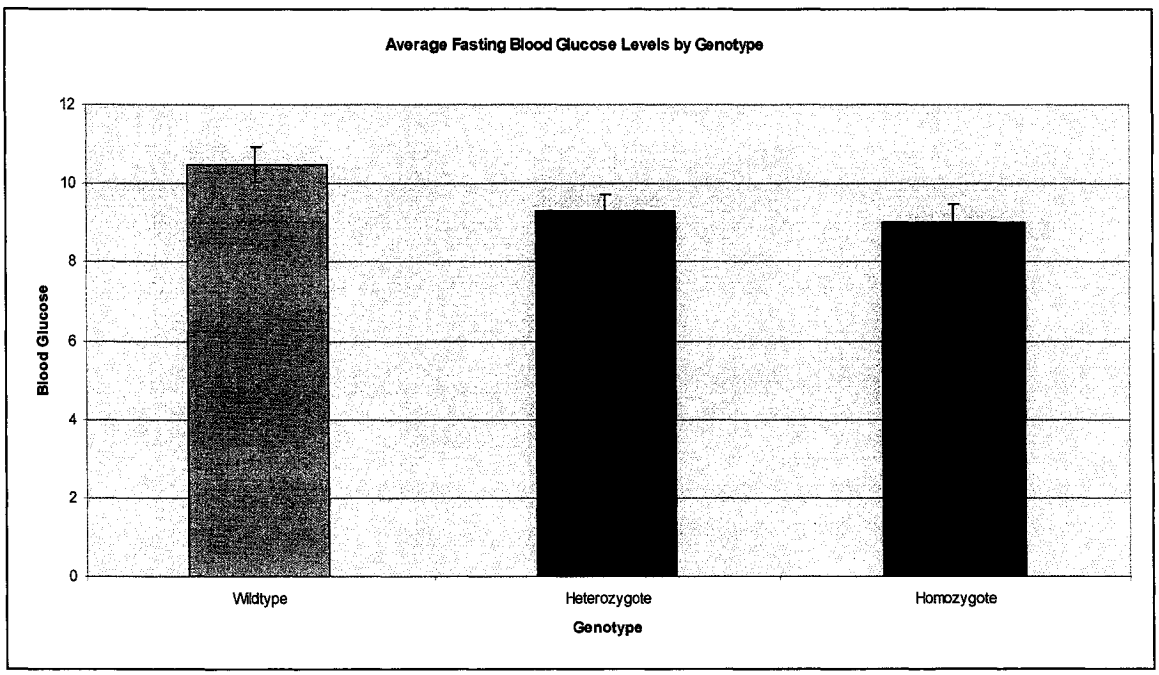

B

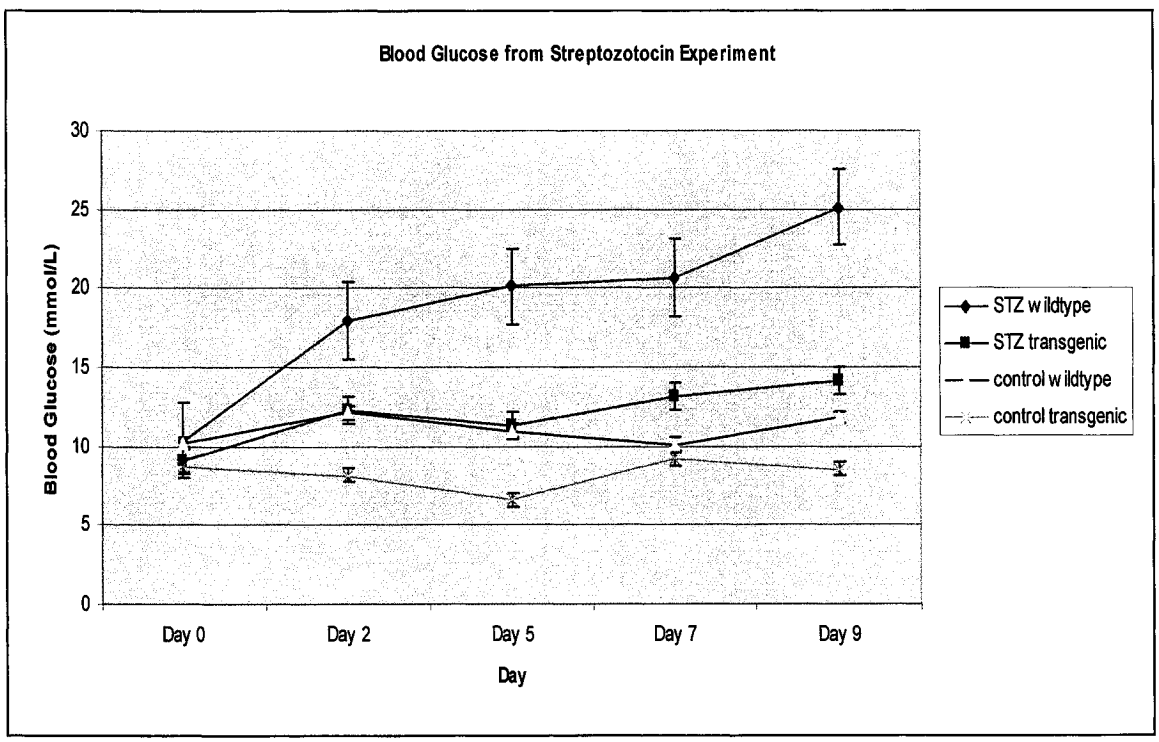

Figure 3-13

The two wildtype mice that received the injections showed significant increases in blood glucose over four readings post-injection while the three transgenic mice maintained blood glucose levels similar to the uninjected control.

The experiment was repeated twice, with eighteen animals and ten animals respectively. The results of all three experiments were pooled and the data shown in figure 3-13b represents the average of all three experiments. In total nine wild types, three heterozygotes, and ten homozygotes received streptozotocin treatment. Four wild types, three heterozygotes and five homozygotes received injections with vehicle only. After three trials, the pooled results show a significant suppression of apoptosis in the transgenic animals as determined using a student's t-test with $p<0.01$.

iii) Insulin immunohistochemistry of pancreas sections after treatment with streptozotocin

Mice that were subjected to streptozotocin treatment were sacrificed and perfused with 4% paraformaldehyde. The pancreas was removed and 10 um sections were cut on a cryostat. Representative sections were probed with anti-insulin. The signal was detected using a biotin-avidin conjugated system. Uninjected mice were used as a control for healthy islet appearance. Sections from three homozygous and two wild type mice were compared (figure 3-14). The control sections show intact islets while the wild type islets show complete destruction. Transgenic islets appeared to be slightly more fragmented than untreated but largely intact. The appearance of the islets after streptozotocin treatment is consistent with the results gathered from both the blood glucose levels and the glucose tolerance test.

Figure 3-14 Insulin expression in the islets after treatment with 150mg/kg streptozotocin

Pancreas sections were probed with an anti-insulin antibody and biotynylated anti-guinea pig secondary antibody. The signal was detected using an avidin biotin detection system and DAB peroxidase substrate.

A) The uninjected mouse has intact islets
B) The wildtype streptozotocin treated mouse has only the remnants of an islet that has been destroyed.
C) The transgenic streptozotocin treated mouse has islets that are slightly fragmented but largely still intact.

A

Uninjected control

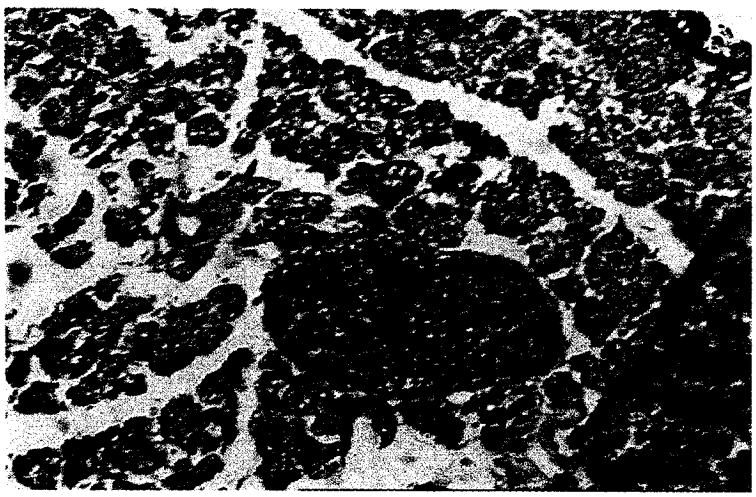

B

Wildtype treated with STZ

C

Transgenic treated with STZ

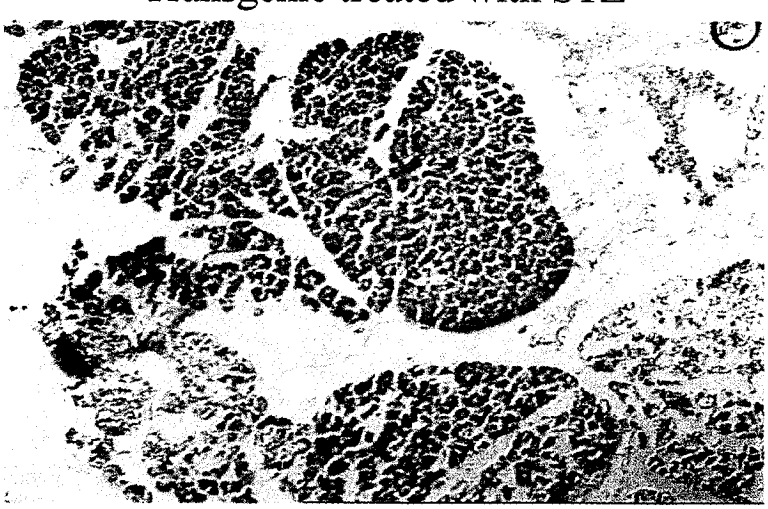

Figure 3-14

Part 3-4: The effects of XIAP over-expression on tumorigenesis

XIAP has a proven role in inhibiting apoptosis and has been shown to promote resistance to chemotherapy and radiation. As anti-sense XIAP therapy makes its way into the clinic it becomes imperative that the role of XIAP in tumorigenesis be fully understood. Furthermore, gene therapy with XIAP has been proposed for halting neuronal cell loss in diseases such as retinitis pigmentosa, spinal chord injury, Parkinson's disease and Huntington's disease. Although suppressing apoptosis is desirable in the context of gene therapy, an unintended effect may be the initiation of cancer.

In terms of its oncogenic potential, XIAP alone does not seem to promote tumorigenesis. In the two years of existence of the transgenic colony, there has not been a single incidence of cancer in the XIAP transgenic mice. None of the other three XIAP over-expressing transgenic mice were reported to have any predisposition to cancer (Wang et al., 2004). Though XIAP does not promote tumorigenesis in single transgenics, a complementary effect may be observed when XIAP is expressed in combination with a known oncogene such as c-myc or in the absence of a tumour suppressor such as p53.

The model system being used has been employed to demonstrate a complementary effect between c-myc and Bcl-x_L overexpression (Pelengaris 2002). Over-expression of Bcl-x_L on its own is considered weakly oncogenic. However, in combination with the oncogene c-myc, a complementary effect demonstrated by significantly accelerated tumorigenesis is observed in double transgenic mice. This effect has also been shown with c-myc and Bcl-2 double transgenics (Heiser et al., 2004). The complementation is derived from the high apoptotic potential of the c-myc oncogene. If the apoptosis can be blocked tumorigenesis

can proceed. The hypothesis is that the same principle can be applied with the XIAP transgenics.

a) Breeding of the UbiC-6 myc XIAP to a line of inducible c-myc transgenics

The model system takes advantage of the proliferative properties of the c-myc oncogene. The inducible c-myc transgene driven by the insulin promoter promotes hyper-proliferation of the beta cells. The increased rate of proliferation triggers an apoptotic response and destruction of the beta cells in the islets of Langerhans.

Double transgenic were created that had the additive effect of the constitutively active XIAP inhibiting apoptosis and the inducible c-myc causing proliferation. The inhibition of apoptosis through XIAP over-expression is hypothesized to create an environment where cells that are undergoing hyper-proliferation will not be eliminated by apoptosis. Instead the proliferating cells will be transformed and neoplastic growth of the islets will create insulinomas.

The PIns-ER^{tam} c-myc transgenics carry the c-myc transgene fused to the estrogen receptor such that the transgene-encoded fusion protein is maintained in the cytoplasm in a complex with the inhibitor of the estrogen receptor. When the mice are treated with 4-hydroxytamoxifen, the inhibitor is displaced and the fusion protein translocates to the nucleus. The inducible gene is driven by the mouse insulin promoter, which limits expression to the beta cells of the islets of Langerhans in the pancreas.

Litters from the XIAP/c-myc cross were genotyped for both transgenes. The c-myc transgene was detected by PCR as shown in figure 3-15A and the XIAP transgene was detected by Southern blot. Double and single transgenic offspring were used in tumorigenesis experiments. Five XIAP transgenic, five c-myc transgenic, five double

transgenic mice and five wild type control mice were given the 4-hydroxytamoxifen on six consecutive days.

b) Effects of the 4-hydroxytamoxifen on blood glucose levels

Myc protein was activated by intraperitoneal injections of 4-hydroxytamoxifen for six days. The animals were monitored for blood glucose levels on days 1, 3, and 6 of injections, and upon sacrifice on day 7 (see figure 3-15). A baseline was established over 3 consecutive days before the initial injection. The transgenic animals had a lower baseline blood glucose level but were still within the normal range for mice.

The first blood glucose reading at 24 hours showed a significant decrease into hypoglycemia for both the single myc transgenics and the myc & XIAP double transgenics. This drop is indicative of beta cell proliferation, which is consistent with observations made by Pelengaris et al. that proliferation begins within 24 hours of c-myc activation. At 72 hours of activation, both the single myc transgenics and the double myc & XIAP transgenics showed a significant increase in blood glucose levels which remained at hyperglycemic levels through day 6 and day 7 until sacrifice. This is consistent with an apoptotic response that destroys the beta cells decreasing the production of insulin.

There was variation in response between animals, especially on day 6 and day 7 when two of the myc & XIAP double transgenics returned to normoglycemia from their hyperglycemic readings at 72 hours.

Figure 3-15 Genotyping of the myc and XIAP double transgenic colony and fasting blood glucose levels by genotype with daily injections of 4-hydroxytamoxifen.

A) Detection of the presence of the c-myc transgene by PCR for the genotyping of single and double transgenics. Genomic DNA was extracted from the tail. Mice were positive if a band was detected. 2137, 2138, 2139, 2145, 2146, 2147, 2166, 2169, 2170, 2173, 2174, 2175 were negative. 2140, 2141, 2142, 2143, 2144, 2167, 2168, 2171 and 2172 were positive. The DNA was then tested by Southern blot for the XIAP transgene. Based on the c-myc PCR and the XIAP Southern blot, animals were assigned to one of four genotypic groups, wild type (myc -/ XIAP -), XIAP only (myc -/XIAP+), myc only (myc+/XIAP -) or double transgenic (myc+/XIAP+).

B) Graphic representation of blood glucose levels for each genotype. The baseline level was determined over 3 consecutive days before injection. Once injections had begun, readings were taken on day 1, 3, 6 and 7. The data points represent the average of the five animals for that time point. Dark blue diamonds represents the myc only animals. The pink squares represent XIAP only animals. The yellow triangles represent myc and XIAP double transgenics and the light blue X represents the control animals. Error bars indicate standard error.

A

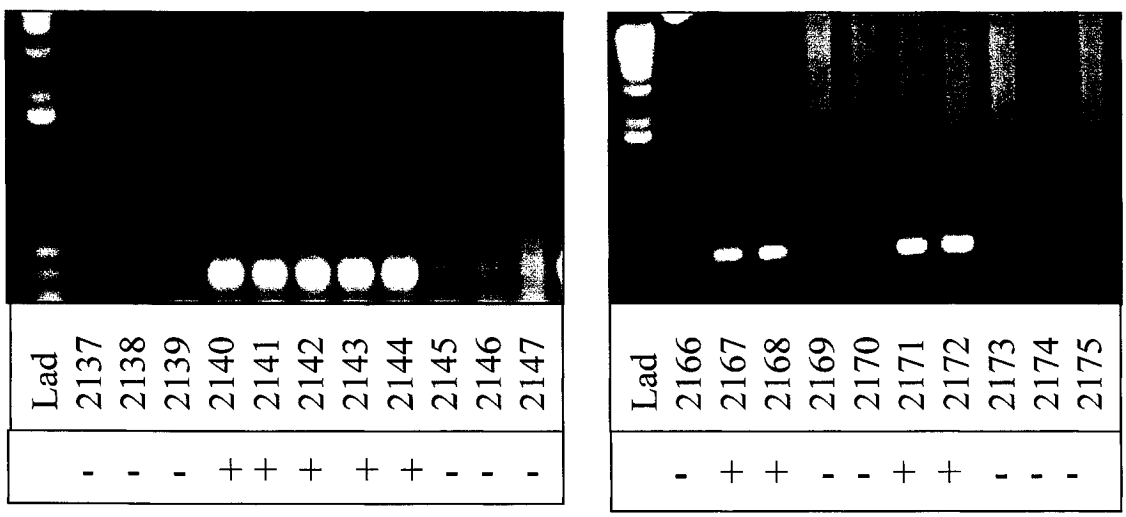

B

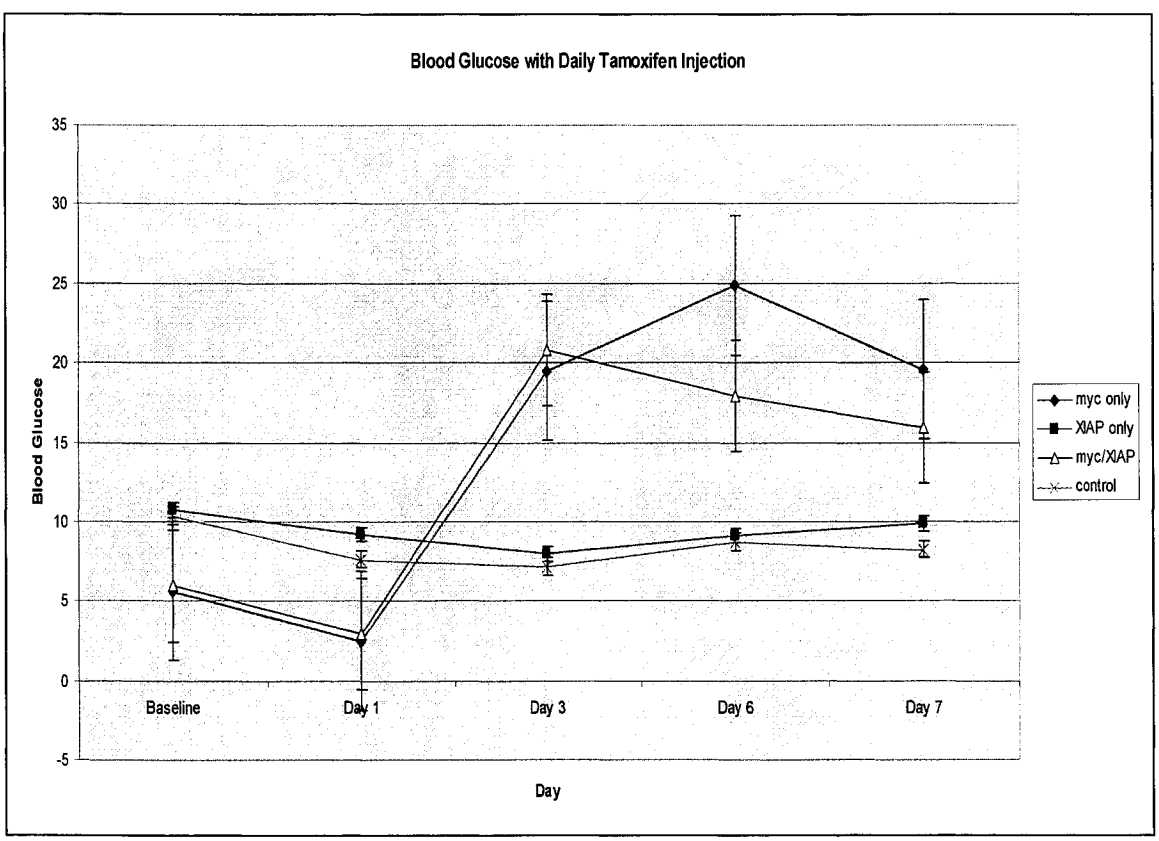

Figure 3-15

There was no significant difference in response between the c-myc single transgenics and the c-myc & XIAP double transgenics. Throughout the experiment both groups showed a similar response and there was no significant difference between the single and double transgenics at any time point as determined by a student's t-test with $p < 0.01$. Neither the XIAP single transgenics nor the wild type controls showed any response to tamoxifen injections. Both groups remained at their baseline normoglycemic levels throughout the experimental period.

b) Analysis of islets by histology and TUNEL

After seven days the mice were sacrificed, the pancreata were removed and 10-micron sections of the pancreas were cut on the cryostat and mounted on slides.

i) Histological analysis by hemotoxylin, phloxine and saffron

Sections were analyzed by hemotoxylin, phloxine and saffron (HPS). Hemotoxylin stains nuclei blue, phloxine stains the cytoplasm, muscle, and myelin red; and saffron stains the connective tissue yellow. HPS was chosen for histology because it is superior to the traditional hemotoxylin and eosin (H &E) because it also recognizes connective tissue. The HPS revealed that the islets in the c-myc single transgenics and the c-myc and XIAP double transgenics were much smaller than the islets in XIAP single transgenics and control animals.

ii) Insulin immunohistochemistry to detect changes in islet morphology

This observation was confirmed by insulin immunohistochemistry. In the c-myc single transgenics and c-myc and XIAP double transgenics the insulin positive cells were concentrated in small round islets while the XIAP single transgenics and the controls had the normal large oval islet morphology.

Figure 3-16 Immunohistochemistry of 4 OH tamoxifen treated myc/XIAP double transgenics including histology by HPS, insulin labelling to detect changes in beta cells and TUNEL labelling to detect cell death

After seven days the mice were sacrificed. The pancreas was removed, sectioned and analyzed for islets loss by hemotoxylin, phloxine, and saffron (HPS), insulin immunohistochemistry, and TUNEL.

1) HPS stains the nuclei blue; the cytoplasm, muscle, and myelin red; and the connective tissue yellow.
2) Insulin immunohistochemistry. Insulin positive cells appear dark brown.
3) TUNEL labels cells undergoing cell death. Dying cells are labelled in green.
    A) XIAP and c-myc double transgenics shown significant reduction in islet size as seen in the HPS and insulin labelling. The apoptotic cells are limited to the islets.
    B) C-myc single transgenics show an identical phenotype to the double transgenics. The islets are fewer in number and smaller as shown in the HPS and insulin labelling. TUNEL positive cells are concentrated in the islets.
    C) The XIAP single transgenics show normal islet morphology and insulin labelling. The only TUNEL positive cells are single cells and indicative of basal levels of apoptosis.
    D) The control animals showed normal islet morphology and insulin labelling. There is a basal level of apoptosis detected by TUNEL that is similar to the XIAP transgenics.

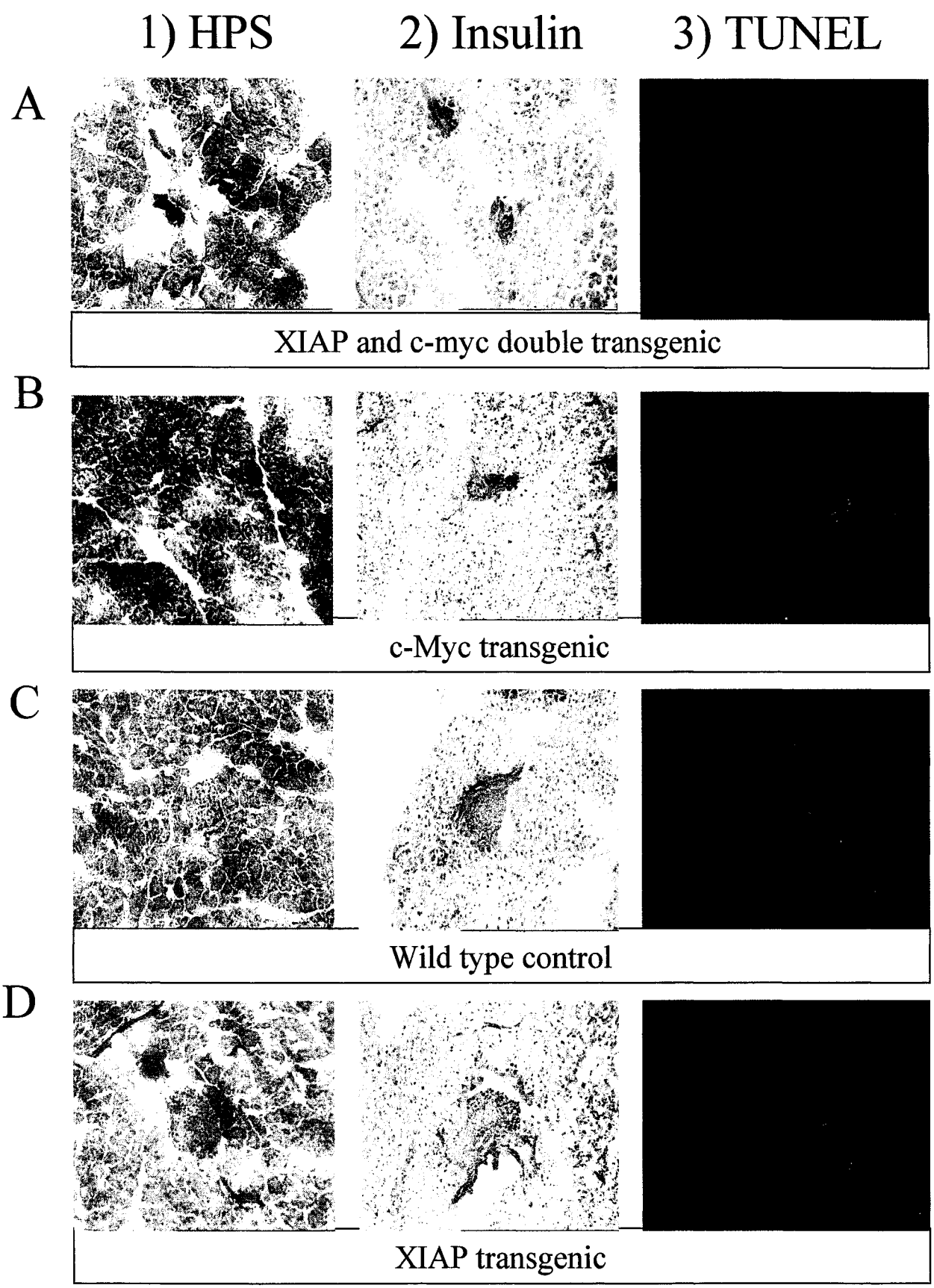
1) HPS
2) Insulin
3) TUNEL
A
XIAP and c-myc double transgenic
B
c-Myc transgenic
C
Wild type control
D
XIAP transgenic

Figure 3-16

iii) Analysis of cell death by TUNEL labelling

TUNEL analysis revealed a concentration of apoptotic cells in islet shaped areas in the double and c-myc single transgenics. The XIAP single transgenics and the control animals had some diffuse apoptosis but in random locations and none that could be considered more than a basal level of cell death.

The histology and TUNEL analysis confirm the observations reported in the blood glucose measurements. There was no significant difference between the c-myc single transgenics and the c-myc and XIAP double transgenics in the appearance of the islets. More significantly, there were signs of cell death present in the double transgenics. The presence of cell death in the islets indicates that XIAP fails to inhibit the cell death induced by the activation the c-myc oncogene.

c) Breeding p53 null mice to XIAP transgenics

An alternate model system that has been initiated employs the elimination of the p53 tumour suppressor, which is eliminated in 50% of all cancers. The p53 null animals have been bred onto the XIAP over-expressing background. P53 null animals already have a high incidence rate of spontaneous tumours; it is hypothesized that the presence of XIAP over-expression will alter that frequency.

The purpose of this second breeding program is to observe spontaneous mutations in XIAP transgenic/p53 null offspring. XIAP transgenic/ p53 +/- animals have been generated and are currently being inter-bred to establish p53 -/-, XIAP transgenic offspring. Once the colony has been established, long-term observation of the mice will begin to determine changes in the spontaneous tumour formation rate. This part of the project has been started but compilation of results is beyond the time frame of this project.

CHAPTER 4: DISCUSSION

A delicate balance exists between excessive cell death and the suppression of cell death in a healthy organism. Either too much or too little cell death can affect survival. Excessive cell death has been associated with neurological disorders including both acute injury such as trauma or stroke and chronic progressive conditions such as Parkinson's disease, Huntington's disease and retinitis pigmentosa. Gene therapy is actively being explored as a means of suppressing the apoptosis induced by these pathological conditions. In the context of gene therapy, it is important to document the effects of long-term over-expression of an apoptosis inhibitor on the entire organism to understand how it affects the body's normal functions and document any adverse effects.

At the same time, it is important to answer the question of how much suppression of cell death is possible without initiating tumorigenesis. Suppression of cell death has been identified as one of the six essential characteristics of all tumours (Hanahan and Weinberg, 2000). Though it has been identified as an important characteristic, it is not known how many of the apoptotic inhibitors are involved. Is suppression of cell death important for initiating tumours or is it more involved in progression, growth, metastasis, and resistance to treatment? The available evidence suggests that alterations in apoptotic pathways alone are not sufficient to induce tumorigenesis (Kaufmann and Vaux, 2003). This evidence comes from studies on the Bcl-2 over-expressing transgenic mice (Coleman et al., 1999; Dubois-Dauphin et al., 1994; Martinou et al., 1994; Zanjani et al., 1997) and several of the caspase knockout mouse models (Hakem et al., 1998; Kuida et al., 1998; Kuida et al., 1996).

There has been significant research on the role of XIAP in resistance to chemotherapy and radiation. XIAP has been shown to be up-regulated in chemotherapy resistant pancreatic (Trauzold et al., 2003), ovarian (Li et al., 2001), prostatic (Amantana et al., 2004)

and breast cancer (Lin et al., 2004) cells. XIAP protein levels have also been shown to increase between early and advanced stage renal cell carcinoma tumours (Yan et al., 2004).

IAPs have also been directly implicated in cancer initiation. The HIAP1/MLT fusion results from the t(11:18)(q21;q21) translocation in mucosa-associated lymphoid tissue (MALT) lymphoma. The fusion protein consists of the three BIR domains of HIAP1 fused to the paracaspase domain of MLT1. The paracaspase domain of the MLT1 protein activates NF-κB (Hosokawa et al., 2004). The HIAP1 promoter is itself NF-κB inducible, thereby generating a positive feedback loop. The relative importance of the HIAP1 BIR domains relative to other NF-κB genes is unknown at present. Numerous genes are induced by NF-κB, including several that have demonstrated an anti-apoptotic function, such as the A20 zinc-finger protein (He and Ting, 2002). Transgenic animal models of MALT1 with HIAP1 BIR domain deletions may be required to resolve this issue.

Several strategies have been used to decrease the level of IAPs and increase the level of apoptosis in tumour cells. These strategies include anti-sense and RNAi, two methods used to reduce the level of expression of IAPs, which enhance sensitivity to chemotherapy and slow tumour progression. XIAP anti-sense has been effective in a wide range of cancer types including breast (Lin et al., 2004), bladder (Bilim et al., 2003), lung (Hu et al., 2003) and leukemia (Carter et al., 2003). XIAP anti-sense therapy has also proven effective in xenograft models of non-small cell lung cancer and has recently entered clinical trials. XIAP RNAi is a newer technology but it appears to create the same or even more effective decrease in IAP expression (Ichim et al., 2004). XIAP RNAi has been shown to enhance the effectiveness of etoposide and doxorubicin in breast cancer (Lima et al., 2004) and to

overcome resistance to ceramide in glioma cell lines (Hatano et al., 2004). XIAP RNAi has also been used to sensitize melanoma cell lines to TRAIL (Chawla-Sarkar et al., 2004).

Difficulties associated with the delivery of antisense oligonucleotides or RNAi vectors make small molecule inhibitors a preferred therapeutic strategy for the pharmaceutical industry. Small molecule inhibitors have been developed that antagonize IAP activity. Embelin, a Japanese herb, exhibits inhibition of XIAP-BIR3-caspase-9 interaction (Nikolovska-Coleska et al., 2004). Peptides mimicking the XIAP inhibitory activity of Smac have been developed (Tamm et al., 2003). A family of polyphenylureas have also been identified that exhibit anti-XIAP activity (Schimmer et al., 2004).

Despite the high incidence of IAP over-expression in cell lines and tumour biopsy samples and the successes in using IAP inhibition in reducing resistance to therapy and slowing tumour progression; there is little direct evidence of the role XIAP plays in tumour establishment, growth, metastasis, and resistance to chemotherapy *in vivo*. The creation of the Ubiquitin-C 6 myc XIAP over-expressing mice provides an important tool to elucidate the role that XIAP plays in tumorigenesis.

A transgenic colony was created and founder lines characterized. The transgene produced physiologically relevant over-expression of mRNA transcripts and protein. XIAP is ubiquitously over-expressed but there is variation in the amount of XIAP expression within and among tissues. This tissue specific variation was consistent with the variability in protein expression seen in the Ubiquitin C promoter -GFP transgenic mice (Tsirigotis et al., 2001). This evidence indicates that tissue specific variation is most likely caused by the promoter and not the over-expressed protein. The protein expression created an approximately two-fold over-expression versus the wild type XIAP. Although transgene

expression levels are higher than in previously reported XIAP transgenic, this over-expression is not as dramatic an increase as that created through adenovirus infection or transfection in cell lines. The effects of long-term ubiquitous over-expression may be more physiologically relevant than artificially high levels created through temporary over-expression.

Founder mice were established by microinjection of C57BL/6 x C3H fertilized oocytes. The heterozygous mice were subsequently backcrossed onto wildtype C57BL/6 to achieve a single strain background and eliminate any effects of a mixed background. A homozygous line of transgenic mice was created. Homozygotes were identified through Phosphor imaging analysis. Homozygous mice produce twice as much protein as heterozygotes. The additive effect creates an approximate four-fold over-expression of XIAP in homozygous transgenics versus wild type.

Apoptosis is an important part of development and cell death is critical to the changes that transform the embryo into a fully developed organism. Several mouse models have been created that have either over-expressed apoptotic inhibitors or knocked out apoptotic effectors. In each of these cases development has been studied. These models include Bcl-2 transgenics(Coleman et al., 1999; Dubois-Dauphin et al., 1994; Martinou et al., 1994; Zanjani et al., 1997), Bax knockouts (White et al., 1998), caspase-9 knockouts (Kuida, 2000), caspase-3 knockouts (Leonard et al., 2002) and Apaf-1 knockouts. Despite major alterations in the expression of these critical proteins most of development proceeded without incident. The only organ system that was affected was the central nervous system and especially the brain. In several of these models there was a tendency for supernumerary neurons. The phenotype is particularly dramatic in the brains of caspase-3 and caspase-9

knockouts (Cowan and Roskams, 2004). Reduced apoptosis in caspase-3 and caspase-9 null mice results in ectopic neuronal tissue protruding from the skull, disruption of cortical structure, expansion of the ventricular zone, and sometimes hydrocephaly (Hakem et al., 1998; Kuida et al., 1998; Kuida et al., 1996).

A survey of critical points in embryogenesis revealed that in the transgenic animals XIAP over-expression does not significantly alter development. The normal transmission frequency of transgenic offspring in the colony was the first significant indication that the ubiquitous over-expression of XIAP does not affect embryogenesis. Any significant alterations in development that decreased embryonic viability would alter the frequency of transgenic offspring. The lack of any significant alterations in gross morphology during development in transgenics was not unexpected because it is consistent with most of the other models that had perturbed apoptotic pathways.

Even though the embryos appeared unaffected, a closer analysis of the brain was undertaken to determine if there was evidence of supernumerary neurons. Because XIAP is such a potent inhibitor of both caspase-3 and caspase-9, if a developmental phenotype existed for the XIAP over-expressing transgenics, it was expected that it would be visible in the brain and might mirror the effects of the caspase knockouts. Several different sections of the brain were probed for neuronal cell bodies and neuronal cell counts were compiled for each of the regions. No significant differences in cell counts were found between the XIAP over-expressing transgenics and the wild-type controls. This is a significant contrast to the caspase knockout phenotypes.

The lack of a developmental phenotype in the brain may be due to the release of endogenous inhibitors. It is possible that upon amplification of the apoptotic signal

increased levels of XIAP could be overwhelmed by the release of endogenous inhibitors such as Smac and Omi. The apoptotic amplification could also cause both endogenous and over-expressed XIAP to be degraded by the proteasome. In either of these cases, the amount of over-expression in the transgenics would not be enough to overcome endogenous regulation of XIAP within the cell.

An alternate explanation is that when caspase-mediated cell death is inhibited by the over-expression of XIAP, the cells undergo autophagy. It has been suggested that autophagy is a critical pathway for PCD during development. This correlates with the observation that cell death caused by growth factor deprivation in neural precursor cells has all the features of autophagy. This type of cell death cannot be inhibited by caspase inhibitors but can still be inhibited by Bcl-2 (Cardenas-Aguayo Mdel et al., 2003). It appears that altering the amount of XIAP does not significantly alter the programmed cell death that is so critical in development. This is consistent with the phenotype of the XIAP knockout, which did not have any visible developmental phenotype (Harlin et al., 2001).

If XIAP cannot interfere with development, is the over-expressed XIAP fully functional during embryogenesis? Primary mouse embryo fibroblasts (MEFs) were isolated from transgenic and wildtype embryos. In cell death assays, the transgene-encoded protein suppressed apoptosis triggered by etoposide in MEFs. The finding that the transgene-encoded protein was suppressing injury-induced apoptosis in cell cultures derived from embryonic tissue was significant because it indicated that XIAP was functional during embryogenesis. The evidence of a fully functional over-expressed XIAP that does not interfere with development during embryogenesis is intriguing. It invites speculation that injury induced apoptosis is differentially regulated from genetically programmed apoptosis.

During embryogenesis, XIAP regulates injury-induced apoptosis but does not affect developmental apoptosis. Perhaps there are other proteins that are specific to developmental apoptosis in the same way that XIAP appears to be specific for injury-induced apoptosis.

Transgenic primary hepatocyte cell cultures were also resistant to apoptosis. The XIAP over-expressing cells suppressed anti-Fas triggered cell death. When the apoptotic signal was elevated by the addition of cyclohexamide and anti-Fas, there was an attenuation of the XIAP mediated suppression of apoptosis. At higher doses of anti-Fas, the combination of general cellular stress induced by the cyclohexamide and the death receptor induced apoptosis caused by Fas activation overwhelmed the protection produced by the over-expression of XIAP. This may be due to the level of over-expression of XIAP. A two-fold over-expression in transgenic cells provides a level of suppression of apoptosis consistent with the amount of protein over-expressed.

To explore XIAP mediated suppression of apoptosis *in vivo,* XIAP over-expressing transgenics and wild type controls were treated with a single high dose of streptozotocin. Both heterozygous and homozygous transgenics showed suppression of apoptosis in this DNA damage inducing beta cell injury model. Not only did the transgenic animals show suppression of apoptosis after streptozotocin treatment, they also showed a significantly better glucose tolerance than the wild type animals. Both heterozygous and homozygous transgenics did not become as hyperglycemic as wild types after a bolus injection of glucose. Transgenic animals also returned to baseline normoglycemic levels faster than wildtypes. This indicates that the transgenic animals could tolerate islet stress better than their wildtype littermates even though their baseline levels were the same.

The suppression of apoptosis observed in the streptozotocin injury model is consistent with data from the thymocyte specific (Conte et al., 2001) and neuronal specific XIAP over-expressing transgenics (Crocker et al., 2003) that over-expression of XIAP can protect animals from injury induced apoptosis *in vivo*. However, the difference in XIAP over-expression between heterozygotes and homozygotes did not seem to affect the overall level of protection *in vivo*. In the results from the glucose challenge and the high dose streptozotocin injury, there was no significant difference between the response of heterozygotes and homozygotes.

XIAP over-expressing transgenic mice were crossed with a line of insulin promoter driven inducible c-myc transgenics. When the c-myc oncogene is induced it causes proliferation followed by apoptosis and destruction of the beta cells of the islets of Langherhans (Pelengaris et al., 2002). It was hypothesized that the XIAP over-expression in the double transgenics would prevent the c-myc induced apoptosis and promote transformation of the islets into insulinomas. This type of complementation had previously been demonstrated with Bcl-x_L in the same c-myc inducible system (Pelengaris et al., 2002). Based on the results of blood glucose measurements, insulin immunohistochemistry and TUNEL labelling it can be concluded that XIAP does not complement the c-myc oncogene and cannot suppress myc-induced apoptosis in this model.

Why does Bcl-x_L promote transformation in this system while XIAP does not? Perhaps it is not just the inhibition of apoptosis that is critical in transformation. Bcl-x_L and XIAP inhibit apoptosis at very different stages of the apoptotic amplification cascade. Bcl-x_L prevents mitochondrial apoptosis pathway activation and arrests the apoptotic signal before the mitochondrial membrane permeability has been compromised.

Cell death in mammary tumours developed in MMTV-c-myc transgenic mice has been observed to occur in the presence of low levels of caspase-3 and little PARP cleavage. Caspase-3 processing and PARP cleavage are two important indicators of classical caspase-dependent apoptosis. The authors suggested that a TUNEL positive, AIF mediated caspase independent cell death involving loss of mitochondrial integrity was occurring and not classical apoptosis (Liao and Dickson, 2003). In this case, even though caspase-dependent cell death is blocked, the loss of mitochondrial membrane integrity promotes a slower, less efficient cell death through the AIF pathway. Mitochondrial damage can also lead to cell death by autophagy. Tolkovsky observed the removal of the entire population of mitochondria by autophagy after toxic insult such as NGF-deprived neurons and staurosporine treated cells in the presence of caspase inhibitors. In this model, Bcl-2 over-expression blocks the removal of mitochondria without preventing death-inducing signals (Tolkovsky et al., 2002).

The placement of Bcl-2 family members upstream of mitochondrial signal amplification may be critical to preventing apoptosis driven by c-myc. XIAP inhibits caspase activation but it is not as effective at preventing caspase-independent apoptosis. The loss of mitochondrial membrane integrity also promotes the release of IAP inhibitors Smac and Omi further weakening the effect of XIAP.

XIAP may not prevent apoptosis in the presence of the c-myc oncogene but this is only one model of tumorigenesis. Fifty percent of all human cancers occur with the elimination of p53. There is a documented link between p53 and XIAP through Akt (Fraser et al., 2003). Because XIAP does play a significant role in the p53 tumour suppressor

pathway, there may be a more significant impact of XIAP over-expression in models involving mutant or deleted p53.

In the final analysis, the ubiquitous over-expression of XIAP in transgenic mice does not appear to be involved in the initiation of tumorigenesis on its own or in the c-myc model system. This is significant for the success of XIAP gene therapy for retinitis pigmentosa, Huntington's disease and Parkinson's disease. It indicates that long-term over-expression of XIAP in the entire organism does not have a risk of cancer initiation. It is not a negative result in the context of anti-sense therapy either. There is a well-documented effect of the role of XIAP in inducing resistance to radiation and chemotherapy in tumours. Etoposide and streptozotocin, two of the toxins used to induce apoptosis in this project are chemotherapeutic agents that have been successfully used in the clinic. If a four-fold over-expression of XIAP can suppress apoptosis then decreasing XIAP levels through anti-sense or RNAi would potentially have just as dramatic an impact on increasing the amount apoptosis. Anti-sense therapy to reduce XIAP levels in combination with these chemotherapeutic agents has the potential to be highly successful.

Taken together, the results indicate that ubiquitous over-expression of XIAP in this transgenic mouse model was successful. The mouse expressed physiologically relevant levels of transgene-encoded messenger RNA and protein in all tissues tested. XIAP does not appear to be involved in suppressing genetically pre-determined apoptosis during embryogenesis but primary cell cultures derived from embryonic tissue are resistant to injury induced apoptosis. The transgenic mouse shows a definite phenotype by being resistant to streptozotocin-induced apoptosis *in vivo*. At the same time, the over-expression

of XIAP does not suppress oncogene-induced apoptosis triggered by the induction of c-myc in the pancreas.

These results suggest a model where XIAP suppresses injury or stress induced apoptosis but is unable to block genetically pre-determined or oncogene-activated apoptosis. This implies that these pathways may be differentially regulated. Both developmental cell death and oncogene-induced cell death occur in situations that are highly controlled by the cell. Developmental apoptosis is genetically pre-determined while oncogene-induced apoptosis is a protective mechanism designed to shield the organism from inappropriate cell proliferation. In both these situations, the stimulus is controlled from within the organism. In contrast, injury induced apoptosis is a reaction to an outside stimulus. The organism is protecting itself by minimizing the damage to the entire organism and eliminating cells that are too damaged and may cause more damage if left intact.

XIAP appears to act as a safety mechanism to prevent unintentional cell death such as an excessive response to injury. It is highly regulated by signalling pathways, endogenous inhibitors such as Smac and Omi and the ubiquitin proteasome pathway. If apoptosis is occurring in response to internal signals such as developmental or oncogene-activated apoptosis then XIAP will be targeted by Smac or Omi and degraded by the proteasome. If the apoptosis is caused by injury or stress, the over-expression of XIAP can give the cell an extra chance to repair itself before it becomes fully committed to die.

References

Altieri, D. C. (2003). Survivin, versatile modulation of cell division and apoptosis in cancer. Oncogene *22*, 8581-8589.

Amantana, A., London, C. A., Iversen, P. L., and Devi, G. R. (2004). X-linked inhibitor of apoptosis protein inhibition induces apoptosis and enhances chemotherapy sensitivity in human prostate cancer cells. Mol Cancer Ther *3*, 699-707.

Arnt, C. R., and Kaufmann, S. H. (2003). The saintly side of Smac/DIABLO: giving anticancer drug-induced apoptosis a boost. Cell Death Differ *10*, 1118-1120.

Assuncao Guimaraes, C., and Linden, R. (2004). Programmed cell deaths. Apoptosis and alternative deathstyles. Eur J Biochem *271*, 1638-1650.

Bartke, T., Pohl, C., Pyrowolakis, G., and Jentsch, S. (2004). Dual Role of BRUCE as an Antiapoptotic IAP and a Chimeric E2/E3 Ubiquitin Ligase. Mol Cell *14*, 801-811.

Bilim, V., Kasahara, T., Hara, N., Takahashi, K., and Tomita, Y. (2003). Role of XIAP in the malignant phenotype of transitional cell cancer (TCC) and therapeutic activity of XIAP antisense oligonucleotides against multidrug-resistant TCC in vitro. Int J Cancer *103*, 29-37.

Blasiak, J., Sikora, A., Wozniak, K., and Drzewoski, J. (2004). Genotoxicity of streptozotocin in normal and cancer cells and its modulation by free radical scavengers. Cell Biol Toxicol *20*, 83-96.

Boatright, K. M., Deis, C., Denault, J. B., Sutherlin, D. P., and Salvesen, G. S. (2004). Activation of caspases 8 and 10 by FLIP L. Biochem J *Pt.*

Bratton, S. B., Lewis, J., Butterworth, M., Duckett, C. S., and Cohen, G. M. (2002). XIAP inhibition of caspase-3 preserves its association with the Apaf-1 apoptosome and prevents CD95- and Bax-induced apoptosis. Cell Death Differ *9*, 881-892.

Byun, D. S., Cho, K., Ryu, B. K., Lee, M. G., Kang, M. J., Kim, H. R., and Chi, S. G. (2003). Hypermethylation of XIAP-associated factor 1, a putative tumor suppressor gene from the 17p13.2 locus, in human gastric adenocarcinomas. Cancer Res *63*, 7068-7075.

Cande, C., Cohen, I., Daugas, E., Ravagnan, L., Larochette, N., Zamzami, N., and Kroemer, G. (2002). Apoptosis-inducing factor (AIF): a novel caspase-independent death effector released from mitochondria. Biochimie *84*, 215-222.

Cardenas-Aguayo Mdel, C., Santa-Olalla, J., Baizabal, J. M., Salgado, L. M., and Covarrubias, L. (2003). Growth factor deprivation induces an alternative non-apoptotic death mechanism that is inhibited by Bcl2 in cells derived from neural precursor cells. J Hematother Stem Cell Res *12*, 735-748.

Carter, B. Z., Milella, M., Tsao, T., McQueen, T., Schober, W. D., Hu, W., Dean, N. M., Steelman, L., McCubrey, J. A., and Andreeff, M. (2003). Regulation and targeting of antiapoptotic XIAP in acute myeloid leukemia. Leukemia *17*, 2081-2089.

Chawla-Sarkar, M., Bae, S. I., Reu, F. J., Jacobs, B. S., Lindner, D. J., and Borden, E. C. (2004). Downregulation of Bcl-2, FLIP or IAPs (XIAP and survivin) by siRNAs sensitizes resistant melanoma cells to Apo2L/TRAIL-induced apoptosis. Cell Death Differ *11*, 915-923.

Cheng, J. Q., Jiang, X., Fraser, M., Li, M., Dan, H. C., Sun, M., and Tsang, B. K. (2002). Role of X-linked inhibitor of apoptosis protein in chemoresistance in ovarian cancer: possible involvement of the phosphoinositide-3 kinase/Akt pathway. Drug Resist Updat *5*, 131-146.

Coleman, G. J., Bernard, C. C., and Bernard, O. (1999). Bcl-2 transgenic mice with increased number of neurons have a greater learning capacity. Brain Res *832*, 188-194.
Conte, D., Liston, P., Wong, J. W., Wright, K. E., and Korneluk, R. G. (2001). Thymocyte-targeted overexpression of xiap transgene disrupts T lymphoid apoptosis and maturation. Proc Natl Acad Sci U S A *98*, 5049-5054.
Cowan, C. M., and Roskams, A. J. (2004). Caspase-3 and caspase-9 mediate developmental apoptosis in the mouse olfactory system. J Comp Neurol *474*, 136-148.
Crocker, S. J., Liston, P., Anisman, H., Lee, C. J., Smith, P. D., Earl, N., Thompson, C. S., Park, D. S., Korneluk, R. G., and Robertson, G. S. (2003). Attenuation of MPTP-induced neurotoxicity and behavioural impairment in NSE-XIAP transgenic mice. Neurobiol Dis *12*, 150-161.
Dan, H. C., Sun, M., Kaneko, S., Feldman, R. I., Nicosia, S. V., Wang, H. G., Tsang, B. K., and Cheng, J. Q. (2004). Akt phosphorylation and stabilization of X-linked inhibitor of apoptosis protein (XIAP). J Biol Chem *279*, 5405-5412.
Debatin, K. M. (2004). Apoptosis pathways in cancer and cancer therapy. Cancer Immunol Immunother *53*, 153-159.
Debatin, K. M., and Krammer, P. H. (2004). Death receptors in chemotherapy and cancer. Oncogene *23*, 2950-2966.
Deveraux, Q. L., and Reed, J. C. (1999). IAP family proteins--suppressors of apoptosis. Genes Dev *13*, 239-252.
Dierlamm, J., Baens, M., Wlodarska, I., Stefanova-Ouzounova, M., Hernandez, J. M., Hossfeld, D. K., De Wolf-Peeters, C., Hagemeijer, A., Van den Berghe, H., and Marynen, P. (1999). The apoptosis inhibitor gene API2 and a novel 18q gene, MLT, are recurrently rearranged in the t(11;18)(q21;q21)p6ssociated with mucosa-associated lymphoid tissue lymphomas. Blood *93*, 3601-3609.
Dubois-Dauphin, M., Frankowski, H., Tsujimoto, Y., Huarte, J., and Martinou, J. C. (1994). Neonatal motoneurons overexpressing the bcl-2 protooncogene in transgenic mice are protected from axotomy-induced cell death. Proc Natl Acad Sci U S A *91*, 3309-3313.
Ekshyyan, O., and Aw, T. Y. (2004). Apoptosis in acute and chronic neurological disorders. Front Biosci *9*, 1567-1576.
Ferri, K. F., and Kroemer, G. (2001). Organelle-specific initiation of cell death pathways. Nat Cell Biol *3*, E255-263.
Fong, W. G., Liston, P., Rajcan-Separovic, E., St Jean, M., Craig, C., and Korneluk, R. G. (2000). Expression and genetic analysis of XIAP-associated factor 1 (XAF1) in cancer cell lines. Genomics *70*, 113-122.
Fraser, M., Leung, B. M., Yan, X., Dan, H. C., Cheng, J. Q., and Tsang, B. K. (2003). p53 is a determinant of X-linked inhibitor of apoptosis protein/Akt-mediated chemoresistance in human ovarian cancer cells. Cancer Res *63*, 7081-7088.
Fulda, S., Wick, W., Weller, M., and Debatin, K. M. (2002). Smac agonists sensitize for Apo2L/TRAIL- or anticancer drug-induced apoptosis and induce regression of malignant glioma in vivo. Nat Med *8*, 808-815.
Glover, C. J., Hite, K., DeLosh, R., Scudiero, D. A., Fivash, M. J., Smith, L. R., Fisher, R. J., Wu, J. W., Shi, Y., Kipp, R. A., *et al.* (2003). A high-throughput screen for identification of molecular mimics of Smac/DIABLO utilizing a fluorescence polarization assay. Anal Biochem *320*, 157-169.

Hakem, R., Hakem, A., Duncan, G. S., Henderson, J. T., Woo, M., Soengas, M. S., Elia, A., de la Pompa, J. L., Kagi, D., Khoo, W., *et al.* (1998). Differential requirement for caspase 9 in apoptotic pathways in vivo. Cell *94*, 339-352.
Hanahan, D., and Weinberg, R. A. (2000). The hallmarks of cancer. Cell *100*, 57-70.
Harlin, H., Reffey, S. B., Duckett, C. S., Lindsten, T., and Thompson, C. B. (2001). Characterization of XIAP-deficient mice. Mol Cell Biol *21*, 3604-3608.
Hatano, M., Mizuno, M., and Yoshida, J. (2004). Enhancement of C2-ceramide antitumor activity by small interfering RNA on X chromosome-linked inhibitor of apoptosis protein in resistant human glioma cells. J Neurosurg *101*, 119-127.
He, K. L., and Ting, A. T. (2002). A20 inhibits tumor necrosis factor (TNF) alpha-induced apoptosis by disrupting recruitment of TRADD and RIP to the TNF receptor 1 complex in Jurkat T cells. Mol Cell Biol *22*, 6034-6045.
Hegde, R., Srinivasula, S. M., Datta, P., Madesh, M., Wassell, R., Zhang, Z., Cheong, N., Nejmeh, J., Fernandes-Alnemri, T., Hoshino, S., and Alnemri, E. S. (2003). The polypeptide chain-releasing factor GSPT1/eRF3 is proteolytically processed into an IAP-binding protein. J Biol Chem *278*, 38699-38706.
Heiser, D., Labi, V., Erlacher, M., and Villunger, A. (2004). The Bcl-2 protein family and its role in the development of neoplastic disease. Exp Gerontol *39*, 1125-1135.
Hill, M. M., Adrain, C., Duriez, P. J., Creagh, E. M., and Martin, S. J. (2004). Analysis of the composition, assembly kinetics and activity of native Apaf-1 apoptosomes. Embo J *23*, 2134-2145.
Holcik, M., and Korneluk, R. G. (2000). Functional characterization of the X-linked inhibitor of apoptosis (XIAP) internal ribosome entry site element: role of La autoantigen in XIAP translation. Mol Cell Biol *20*, 4648-4657.
Hosokawa, Y., Suzuki, H., Suzuki, Y., Takahashi, R., and Seto, M. (2004). Antiapoptotic function of apoptosis inhibitor 2-MALT1 fusion protein involved in t(11;18)(q21;q21) mucosa-associated lymphoid tissue lymphoma. Cancer Res *64*, 3452-3457.
Hu, S., and Yang, X. (2003). Cellular inhibitor of apoptosis 1 and 2 are ubiquitin ligases for the apoptosis inducer Smac/DIABLO. J Biol Chem *278*, 10055-10060.
Hu, Y., Cherton-Horvat, G., Dragowska, V., Baird, S., Korneluk, R. G., Durkin, J. P., Mayer, L. D., and LaCasse, E. C. (2003). Antisense oligonucleotides targeting XIAP induce apoptosis and enhance chemotherapeutic activity against human lung cancer cells in vitro and in vivo. Clin Cancer Res *9*, 2826-2836.
Huang, Y., Rich, R. L., Myszka, D. G., and Wu, H. (2003). Requirement of both the second and third BIR domains for the relief of X-linked inhibitor of apoptosis protein (XIAP)-mediated caspase inhibition by Smac. J Biol Chem *278*, 49517-49522.
Ichim, T. E., Li, M., Qian, H., Popov, I. A., Rycerz, K., Zheng, X., White, D., Zhong, R., and Min, W. P. (2004). RNA interference: a potent tool for gene-specific therapeutics. Am J Transplant *4*, 1227-1236.
Kamsteeg, M., Rutherford, T., Sapi, E., Hanczaruk, B., Shahabi, S., Flick, M., Brown, D., and Mor, G. (2003). Phenoxodiol--an isoflavone analog--induces apoptosis in chemoresistant ovarian cancer cells. Oncogene *22*, 2611-2620.
Kaufmann, S. H., and Vaux, D. L. (2003). Alterations in the apoptotic machinery and their potential role in anticancer drug resistance. Oncogene *22*, 7414-7430.
Kerr, J. F. (2002). History of the events leading to the formulation of the apoptosis concept. Toxicology *181-182*, 471-474.

Kim, E. H., Kim, S. U., Shin, D. Y., and Choi, K. S. (2004). Roscovitine sensitizes glioma cells to TRAIL-mediated apoptosis by downregulation of survivin and XIAP. Oncogene *23*, 446-456.
Kipp, R. A., Case, M. A., Wist, A. D., Cresson, C. M., Carrell, M., Griner, E., Wiita, A., Albiniak, P. A., Chai, J., Shi, Y., *et al.* (2002). Molecular targeting of inhibitor of apoptosis proteins based on small molecule mimics of natural binding partners. Biochemistry *41*, 7344-7349.
Kirkin, V., Joos, S., and Zornig, M. (2004). The role of Bcl-2 family members in tumorigenesis. Biochim Biophys Acta *1644*, 229-249.
Korhonen, L., Belluardo, N., and Lindholm, D. (2001). Regulation of X-chromosome-linked inhibitor of apoptosis protein in kainic acid-induced neuronal death in the rat hippocampus. Mol Cell Neurosci *17*, 364-372.
Kugler, S., Straten, G., Kreppel, F., Isenmann, S., Liston, P., and Bahr, M. (2000). The X-linked inhibitor of apoptosis (XIAP) prevents cell death in axotomized CNS neurons in vivo. Cell Death Differ *7*, 815-824.
Kuida, K. (2000). Caspase-9. Int J Biochem Cell Biol *32*, 121-124.
Kuida, K., Haydar, T. F., Kuan, C. Y., Gu, Y., Taya, C., Karasuyama, H., Su, M. S., Rakic, P., and Flavell, R. A. (1998). Reduced apoptosis and cytochrome c-mediated caspase activation in mice lacking caspase 9. Cell *94*, 325-337.
Kuida, K., Zheng, T. S., Na, S., Kuan, C., Yang, D., Karasuyama, H., Rakic, P., and Flavell, R. A. (1996). Decreased apoptosis in the brain and premature lethality in CPP32-deficient mice. Nature *384*, 368-372.
LaCasse, E. C., Baird, S., Korneluk, R. G., and MacKenzie, A. E. (1998). The inhibitors of apoptosis (IAPs) and their emerging role in cancer. Oncogene *17*, 3247-3259.
Leaman, D. W., Chawla-Sarkar, M., Vyas, K., Reheman, M., Tamai, K., Toji, S., and Borden, E. C. (2002). Identification of X-linked inhibitor of apoptosis-associated factor-1 as an interferon-stimulated gene that augments TRAIL Apo2L-induced apoptosis. J Biol Chem *277*, 28504-28511.
Leonard, J. R., Klocke, B. J., D'Sa, C., Flavell, R. A., and Roth, K. A. (2002). Strain-dependent neurodevelopmental abnormalities in caspase-3-deficient mice. J Neuropathol Exp Neurol *61*, 673-677.
Levkau, B., Garton, K. J., Ferri, N., Kloke, K., Nofer, J. R., Baba, H. A., Raines, E. W., and Breithardt, G. (2001). xIAP induces cell-cycle arrest and activates nuclear factor-kappaB : new survival pathways disabled by caspase-mediated cleavage during apoptosis of human endothelial cells. Circ Res *88*, 282-290.
Lewis, J., Burstein, E., Reffey, S. B., Bratton, S. B., Roberts, A. B., and Duckett, C. S. (2004). Uncoupling of the signaling and caspase-inhibitory properties of X-linked inhibitor of apoptosis. J Biol Chem *279*, 9023-9029.
Li, J., Feng, Q., Kim, J. M., Schneiderman, D., Liston, P., Li, M., Vanderhyden, B., Faught, W., Fung, M. F., Senterman, M., *et al.* (2001). Human ovarian cancer and cisplatin resistance: possible role of inhibitor of apoptosis proteins. Endocrinology *142*, 370-380.
Liao, D. J., and Dickson, R. B. (2003). Cell death in MMTV-c-myc transgenic mouse mammary tumors may not be typical apoptosis. Lab Invest *83*, 1437-1449.
Lima, R. T., Martins, L. M., Guimaraes, J. E., Sambade, C., and Vasconcelos, M. H. (2004). Specific downregulation of bcl-2 and xIAP by RNAi enhances the effects of

chemotherapeutic agents in MCF-7 human breast cancer cells. Cancer Gene Ther *11*, 309-316.
Lin, M. T., Chang, C. C., Chen, S. T., Chang, H. L., Su, J. L., Chau, Y. P., and Kuo, M. L. (2004). Cyr61 Expression Confers Resistance to Apoptosis in Breast Cancer MCF-7 Cells by a Mechanism of NF-{kappa}B-dependent XIAP Up-Regulation. J Biol Chem *279*, 24015-24023.
Liston, P., Fong, W. G., Kelly, N. L., Toji, S., Miyazaki, T., Conte, D., Tamai, K., Craig, C. G., McBurney, M. W., and Korneluk, R. G. (2001). Identification of XAF1 as an antagonist of XIAP anti-Caspase activity. Nat Cell Biol *3*, 128-133.
Liston, P., Fong, W. G., and Korneluk, R. G. (2003). The inhibitors of apoptosis: there is more to life than Bcl2. Oncogene *22*, 8568-8580.
Malaguarnera, L. (2004). Implications of apoptosis regulators in tumorigenesis. Cancer Metastasis Rev *23*, 367-387.
Martinou, J. C., Frankowski, H., Missotten, M., Martinou, I., Potier, L., and Dubois-Dauphin, M. (1994). Bcl-2 and neuronal selection during development of the nervous system. J Physiol Paris *88*, 209-211.
McDonald, E. R., 3rd, and El-Deiry, W. S. (2004). Suppression of caspase-8- and -10-associated RING proteins results in sensitization to death ligands and inhibition of tumor cell growth. Proc Natl Acad Sci U S A *101*, 6170-6175.
Miller, L. K. (1999). An exegesis of IAPs: salvation and surprises from BIR motifs. Trends Cell Biol *9*, 323-328.
Mirkes, P. E. (2002). 2001 Warkany lecture: to die or not to die, the role of apoptosis in normal and abnormal mammalian development. Teratology *65*, 228-239.
Nachmias, B., Ashhab, Y., and Ben-Yehuda, D. (2004). The inhibitor of apoptosis protein family (IAPs): an emerging therapeutic target in cancer. Semin Cancer Biol *14*, 231-243.
Nemoto, T., Kitagawa, M., Hasegawa, M., Ikeda, S., Akashi, T., Takizawa, T., Hirokawa, K., and Koike, M. (2004). Expression of IAP family proteins in esophageal cancer. Exp Mol Pathol *76*, 253-259.
Nikolovska-Coleska, Z., Xu, L., Hu, Z., Tomita, Y., Li, P., Roller, P. P., Wang, R., Fang, X., Guo, R., Zhang, M., *et al.* (2004). Discovery of embelin as a cell-permeable, small-molecular weight inhibitor of XIAP through structure-based computational screening of a traditional herbal medicine three-dimensional structure database. J Med Chem *47*, 2430-2440.
Norbury, C. J., and Zhivotovsky, B. (2004). DNA damage-induced apoptosis. Oncogene *23*, 2797-2808.
Oppenheim, R. W. (1991). Cell death during development of the nervous system. Annu Rev Neurosci *14*, 453-501.
Orrenius, S. (2004). Mitochondrial regulation of apoptotic cell death. Toxicol Lett *149*, 19-23.
Pei, Z., Chu, L., Zou, W., Zhang, Z., Qiu, S., Qi, R., Gu, J., Qian, C., and Liu, X. (2004). An oncolytic adenoviral vector of Smac increases antitumor activity of TRAIL against HCC in human cells and in mice. Hepatology *39*, 1371-1381.
Pelengaris, S., Khan, M., and Evan, G. I. (2002). Suppression of Myc-induced apoptosis in beta cells exposes multiple oncogenic properties of Myc and triggers carcinogenic progression. Cell *109*, 321-334.

Perrelet, D., Perrin, F. E., Liston, P., Korneluk, R. G., MacKenzie, A., Ferrer-Alcon, M., and Kato, A. C. (2004). Motoneuron resistance to apoptotic cell death in vivo correlates with the ratio between X-linked inhibitor of apoptosis proteins (XIAPs) and its inhibitor, XIAP-associated factor 1. J Neurosci *24*, 3777-3785.
Raff, M. (1998). Cell suicide for beginners. Nature *396*, 119-122.
Roy, N., Mahadevan, M. S., McLean, M., Shutler, G., Yaraghi, Z., Farahani, R., Baird, S., Besner-Johnston, A., Lefebvre, C., Kang, X., and et al. (1995). The gene for neuronal apoptosis inhibitory protein is partially deleted in individuals with spinal muscular atrophy. Cell *80*, 167-178.
Saelens, X., Festjens, N., Walle, L. V., van Gurp, M., van Loo, G., and Vandenabeele, P. (2004). Toxic proteins released from mitochondria in cell death. Oncogene *23*, 2861-2874.
Salvesen, G. S., and Abrams, J. M. (2004). Caspase activation - stepping on the gas or releasing the brakes? Lessons from humans and flies. Oncogene *23*, 2774-2784.
Sanna, M. G., da Silva Correia, J., Ducrey, O., Lee, J., Nomoto, K., Schrantz, N., Deveraux, Q. L., and Ulevitch, R. J. (2002a). IAP suppression of apoptosis involves distinct mechanisms: the TAK1/JNK1 signaling cascade and caspase inhibition. Mol Cell Biol *22*, 1754-1766.
Sanna, M. G., da Silva Correia, J., Luo, Y., Chuang, B., Paulson, L. M., Nguyen, B., Deveraux, Q. L., and Ulevitch, R. J. (2002b). ILPIP, a novel anti-apoptotic protein that enhances XIAP-mediated activation of JNK1 and protection against apoptosis. J Biol Chem *277*, 30454-30462.
Schimmer, A. D., Welsh, K., Pinilla, C., Wang, Z., Krajewska, M., Bonneau, M. J., Pedersen, I. M., Kitada, S., Scott, F. L., Bailly-Maitre, B., *et al.* (2004). Small-molecule antagonists of apoptosis suppressor XIAP exhibit broad antitumor activity. Cancer Cell *5*, 25-35.
Sedivy, R., Wolf, B., Kalipciyan, M., Steger, G. G., Karner-Hanusch, J., and Mader, R. M. (2000). Genetic analysis of multiple synchronous lesions of the colon adenoma-carcinoma sequence. Br J Cancer *82*, 1276-1282.
Shankar, S., and Srivastava, R. K. (2004). Enhancement of therapeutic potential of TRAIL by cancer chemotherapy and irradiation: mechanisms and clinical implications. Drug Resist Updat *7*, 139-156.
Sharpe, J. C., Arnoult, D., and Youle, R. J. (2004). Control of mitochondrial permeability by Bcl-2 family members. Biochim Biophys Acta *1644*, 107-113.
Shi, Y. (2004). Caspase activation: revisiting the induced proximity model. Cell *117*, 855-858.
Shin, H., Okada, K., Wilkinson, J. C., Solomon, K. M., Duckett, C. S., Reed, J. C., and Salvesen, G. S. (2003). Identification of ubiquitination sites on the X-linked inhibitor of apoptosis protein. Biochem J *373*, 965-971.
Shiozaki, E. N., Chai, J., Rigotti, D. J., Riedl, S. J., Li, P., Srinivasula, S. M., Alnemri, E. S., Fairman, R., and Shi, Y. (2003). Mechanism of XIAP-mediated inhibition of caspase-9. Mol Cell *11*, 519-527.
Sorenson, C. M. (2004). Bcl-2 family members and disease. Biochim Biophys Acta *1644*, 169-177.
Strasser, A., Harris, A. W., and Cory, S. (1993). E mu-bcl-2 transgene facilitates spontaneous transformation of early pre-B and immunoglobulin-secreting cells but not T cells. Oncogene *8*, 1-9.

Suzuki, Y., Nakabayashi, Y., and Takahashi, R. (2001). Ubiquitin-protein ligase activity of X-linked inhibitor of apoptosis protein promotes proteasomal degradation of caspase-3 and enhances its anti-apoptotic effect in Fas-induced cell death. Proc Natl Acad Sci U S A *98*, 8662-8667.

Tamm, I., Trepel, M., Cardo-Vila, M., Sun, Y., Welsh, K., Cabezas, E., Swatterthwait, A., Arap, W., Reed, J. C., and Pasqualini, R. (2003). Peptides targeting caspase inhibitors. J Biol Chem *278*, 14401-14405.

Tolkovsky, A. M., Xue, L., Fletcher, G. C., and Borutaite, V. (2002). Mitochondrial disappearance from cells: a clue to the role of autophagy in programmed cell death and disease? Biochimie *84*, 233-240.

Trapp, T., Korhonen, L., Besselmann, M., Martinez, R., Mercer, E. A., and Lindholm, D. (2003). Transgenic mice overexpressing XIAP in neurons show better outcome after transient cerebral ischemia. Mol Cell Neurosci *23*, 302-313.

Trauzold, A., Schmiedel, S., Roder, C., Tams, C., Christgen, M., Oestern, S., Arlt, A., Westphal, S., Kapischke, M., Ungefroren, H., and Kalthoff, H. (2003). Multiple and synergistic deregulations of apoptosis-controlling genes in pancreatic carcinoma cells. Br J Cancer *89*, 1714-1721.

Tsirigotis, M., Thurig, S., Dube, M., Vanderhyden, B. C., Zhang, M., and Gray, D. A. (2001). Analysis of ubiquitination in vivo using a transgenic mouse model. Biotechniques *31*, 120-126, 128, 130.

Vaux, D. L., and Silke, J. (2003). Mammalian mitochondrial IAP binding proteins. Biochem Biophys Res Commun *304*, 499-504.

Wang, X., Zhu, C., Hagberg, H., Korhonen, L., Sandberg, M., Lindholm, D., and Blomgren, K. (2004). X-linked inhibitor of apoptosis (XIAP) protein protects against caspase activation and tissue loss after neonatal hypoxia-ischemia. Neurobiol Dis *16*, 179-189.

White, F. A., Keller-Peck, C. R., Knudson, C. M., Korsmeyer, S. J., and Snider, W. D. (1998). Widespread elimination of naturally occurring neuronal death in Bax-deficient mice. J Neurosci *18*, 1428-1439.

Xu, D., Bureau, Y., McIntyre, D. C., Nicholson, D. W., Liston, P., Zhu, Y., Fong, W. G., Crocker, S. J., Korneluk, R. G., and Robertson, G. S. (1999). Attenuation of ischemia-induced cellular and behavioral deficits by X chromosome-linked inhibitor of apoptosis protein overexpression in the rat hippocampus. J Neurosci *19*, 5026-5033.

Yan, Y., Mahotka, C., Heikaus, S., Shibata, T., Wethkamp, N., Liebmann, J., Suschek, C. V., Guo, Y., Gabbert, H. E., Gerharz, C. D., and Ramp, U. (2004). Disturbed balance of expression between XIAP and Smac/DIABLO during tumour progression in renal cell carcinomas. Br J Cancer.

Yang, Q. H., Church-Hajduk, R., Ren, J., Newton, M. L., and Du, C. (2003). Omi/HtrA2 catalytic cleavage of inhibitor of apoptosis (IAP) irreversibly inactivates IAPs and facilitates caspase activity in apoptosis. Genes Dev *17*, 1487-1496.

Yang, Y., and Yu, X. (2003). Regulation of apoptosis: the ubiquitous way. Faseb J *17*, 790-799.

Yoshida, H., Kong, Y. Y., Yoshida, R., Elia, A. J., Hakem, A., Hakem, R., Penninger, J. M., and Mak, T. W. (1998). Apaf1 is required for mitochondrial pathways of apoptosis and brain development. Cell *94*, 739-750.

Zanjani, H. S., Vogel, M. W., Delhaye-Bouchaud, N., Martinou, J. C., and Mariani, J. (1997). Increased inferior olivary neuron and cerebellar granule cell numbers in transgenic mice overexpressing the human Bcl-2 gene. J Neurobiol *32*, 502-516.
Zhou, M., Gu, L., Li, F., Zhu, Y., Woods, W. G., and Findley, H. W. (2002). DNA damage induces a novel p53-survivin signaling pathway regulating cell cycle and apoptosis in acute lymphoblastic leukemia cells. J Pharmacol Exp Ther *303*, 124-131.

National Capital Region YMCA-YWCA Bonenfant Outdoor Centre
Supervised outdoor education program staff. Acted as a liaison between teachers, group leaders and the YMCA. Created program schedules and staff schedules. Created specialized programs tailored to individual group needs.

CPR INSTRUCTOR September 2001 – April 2002
University of Guelph Athletics
Instructor for Cardio-Pulmonary Resuscitation (CPR) courses to university students and staff.

ASSISTANT DAY CAMP DIRECTOR May to August 2001
YMCA-YWCA of Guelph
Supervised staff and assisted in planning and running staff training. Wrote staff manual, designed program activities and set up program schedules. Responsible for all first aid and medication administered to campers.

HEAD LIFEGUARD AND LIFEGUARD September 1998 to April 2002
University of Guelph Athletics
Head lifeguard (2000-2001) worked as a member of a team to hire and train lifeguards and manage all aspects of the operation of the aquatic facility, also responsible for all first aid equipment. Lifeguard (1998-2002) supervised pool users and taught swimming lessons to adults and children.

WATERFRONT COORDINATOR May to August 1999 and 2000
OUTDOOR EDUCATION PROGRAM STAFF
National Capital Region YMCA YWCA Outdoor Centre
Coordinator duties included supervising eight waterfront staff, teaching canoeing, kayaking, swimming and lifesaving, and training staff for emergencies. Responsible for waterfront maintenance, staff scheduling and first aid.

VOLUNTEER EXPERIENCE

VOLUNTEER PARTNER September 2002 to present
Let's Talk Science Partnership Program
Performing demonstrations in biology, genetics, forensics, HIV/AIDS and ecology for elementary and secondary school students

MODERATOR FOR THE YOUTH GENOME FORUM May 2003
Youth Genome Forum at the Canadian Museum of Nature
Helping high school students interpret presentations from experts on genetically modified organisms, genomics, and cancer genetics.

GRADUATE STUDENT REPRESENTATIVE September 2002 to present
Faculty Council for the University of Ottawa Faculty of Medicine

STUDENT REPRESENTATIVE September 2000 to April 2001
Department of Athletics Health and Safety Committee
University of Guelph Athletics

MEMBER OF THE ORGANIZING COMMITTEE September 2000 to March 2001
ONTARIO UNIVERSITY LIFEGUARD CHAMPIONSHIP 2001
University of Guelph Athletics

VOLUNTEER CAMPUS TOUR GUIDE September 1999 to April 2002
University of Guelph Admissions